1-1-2015

Advancement And Validation Of A Plug-In Hybrid Electric Vehicle Model Utilizing Experimental Data From Vehicle Testing

Kevin Lloyd Snyder
Wayne State University,

ADVANCEMENT AND VALIDATION OF A PLUG-IN HYBRID ELECTRIC VEHICLE MODEL UTILIZING EXPERIMENTAL DATA FROM VEHICLE TESTING

by

KEVIN SNYDER

THESIS

Submitted to the Graduate School

of Wayne State University,

Detroit, Michigan

in partial fulfillment of the requirements

for the degree of

MASTER OF SCIENCE

2015

MAJOR: ELECTRIC-DRIVE VEHICLE ENGINEERING

Approved By:

_____

Advisor   Date

ACKNOWLEDGMENTS

TABLE OF CONTENTS

LIST OF TABLES

LIST OF FIGURES

xi

LIST OF ABBREVIATIONS

ACCM	(Electric) Air Conditioning Compressor Module, replaces conventional compressor belt driven by engine
APM	Auxiliary Power Module, a DC-DC voltage converter from ESS to 12 V system, replaces conventional alternator belt driven by engine
ATF	Automatic Transmission Fluid
AWD	All Wheel Drive
BAS	Belt Alternator Starter, a mild hybrid system, capable of engine start/stop and mild boost/regen
BCM	Battery Control Module
CAD	Computer Aided Design
CAN	Controller Area Network, a network communication standard
CD mode	Charge Depletion mode, where propulsion energy comes from the ESS, primarily or exclusively
CO	Carbon Monoxide (a pollutant)
CS mode	Charge Sustaining mode, where the propulsion energy comes from the fuel converter (internal combustion engine, fuel cell)
CSM	Current Sense Module
DUT	Device Under Test
E2D2	Ethanol-Electric Dual-Drivetrain, the name chosen for the team's reengineered vehicle
E85	Alternative fuel for internal combustion engine, nominally 85% ethanol and 15% gasoline, for use in Flex Fuel capable engines
E&EC	Emissions & Energy Consumption (competition event)
ECU	Electronic Control Unit - the generic term for ECM, TCM, HCU, etc.

ECM	Engine Control Module
EDM	Electrical Distribution Module
EPA	Environmental Protection Agency of the United States of America
ESS	Energy Storage System (the high voltage traction battery pack)
EVT	Electrically Variable Transmission
FCHEV	Fuel Cell Hybrid Electric Vehicle
FWD	Front Wheel Drive
GHG	Green House Gases
GM	General Motors corporation
GPS	Global Positioning System, satellite based location awareness
GUI	Graphical User Interface
HCU	Hybrid Control Unit (supervisory controller)
HEV	Hybrid Electric Vehicle, small ESS in vehicle, no plug-in charging
HIL	Hardware In the Loop
HV	High Voltage, greater than 60 V
HWFET	EPA drive cycle, moderate, highway speeds
ICE	Internal Combustion Engine
IMS	Internal Mode Switch - of the transmission for controlling transmission ranges: P, R, N, D, L
IO	Inputs/Outputs, for controller to sense and actuate
J1772	SAE specification for Electric Vehicle Conductive Charge Coupler

MIL	Model In the Loop
MORA	Model Order Reduction Algorithm
MPGe	Miles Per Gallon gasoline equivalent
MSD	Manual Service Disconnect
NOx	Nitrogen Oxides (a pollutant)
NVH	Noise, Vibration, Harshness (undesirable vehicle characteristics)
OBC	On-Board Charger, converts grid/wall AC electricity to DC electricity during plug-in charging to charge the ESS
OBD	On Board Diagnostics
OOR	Out Of Range, an invalid or unacceptable value returned from simulation
PHEV	Plug-in Hybrid Electric Vehicle, grid/wall AC electrical energy is used for plug-in charging of a large ESS in the vehicle, AC electricity displaces some portion of fuel for propulsion energy
PI	Proportional Integral (feedback control method for simulation Driver model)
PTTR	Parallel-Through-The-Road (hybrid powertrain architecture)
PWM	Pulse Width Modulated
RWD	Rear Wheel Drive
SAE	Society of Automotive Engineers
SIL	Software In the Loop
SOC	State-of-Charge of the ESS (0% empty, 100% full)
TCM	Transmission Control Module
THC	Total Hydrocarbons, incomplete combustion (a pollutant)

UDDS   EPA drive cycle, moderate, city speeds, many stops

UF   Utility Factor, from SAE J1711 standard for measuring the exhaust emissions and fuel economy of HEV's and PHEV's [1]

US06   EPA drive cycle, aggressive, city and highway speeds

VTS   Vehicle Technical Specifications

WEG   Water Ethylene Glycol

WSU   Wayne State University

WTW   Well-To-Wheel, from source extraction through processing, distribution, and ending at point of consumption

Y1   Year 1 (of 3 in the EcoCAR2 competition)

Y2   Year 2 (of 3 in the EcoCAR2 competition)

Y3   Year 3 (of 3 in the EcoCAR2 competition)

CHAPTER 1. INTRODUCTION

1.1. EcoCAR 2 Competition

The research for this thesis came from participating in the Wayne State University (WSU) student team that competed in the three year EcoCAR 2 student design competition sponsored by the US Department of Energy and managed by Argonne National Laboratory to reengineer a mid-sized sedan into a Plug-in Hybrid Electric Vehicle (PHEV).

Competition goals included reducing petroleum consumption, Well-To-Wheel (WTW) Green House Gas (GHG) emissions, energy consumption, and training next generation of students in advanced vehicle technologies. The students learned by using hands-on tasks, math-based tools, and performing simulations. The students reengineering process followed the EcoCAR Vehicle Development Process, which mimics the General Motors (GM) Corporation's Global Vehicle Development Process [2]. There were 15 university teams competing in EcoCAR 2.

An EcoCAR "4-Cycle" drive cycle was created from a weighted combination of EPA cycles (US06, UDDS, HWFET) and used in the Final Competition for Emissions & Energy Consumption (E&EC) results. The test track "On Road Competition" drive cycles for E&EC were approximations of the EcoCAR "4-Cycle," having similar road loads. The E&EC "On Road Competition" drive cycles for Year 2/Year 3 were 104.5/103.7 mile [168/167 km] long drive cycles on a GM proving ground track.

The Final Competition had other scored events including:

- Dynamic: 0-60 mph & 50-70 mph Acceleration, 60-0 mph Braking Distance, Maximum Lateral Acceleration, and Autocross, Dynamic Consumer Acceptability (Noise, Vibration, Harshness - NVH)
- Static: Vehicle Testing Complete, Static Consumer Acceptability
- Presentations: Business, Communications, Engineering (Mechanical, Electrical, and Controls)

The team's reengineering included mechanical, electrical, and controls software tasks, with the vehicle architecture shown in Figure 1-1. The team ended up adding an A123 19 kWh high voltage Energy Storage System (ESS) that powered a Rear Wheel Drive (RWD) powertrain consisting of a Rinehart 150 kW inverter connected to a Remy 150 kW electric traction motor, but the motor was current limited by the inverter to 115 kW / 95 kW (peak/cont.) mechanical output. The team swapped out the GM 2.4 L eAssist mild hybrid (Belt Alternator Starter – BAS) engine and installed a 2.4 L E85 flex fuel engine, to be able to run the engine on E85 instead of gasoline as the

only modification to the Front Wheel Drive (FWD) powertrain. Since E85 is nominally 85% ethanol (a renewable, vegetation based fuel) and 15% gasoline (non-renewable, petroleum oil based fuel), a significant amount of petroleum oil reduction can be accomplished by fuel choice. The team's reengineering efforts successfully converted the mid-sized sedan into a Parallel-Through-The-Road (PTTR) hybrid architecture, where the road was the mechanical connection between the two powertrains, creating the parallel hybrid. The reengineered WSU PTTR PHEV final curb weight was 2072 kg (4568 lbs.).
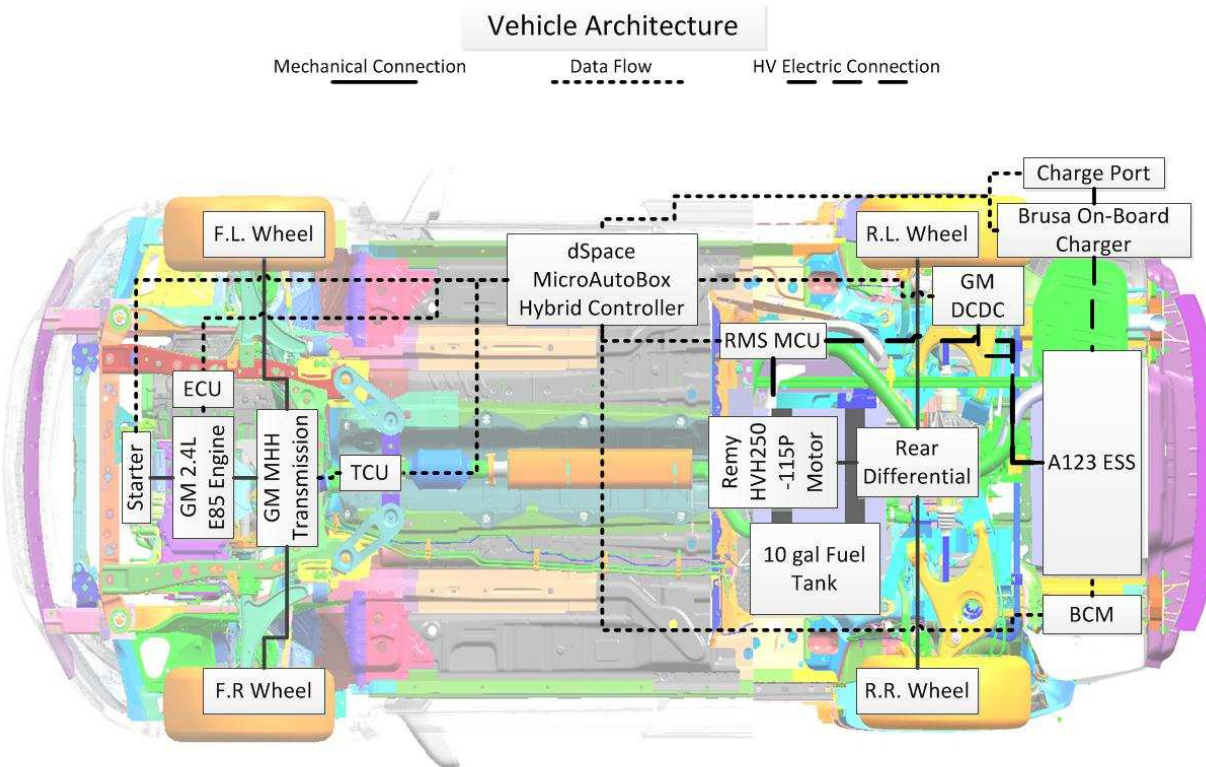
Figure 1-1. WSU's Plug-In Hybrid Vehicle Powertrain Architecture.

To reengineer the GM donated 2013 Chevrolet Malibu eAssist mild hybrid into a plug-in hybrid, the team went through a three year process that broke down to the following annual phases:

- Year 1 (Y1) – Chose a plug-in hybrid powertrain architecture and components, then reengineered the design of the vehicle to incorporate the new hybrid powertrain

- Year 2 (Y2) – Build the re-design and debug to the point of a rough running "engineering mule" vehicle, with all hardware functional

- Year 3 (Y3) – Refine, debug, and optimize the design hardware and controls software to be well running, near production ready vehicle

1.2. Problem Statement and Research Objective

Transportation energy mainly comes from petroleum oil (over 90% [3]) and 71% of petroleum oil production is used for transportation [4]. Petroleum oil is not a renewable energy source and is therefore not a sustainable source of energy.

Ground vehicle exhaust emissions contain both pollutants and Green House Gases (GHG) from the combustion of hydrocarbon fuels to propulsion energy. There are also emissions of pollutants and GHG in the supply chain to get the fuel all the way to the fuel tank in the vehicle: extraction of the raw feedstock (drilling & pumping oil), processing of the feedstock to fuel (oil refinery), and distribution of the fuel to the retail points (gas stations). For the United States of America in 2012, 28% of GHG came from the transportation sector [5].

Improvements are needed to reduce petroleum oil usage and emissions in order to:

- Achieve energy sustainability in preparation for when petroleum oil becomes scarce

- Prevent further degradation of the environment we live in

The objective of the research was to investigate improvements to automotive powertrains to reduce energy consumption, especially petroleum oil and to also reduce overall emissions from Well-To-Wheel (WTW), while still maintaining consumer acceptability of vehicle performance, utility, and safety [2].

This thesis's research into modeling and simulation provides an iterative improvement to the team's math-based design tools for use in evaluating different outcomes based on hybrid powertrain architecture tweaks, controls code development, and testing to provide the best solution for the problem statement.

This thesis also includes the results of the WSU team's efforts in the EcoCAR 2 competition to create and test a PHEV for reducing petroleum oil and emissions.

1.3. Research Methodology

The research utilized both analytical and empirical methods. Powertrain improvements were investigated by modeling and simulation by the analytical method. As the conventional vehicle was reengineered into a PHEV

and tested throughout the EcoCAR 2 competition, the empirical method was used to take the experimental test data and compare it to the simulation results, to then make advancements on the vehicle plant model.

Advancements to vehicle plant model improved the quality of the team's control software testing by providing more realistic vehicle behavior for the testing. The "V-diagram" software process shown in Figure 1-2 was used to design, build, and test team's control software for the reengineered PHEV. The model advancement affects improvement in two major test steps of the "V-diagram" (yellow highlighted boxes):

1) Create driver cycle/s using the test vectors and check all requirements are met

2) Test "Development" Code on the HIL
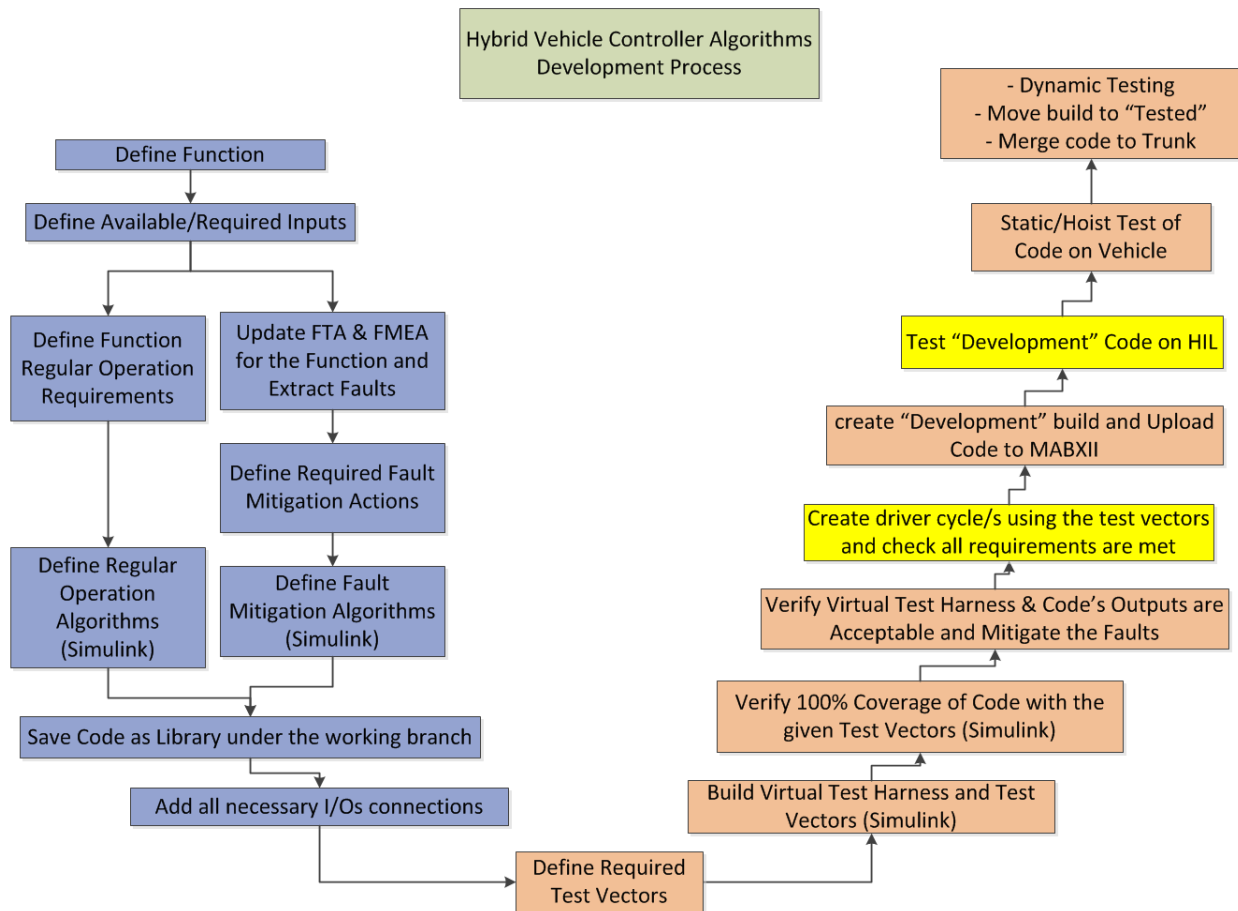
Figure 1-2. WSU's "V-diagram" software development process.

The "V-diagram" is also an iterative process for software controls and plant model development: each iteration loop would have improvements to the plant model to reduce the most pressing discrepancies between the actual vehicle results and the simulated results.

1.4. Literature Review

Plant model validation for vehicles is performed at both the component level and the vehicle level. Plant models for energy consumption need enough equation fidelity and meaningful input parameters to accurately predict the vehicle responses for a given drive cycle. Adding more than necessary complexity, fidelity, to the model decreases the efficiency of the model, increasing the run time significantly, for diminishing improvements to model accuracy.

In [6], Waldner described his team's development of a complete vehicle model with Mathworks Simulink environment using SimDriveline, a part of the SimScape library. The vehicle model was a PHEV comprised of a 2009 Saturn Vue (sport utility vehicle) with an A123 21 kWh ESS for powering the electric motors. A GM 2.4 L E85 flex fuel engine coupled to a GM 2-Mode transmission (2 electric motors, 2 Electrically Variable Transmission (EVT) ranges for city driving/acceleration, plus 4 fixed gear ratios for cruising efficiency) which powered the front wheels. An UQM PP-145 motor/inverter coupled to a BorgWarner 31-01 single speed transaxle (8.28:1 gear ratio) which powered the rear wheels. Axle torque, engine speed, engine fuel mass flow, and ESS power from simulation were validated with vehicle test data. Plots of each were shown comparing the simulation trace to the vehicle data trace.

In [7], Crain described his team's development of a complete vehicle model as a combination of Argonne National Lab's Autonomie models and dSPACE's Automotive Simulation Models based upon a Mathworks MATLAB/Simulink environment. The vehicle model was a 2160 kg PHEV comprised of a 2013 Chevrolet Malibu (mid-sized sedan) with an A123 19 kWh ESS for powering the electric motors. A GM 1.7 L turbo diesel engine running on B20 biodiesel coupled to a GM conventional 6 speed automatic transmission which powered the front wheels. A Rinehart inverter controlled a Remy 150 kW motor coupled to a GKN single speed transaxle (9.7:1 gear ratio) which powered the rear wheels. Engine fuel mass flow and ESS voltage from simulation were validated with vehicle test data. Plots of each were shown comparing the simulation trace to the vehicle data trace.

In [8], Wilhelm described his team's development of a complete vehicle model using empirical models in Mathworks MATLAB/Simulink for the motor, fuel cell, battery, and most other powertrain components, except the

SimDriveLine library was used for the vehicle dynamics model. The vehicle model was a Fuel Cell Hybrid Electric Vehicle (FCHEV), 2178 kg, and based on a 2005 Chevrolet Equinox. Dynetek ZM180 gaseous hydrogen tank (4.3 kg @ 5075 psi) fed a Hydrogenics HyPM 65kW Fuel Cell whose output was boosted by a custom team designed and constructed DC-DC converter to supply the high voltage bus. On the high voltage bus was a Cobasys 2.4 kWh ESS with a Ballard 312V67 67 kW motor/inverter powering the front wheels and another Ballard 312V67 67 kW motor/inverter powering the rear wheels. Fuel Cell bus voltage and ESS bus voltage from simulation were validated with vehicle test data. Plots of each were shown comparing the simulation trace to the vehicle data trace.

In [9], Syed *et al.* constructed a complete vehicle plant model of a power-split HEV using Mathworks MATLAB/Simulink where empirical data was used with a first or second order transfer function in an iterative approach to model the engine and electric motor/generator. The ESS State-of-Charge (SOC) was also modeled also with an iterative approach using experimental data curves of battery parameters, similar to the Peukert's equation approach. The planetary gear set dynamic system was modeled with a state-space equation. The vehicle model was a 1820 kg Ford Escape HEV with a 2.3 L engine Atkinson Cycle (124 Nm @ 4250 rpm), a 70 kW electric machine, and a 2 kWh ESS. Vehicle speed, wheel torque, engine speed, engine torque, generator speed, generator torque, motor speed, motor torque, ESS voltage, ESS power, and ESS SOC were validated with vehicle test data. Plots of each were shown comparing the simulation trace to the vehicle data trace.

In [10], Browne constructed a complete energy based (bond graph) vehicle model then performs model reduction using Model Order Reduction Algorithm (MORA). Browne simulated two conventional vehicles: 2004 Chevrolet Optra (1250 kg, 2.0 L compact sedan) and a 2003 Honda CR-V (1525 kg, 2.4 L sport utility vehicle). Browne then used GPS combined with vehicle On Board Diagnostics (OBD) data to validate engine manifold pressure, engine crankshaft speed, and vehicle speed. Plots of each were shown comparing the simulation trace to the vehicle data trace and Coefficients of Determination (R^2) were calculated for each.

CHAPTER 2. SIMULATION RESULTS AND COMPARISON TO EXPERIMENTAL DATA

2.1.   Component and Vehicle Testing Methodologies

Vehicle testing methodologies and equipment are extensive and not all were used for the research for this thesis in the area of energy consumption and emissions. Testing comprises two general categories:

- Low level testing of the unit, or subsystem, or component (i.e. engine, electric motor, ESS, etc.)

- High level testing of the system (i.e. vehicle or vehicle towing a trailer), integration testing of all the subsystems

Test equipment can span from simple test equipment to extremely complex and expensive test cell setups, to freely available public roads in cities & highways, and extreme/remote locations:

- Component Dynamometer (dyno): engine, transmission, electric motor

- Component Test Benches: thermal systems, fuel systems, vehicle 12 V wiring and control, battery cell, battery module, battery pack (ESS), etc.

- Hardware-In-the-Loop (HIL) Test Benches: simulate an entire vehicle's powertrain and chassis for a safe initial test environment where nobody is hurt if there are torque control errors and a crash

- Chassis Dynamometer (chassis dyno) [11]: emulated road load applied to test vehicle's driven wheels (2WD, 4WD chassis dynos) with tailpipe exhaust emissions data collection, sometimes with environmental features (wind, hot/cold ambient temperature, altitude)

    o   However, the smooth, low friction surface of the 48 inch diameter steel dyno rollers are not suitable for highly dynamic testing: acceleration testing of 0-60 mph & 50-70 mph, braking distance testing from 60-0 mph, autocross course time testing, maximum lateral acceleration, Dynamic Consumer Acceptability (DCA) which includes Noise, Vibration, Harshness (NVH) and suspension handling, drive quality, highway gradeability, on road safety evaluation, and emissions & energy consumption

- Test Track: testing vehicle on closed course of various configurations, can perform aggressive maneuvers at or beyond the limits of the vehicle, can test with or without towing an instrumented trailer for emissions, or trailer dyno for simulated grade (applies extra variable load to test vehicle), snow/ice traction testing. The test track is the only safe way to test an entire vehicle in dynamic events:

- o Emissions & energy consumption: "*The Emissions and Energy Consumption (E&EC) Event consists of four individual event categories that are scored from the data collected over a 103-mile trip on the Circle Track:*
    - *Energy Consumption*
    - *Well-to-Wheel Petroleum Energy Use*
    - *Well-to-Wheel Criteria Emissions*
    - *Well-to-Wheel Greenhouse Gas Emissions*

  Greenhouse Gas, Criteria Emissions and Petroleum Energy Usage (PEU) factors can be found in the NYS Rules. Tailpipe emissions are measured and logged with a SEMTECH DS exhaust gas analyzer, which is installed by the competition organizers." [12]

- o Acceleration testing of 0-60 mph & 50-70 mph: "*Acceleration times, vehicle speeds, and stopping distances are recorded using V-Box instrumentation*" [13]

- o Braking distance testing from 60-0 mph [13]

- o Autocross course time testing: "*This event will test the vehicle's dynamic handling ability through a timed autocross style course. This event is designed to test the vehicle's balance and stability at higher than average maneuvering speeds, and it must be performed in the team's normal control strategy*" [14]

- o Maximum lateral acceleration: "*This event evaluates the maximum lateral acceleration as the vehicle negotiates a decreasing radius turn at a preset vehicle speed without excessive sliding or body lean. The event is a test of how well the vehicle handles with the new powertrain and mass characteristics by objectively evaluating the vehicle's weight distribution, spring and bar selection, and tire characteristics."* [15]

- o Dynamic Consumer Acceptability (DCA): "*This event will include subjective evaluations and objective noise measurements to score teams. Noise and vibration should be controlled properly through powertrain mounts, proper intake and exhaust systems, interior noise abatement, etc. Vehicle ride and handling should be at production levels in regards to vehicle systems such as the steering, brakes, and suspension."* [16]

- o Drive quality: "*The balance between fuel economy and drive quality is one of the most difficult and important tasks in the Vehicle Development Process. The objective of this event is to assess the vehicle's drive quality. The main tool that will be used for this drive quality assessment is AVL Drive.*" [17]

- o Highway gradeability: "*The vehicles will tow a dynamometer that simulates a 3.5% grade at a constant speed of 60 MPH for 20 miles. Vehicle speed cannot slip below 50 MPH or exceed 70 MPH during the event.*" [18]

- o On road safety evaluation: "*The On Road Safety Evaluation (ORSE) event is designed to evaluate the vehicle's dynamic handling characteristics and verify the ability of the vehicle to safely perform dynamic maneuvers and stop within a safe distance. Vehicles will be evaluated to make sure that no interference with the steering or suspension system exists, that the anti-lock brake system (ABS) is functioning, and that the vehicle exhibits stability at high and low speeds.*" [19]

- Public Road: test vehicle in real world conditions of city and highway traffic, on extreme mountain grades, extreme high altitude engine testing, extreme hot/cold locations in worst seasons (desert in summer, extreme North/South locations in the winter), snow storm/sand storm particulate ingestion, etc.

2.2. Road Load Physics and other Equations for Simulation

The equations used for modeling and simulation involve the vehicle chassis motion due to forces acting on it from the dual powertrains combined with the environment the vehicle is experiencing. Newton's Second Law of Motion, the vector sum of the forces equals the product of the total mass and the acceleration vector [20]:

$$\sum_i \bar{F}_i = m\bar{a} \tag{1}$$

Drive cycle simulations for fuel economy and linear acceleration simplify the force and acceleration from vectors to scalars as the longitudinal forces dominate over the lateral forces for these drive cycles.

$$\sum_i F_i = ma \tag{2}$$

Equation 2 is rewritten to solve for the vehicle linear acceleration. The total mass and the sum of the forces need to be determined to solve for the acceleration:

$$a = \frac{1}{m} \sum_i F_i \tag{3}$$

$$a = \frac{d}{dt} v = \frac{1}{m} \sum_i F_i \tag{4}$$

The total mass is the sum of the vehicle mass and the effective mass from the rotational drivetrain components (wheels, gears, engine, and electric motor) [21]:

$$m = m_{vehicle} + m_{equivalent\_rotational} \tag{5}$$

The sum of the forces are comprised of the individual forces listed below [21] and are graphically shown in Figure 2-1:

$$\sum_i F_i = F_{tractive} - F_{roll} - F_{aero} - F_{grade} - F_{brakes} \tag{6}$$

- $F_{tractive}$ is the tractive force resulting from the sum of both FWD & RWD powertrains in the PTTR PHEV
- F_{roll} is the rolling resistance force

- F_{aero} is the aerodynamic drag force

- F_{grade} is the hill climb or descent force, where the angle of the grade is the slope of the hill

- F_{brakes} is the force of the friction braking system of the vehicle
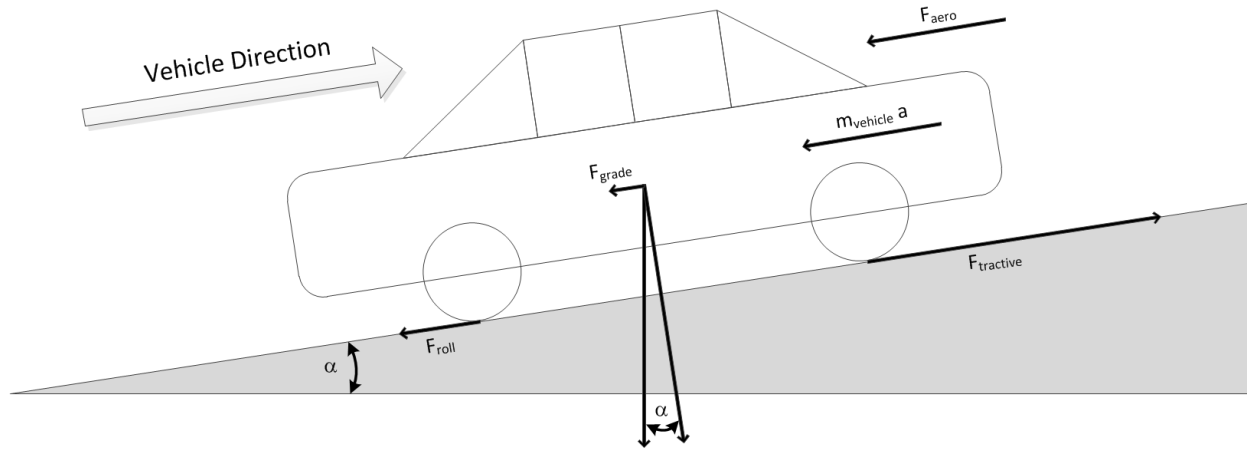
Figure 2-1. Forces acting on a vehicle accelerating up a grade.

$$F_{tractive} = F_{FWD} + F_{RWD} \tag{7}$$

$$F_{roll} = \mu_{roll} mg \, \cos(\alpha) \tag{8}$$

For rolling resistance, μ_{roll} is the coefficient of rolling resistance (dimensionless), g is the acceleration due to gravity, and α is the angle of the grade. Rolling resistance is due to the tire flexing/deforming with the road, road conditions/composition, and also friction in the bearings of the rotating components [22].

$$F_{aero} = \frac{1}{2} \rho A_f C_d v^2 \tag{9}$$

Aerodynamic drag is comprised of: ρ density of air along the road (depends on altitude, temperature, and humidity) [22], A_f frontal area of the vehicle, C_d drag coefficient (dimensionless), and v velocity of the vehicle to the air (wind speed plus vehicle speed, usually assume zero wind speed for simulations, so only have vehicle speed).

$$F_{grade} = mg \sin(\alpha) \tag{10}$$

The equivalent mass from the inertial acceleration of the rotational components are calculated for both the front axle and the rear axle by [23]:

$$m_{equivalent\_rotational} = \frac{1}{r^2_{whl}} \left(J_{whl} + J_{whl\_in} \right) \tag{11}$$

Where J_{whl} is the rotational inertia of a pair of wheels on the same axle (either the FWD or RWD wheels), r_{whl} is the wheel radius, and J_{whl_in} is the rotational inertia into the wheel from upstream components, passed on from the differential output.

$$J_{whl\_in} = J_{diff\_out} = J_{diff\_gear\_out} + \gamma^2_{diff} \left(J_{diff\_gear\_in} + J_{diff\_in} \right) \tag{12}$$

The differential rotational inertia out to the wheel is comprised of the differential output ring gear's rotational inertia $J_{diff\_gear\_out}$, the differential gear ratio γ_{diff}, the differential input pinion gear's rotational inertia $J_{diff\_gear\_in}$, and the J_{diff_in} rotational inertia into the differential from the gearbox (single speed reducer or multispeed transmission) and upstream components.

$$J_{diff\_in} = J_{gb\_out} = J_{gb\_gear\_out} + \gamma^2_{gear} \left(J_{gb\_gear\_in} + J_{gb\_in} \right) \tag{13}$$

The gearbox rotational inertia out to the differential comprises the rotational inertia of the output gear $J_{gb\_gear\_out}$, the gearbox current gear ratio γ_{gear}, the gearbox input gear's rotational inertia $J_{gb\_gear\_in}$, and the J_{gb_in} rotational inertia into the gearbox from the electric traction motor or the internal combustion engine.

$$J_{gb\_in} = J_{motor\_or\_engine} \qquad (14)$$

Figure 2-2 shows the linear and rotational inertias, torques, forces, masses, forms of energy, and flow through the dual powertrains of the PTTR PHEV.
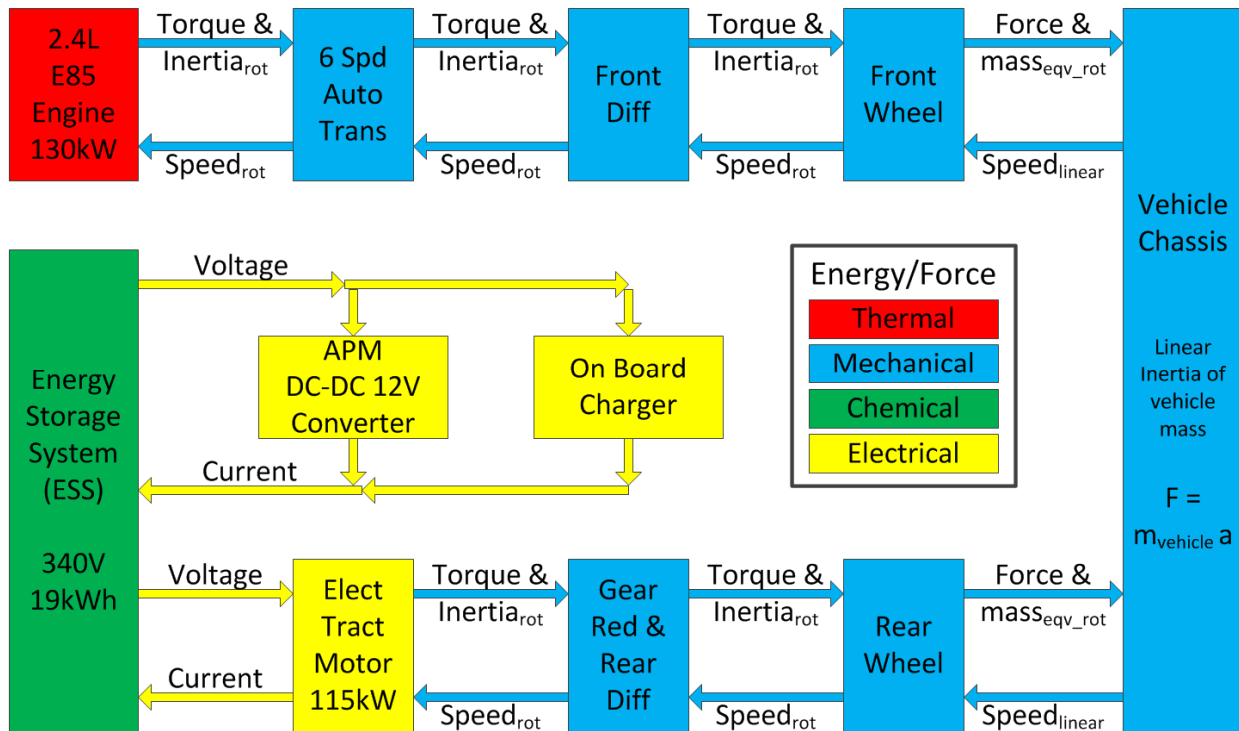
Figure 2-2. Energy & Force forms & flows of the Wayne State University team's PTTR PHEV.

The maximum braking force at the front and rear wheels in the simplest form, assuming no wheel slip, is braking torque T from the force of the friction brake pads on the rotors [24]:

$$F_{front\_brakes} = \frac{T_{front\_brakes}}{r_{whl}} \tag{15}$$

$$F_{brakes} = F_{front\_brakes} + F_{rear\_brakes} \tag{16}$$

The tractive force of the FWD & RWD powertrains use the same equations for the wheels, differentials, and gears. The tractive force at the wheel is the

$$F_{FWD} = \frac{T_{front\_whl}}{r_{whl}} \tag{17}$$

The torque of the wheel from the output of the differential is [24]:

$$T_{whl} = \gamma_{diff} \, \eta_{diff} \, T_{diff\_in} \tag{18}$$

Where γ_{diff} is the gear ratio of the differential, η_{diff} is the efficiency of the gears and bearings in the differential, T_{diff_in} is the input torque to the differential.

$$T_{diff\_in} = \gamma_{gear} \, \eta_{gear} \, T_{gearbox\_in} \tag{19}$$

Where γ_{gear} is the current gear in use, η_{gear} is the efficiency, and $T_{gearbox\_in}$ is the torque into the gearbox. The gearbox is either the 6 speed automatic transmission on the FWD powertrain or the single speed gear reducer on the RWD powertrain.

$$T_{gearbox\_in} = T_{engine} \tag{20}$$

The engine torque comes from a 2-D experimentally created fuel mass flow ($\dot{m}$ in kg/s) map from engine dyno testing by the manufacturer that has engine speed (ω in rad/sec) and engine torque for the two axes. The engine torque and fuel mass flow equations are [23]:

$$T_{engine} = f\left(\omega_{engine}, APP_{engine}\right) \tag{21}$$

$$\dot{m}_{fuel\_flow} = f\left(\omega_{engine}, T_{engine}\right) \tag{22}$$

APP_{engine} is the driver's torque request through the Accelerator Pedal Position (APP) that ranges from 0.0 - 1.0 (0% - 100% travel). In the hybrid supervisory controller, the controls code will decide how much torque to request of the engine and how much to request of the motor, depending on which operating more the vehicle is in and the driver's demand.

$$P_{engine\_mech} = \omega_{engine}\, T_{engine} \tag{23}$$

$$P_{fuel} = \dot{m}_{fuel\_flow}\, \text{SE}_{\text{LHV}} \tag{24}$$

The Specific Energy (at the Lower Heating Value) SE_{LHV} is in J/kg and is used to convert the fuel mass flow in kg/s to fuel power in J/s. This is then used to convert fuel power to fuel energy:

$$E_{fuel} = \int_{t0}^{t1} P_{fuel}\, dt \tag{25}$$

The motor torque comes from a 2-D experimentally created motor efficiency map from motor dyno testing by the manufacturer that has motor speed and motor torque for the two axes. The motor equations are [23]:

$$T_{motor} = f(\omega_{motor}, APP_{motor}) \tag{26}$$

$$P_{motor\_loss} = f(\omega_{motor}, T_{motor}) \tag{27}$$

$$I_{motor\_DC} = \frac{1}{V_{DC\_bus}} \left(P_{motor\_mech} + P_{motor\_loss} \right) \tag{28}$$

The high voltage DC bus V_{DC_bus} connects the motor to the ESS, P_{motor_mech} is the mechanical power output of the motor, P_{motor_loss} is the power loss from the motor efficiency map, and I_{motor_DC} is the DC current draw of the motor due to the torque output and inefficiencies.

$$P_{motor\_mech} = \omega_{motor} \, T_{motor} \tag{29}$$

$$P_{motor\_elect} = V_{DC\_bus} \, I_{motor\_DC} \tag{30}$$

The Auxillary Power Module (APM) DC-DC voltage converter runs in buck mode, reducing the nominal 340 V V_{DC_bus} voltage down to 13 V to keep the vehicle's 12 V system maintained. The APM electrical equations are below, where η_{APM} is the efficiency of the voltage conversion:

$$P_{APM} = \frac{1}{\eta_{APM}} P_{accessory\_loads} \tag{31}$$

$$I_{APM\_DC} = \frac{1}{V_{DC\_bus}} P_{APM} \tag{32}$$

The On Board Charge (OBC) is not simulated in the drive cycles, so the equations are not discussed other than I_{OBC_DC} is always zero current for the simulations. The OBC plant model is currently only used for Software-In-the-Loop (SIL) testing.

The ESS equations for current and State of Charge *SOC* are:

$$I_{ESS\_DC} = I_{motor\_DC} + I_{APM\_DC} + I_{OBC\_DC} \tag{33}$$

$$SOC_{current} = SOC_{initial} - \Delta SOC \tag{34}$$

$$\Delta SOC = \frac{1}{3600 \, C_{ESS}} \int_{t0}^{t1} I_{ESS\_DC} \, dt \tag{35}$$

ESS capacity C_{ESS} is in Amp hours so it is multiplied by 3600 to convert hours to seconds. The ESS equation for internal resistance R_{int} and ESS terminal voltage V_{term} are:

$$R_{int} = f(SOC, [charging|discharging]) \tag{36}$$

$$V_{term} = OCV + I_{ESS\_DC} \, R_{int} \tag{37}$$

The Open Circuit Voltage *OCV* is the no load, zero current voltage of the battery cells and I_{ESS_DC} is negative for discharging and positive for charging. The V_{DC_bus} voltage is the ESS V_{term} voltage if there is no bus conductor resistance modeled:

$$V_{DC\_bus} = V_{term} + I_{ESS\_DC} \, R_{bus\_conductor} \tag{38}$$

2.3. Wayne State University PTTR Vehicle Plant Models

The WSU vehicle plant model is shown in Figure 2-3 and it is comprised of component sub-models that make up two parallel independent powertrains, the combustion engine for the FWD and the electric traction motor for the RWD.
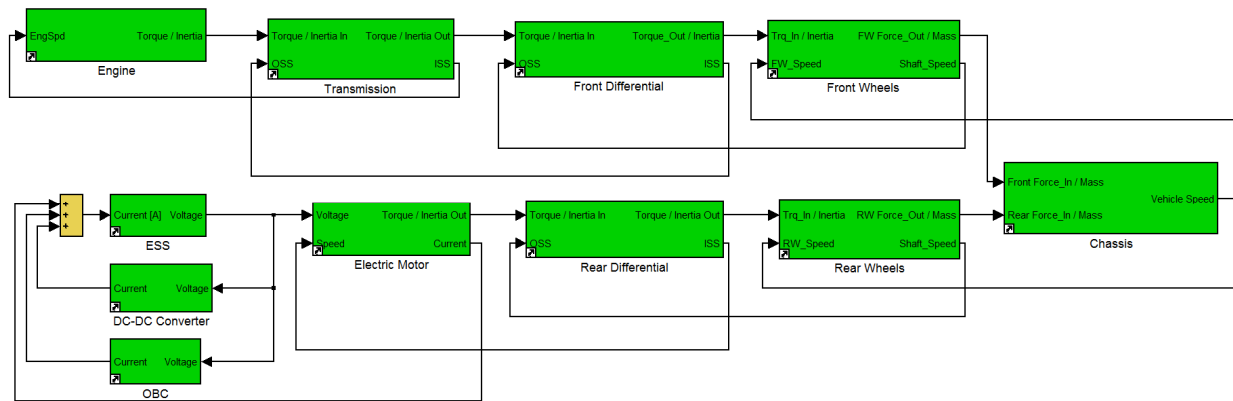
Figure 2-3. WSU's vehicle plant model for the team's PTTR PHEV.

The FWD powertrain has a 130 kW 2.4L engine using E85 for fuel, so an E85 specific fuel mass flow map for speed versus torque was obtained for use in the component plant model. The engine model was a LE9 ECOTEC 2.4L inline 4 cylinder with dual overhead cams having variable valve timing and a 10.4 compression ratio [25] shown in Figure 2-4.
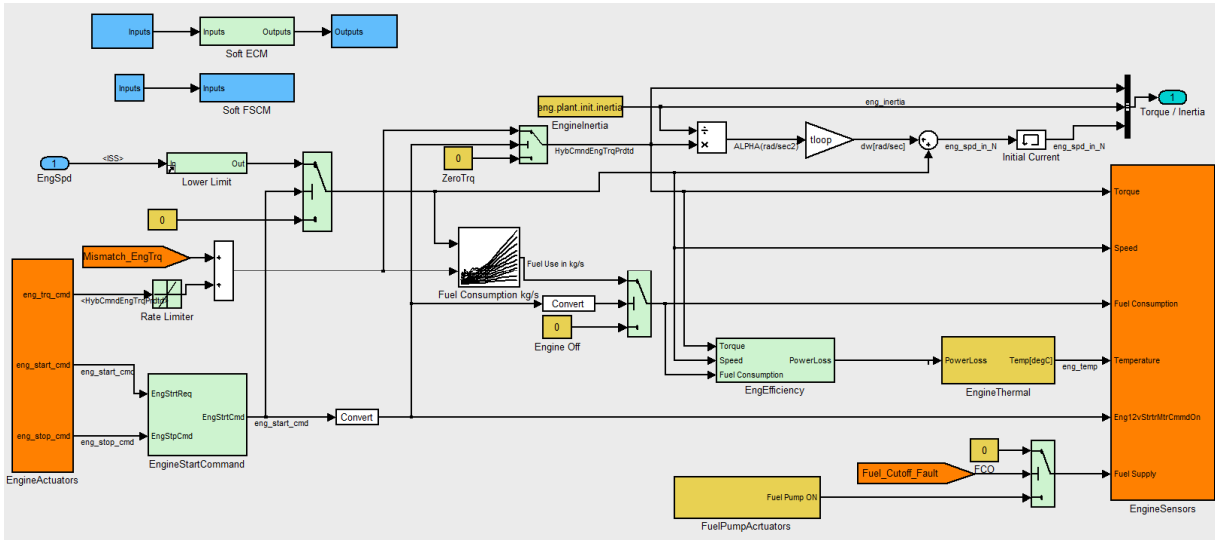
Figure 2-4. Internal Combustion Engine (ICE) plant model.

The WSU team obtained a gear efficiency map (based on torque and speed) and a gear shift schedule map (based on accelerator pedal position and vehicle speed) that were representative for the 6 speed automatic transmission in the GM donated 2013 Chevrolet Malibu. The transmission model was a 6T40 w/Aux Pump (MHH) having gear ratios: 4.58, 2.96, 1.91, 1.45, 1.00, 0.75 [26], the component plant model is shown in Figure 2-5.
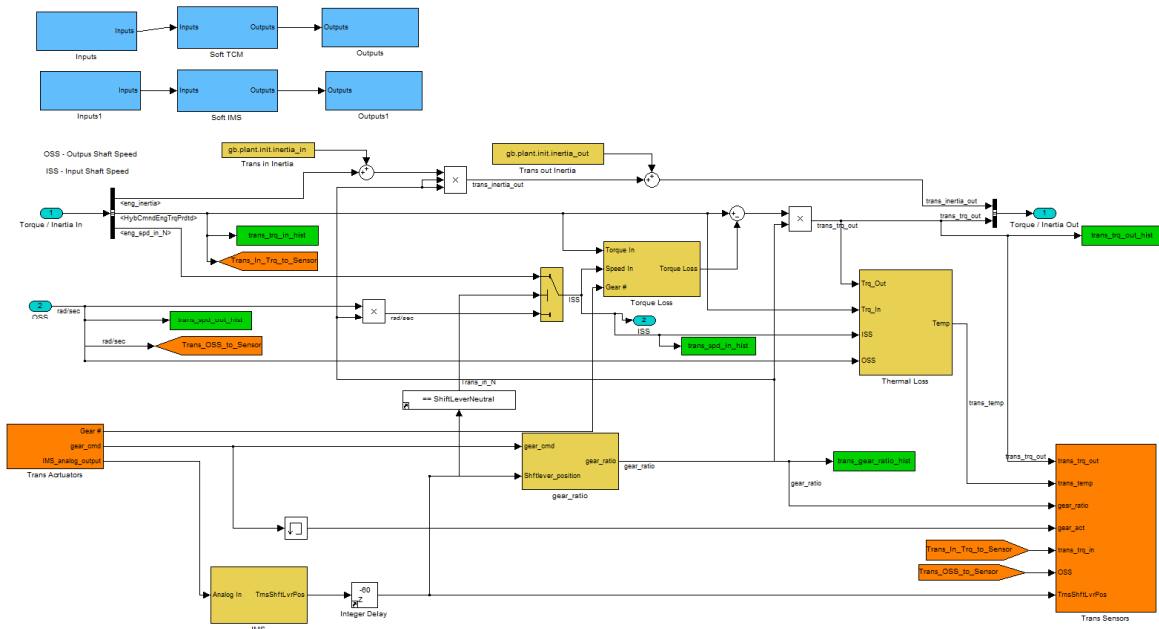
Figure 2-5. 6 Speed Automatic Transmission plant model.

The front differential ratio of 2.64 [27] and an assumed 99% constant efficiency were used in the front differential component plant model, shown in Figure 2-6.
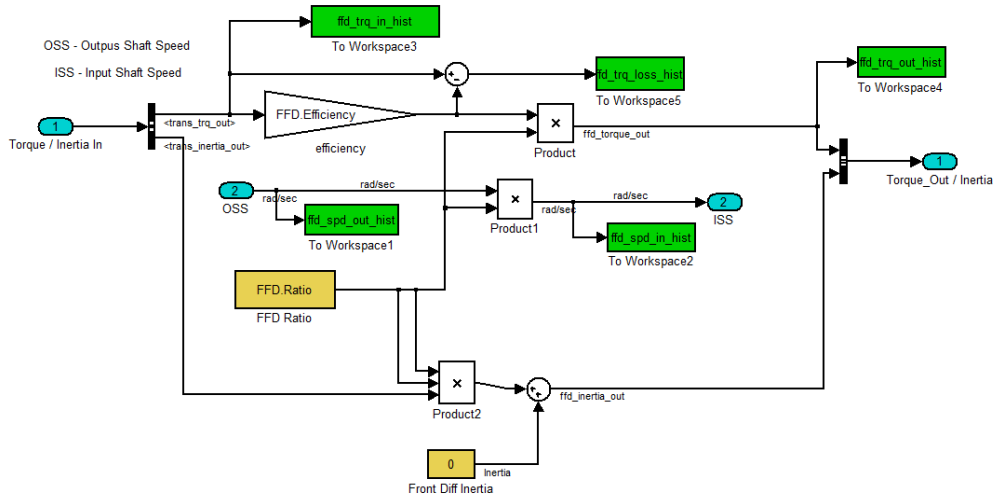
Figure 2-6. Front Differential plant model.

A wheel radius of 0.343 m and a rotational inertia of 1.2 kg m^2 were used in the front wheel component plant model for the Goodyear "Assurance Fuel Max" P225/55R17 tires on 17" alloy wheels, shown in Figure 2-7.
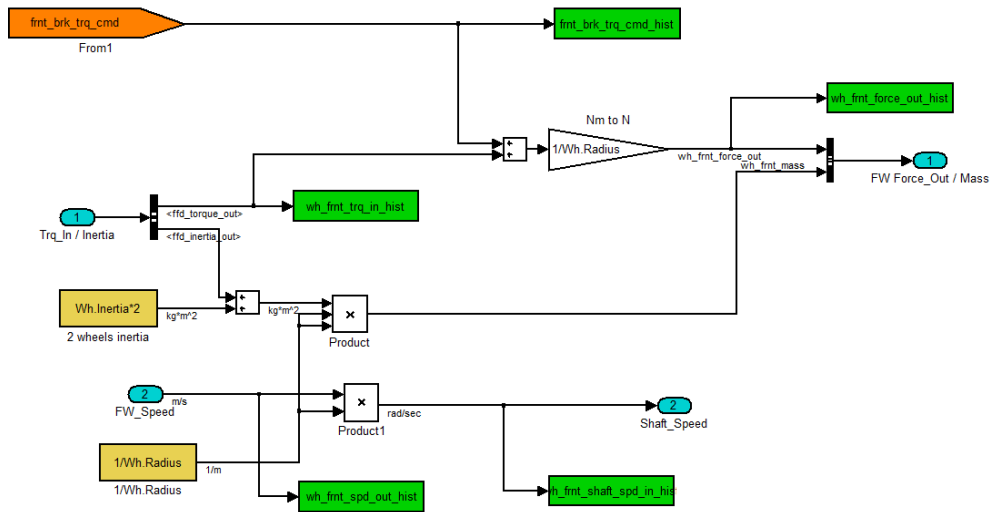
Figure 2-7. Front Wheel plant model.

The chassis is where the road load forces, tractive forces, and braking force all come together to determine the resulting acceleration of the vehicle. The chassis parameters used for the PTTR PHEV were mass = 2240 kg, $\mu_{roll} = 0.01$, $\rho = 1.225$, $C_d = 0.295$, and $A_f = 2.295$. The chassis component plant model is shown in Figure 2-8.
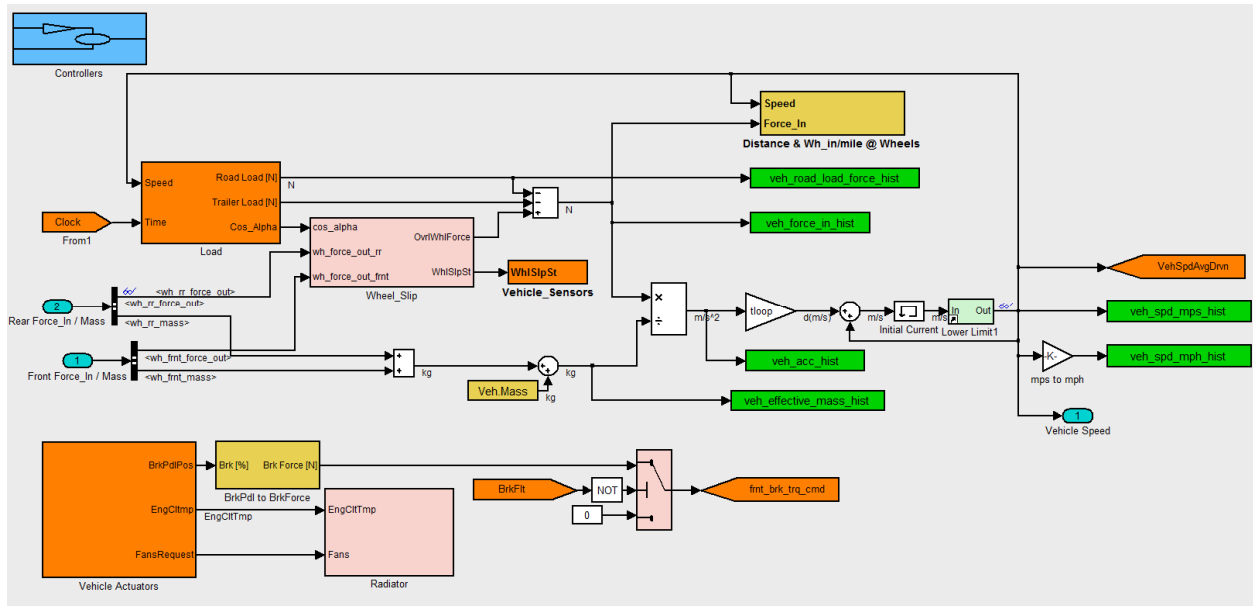
Figure 2-8. Chassis plant model.

The A123 high voltage battery pack (Energy Storage System – ESS) had a nominal pack voltage of 340 V and a nominal capacity of 19 kWh [28]. The team used an internal resistance map based on SOC and current for determining the internal resistance and then the resulting voltage drop from OCV to the battery terminals during discharge. The ESS component plant model is shown in Figure 2-9.
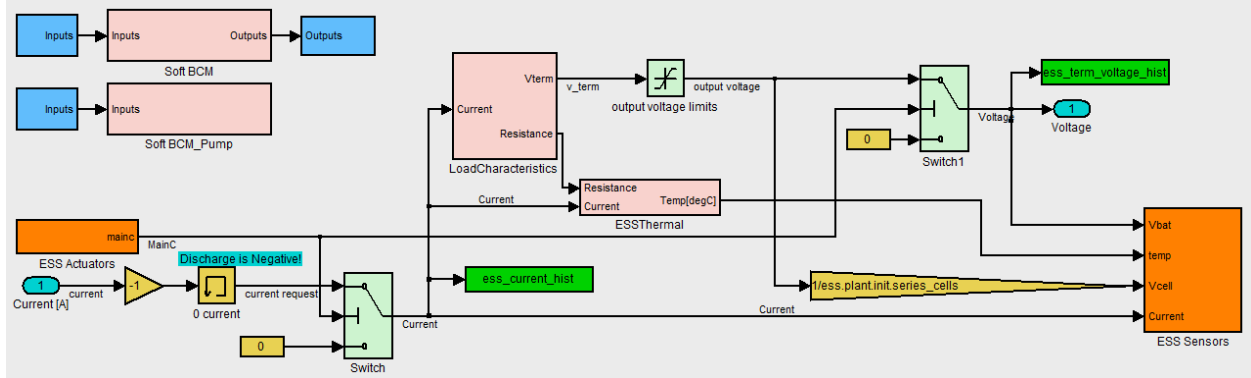
Figure 2-9. ESS plant model.

The RWD powertrain has a 115 kW mechanical output from a Remy motor / Rinehart inverter combination. A motor efficiency map was obtained and the team made an assumption of a constant 97% efficiency for the inverter. These were used in the component plant model, shown in Figure 2-10.
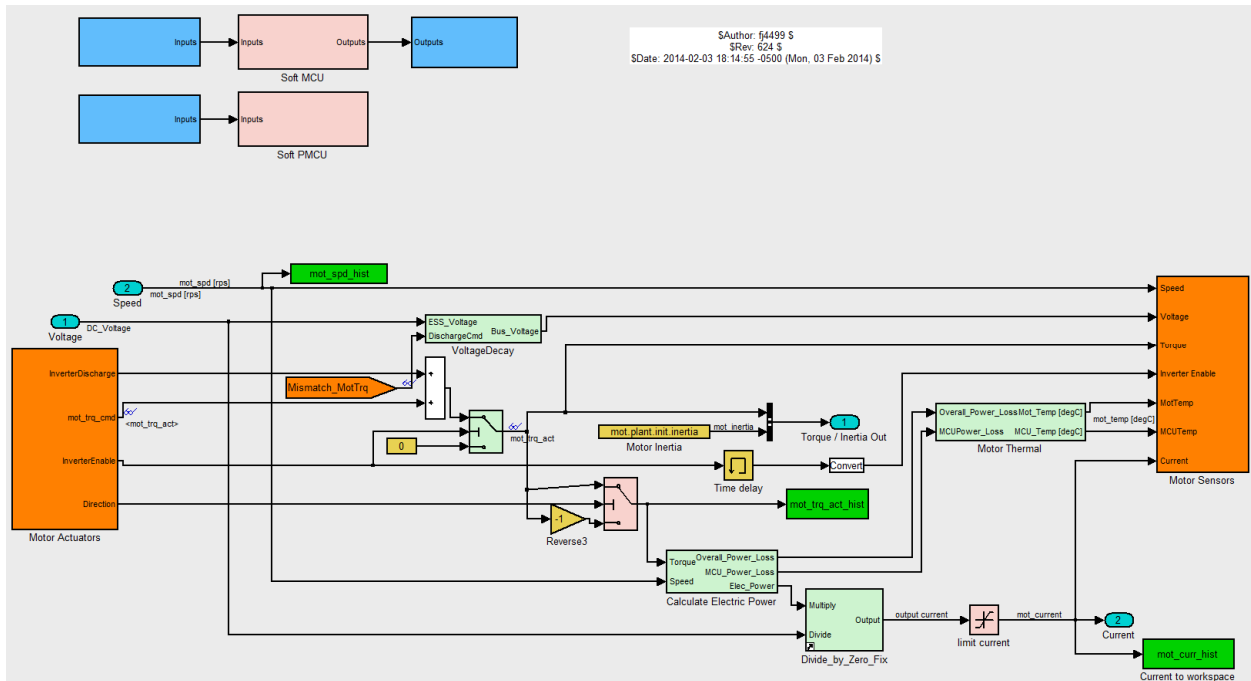
Figure 2-10. Electric Traction Motor plant model.

The rear differential ratio of 2.77 was determined by accessing the specifications on the GM website [27] and an assumed 99% constant efficiency was used. However, the team's belt & pulley reducer with a ratio of 2.57 was also lumped in with the rear differential for a total ratio of 7.12 (2.77 x 2.57). The rear differential component plant model is shown in Figure 2-11.
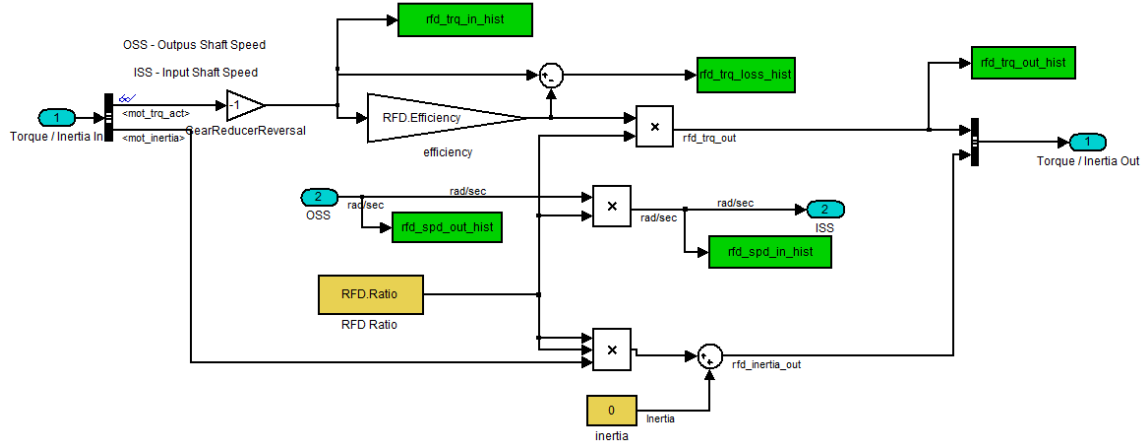
Figure 2-11. Rear Differential plant model (also includes Belt & Pulley Reducer).

The team's rear wheel was modeled identically to the front wheel model, except for braking force, where all braking force went to the front wheels. The rear wheel component plant model is shown in Figure 2-12.
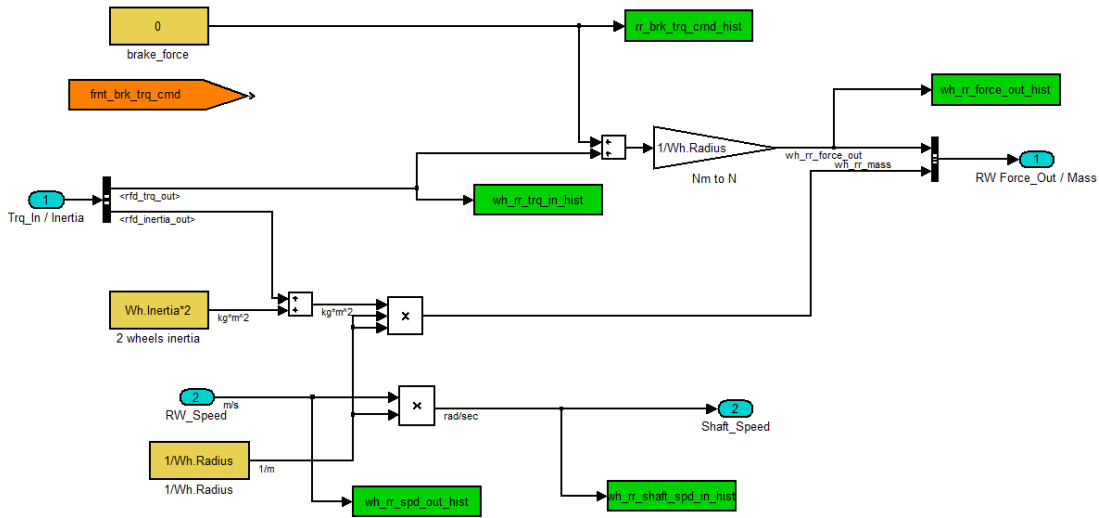
Figure 2-12. Rear Wheel plant model.

The team used an efficiency map for the APM to determine the losses through the DC-DC conversion from the 340 V high voltage DC bus down to the 12 V system. The APM component plant model is shown in Figure 2-13.
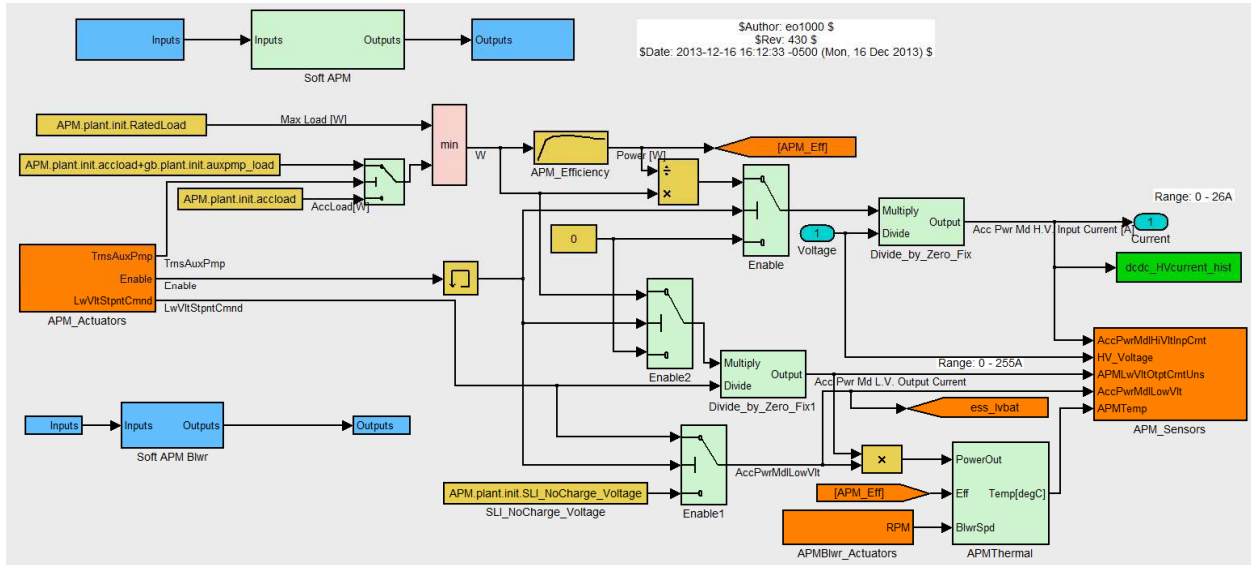
Figure 2-13. APM DC-DC Converter plant model.

The OBC component plant model was only used for SIL testing controls code, it was not used for drive cycle simulations. The component plant model is shown in Figure 2-14.
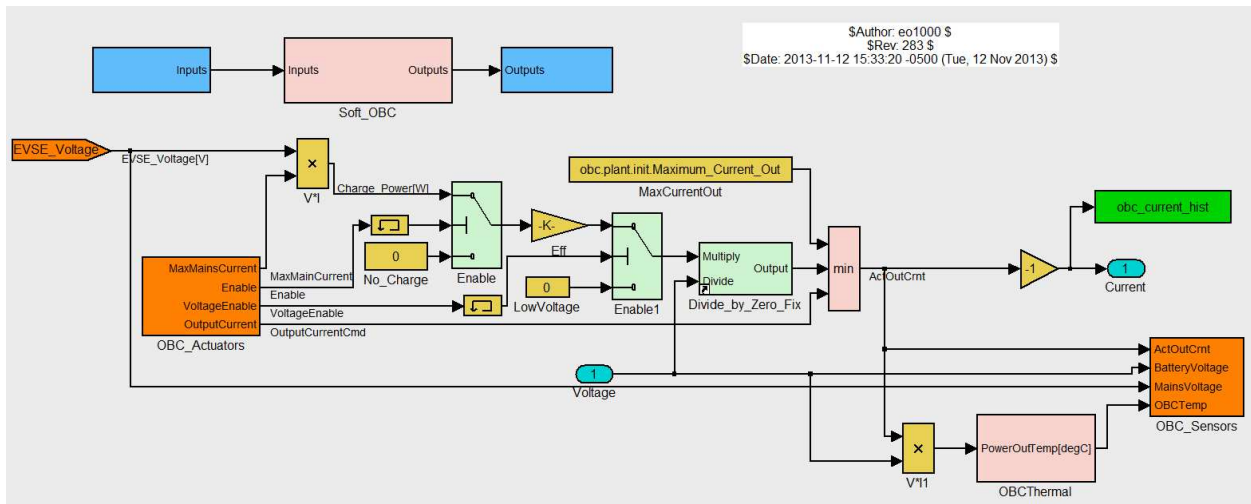
Figure 2-14. On Board Charger (OBC) plant model.

2.4. Dynamic Performance

The dynamic performance of the WSU PTTR PHEV was measured across several competition events, however not all events manifested into Vehicle Technical Specifications (VTS), so not all events were modeled & simulated:

1. Maximum Lateral Acceleration *(not simulated, not a VTS requirement)*

2. Autocross *(not simulated, not a VTS requirement)*

3. AVL Drive quality *(not simulated, not a VTS requirement)*

4. Dynamic Consumer Acceptability *(NVH event, not simulated, not a VTS requirement)*

5. 0-60 mph Acceleration

6. 50-70 mph Acceleration

7. Braking Distance, 60-0 mph deceleration

Table 2-1 shows the dynamic performance comparison of the stock vehicle, the competition targets and minimum requirements, the actual experimental data, and the WSU PTTR simulation results.

Table 2-1. WSU PTTR simulation results for Dynamic Performance compared to experimental data.

EcoCAR 2 Vehicle Technical Specifications (VTS) - **Dynamic Performance**	Production 2013 Chevy Malibu (eAssist)	EcoCAR2 Competition Design Target	EcoCAR2 Competition Requirement	WSU PTTR Y3 E85 Experimental Data	WSU PTTR Y3 E85 Simulation Prediction
Acceleration 0-60 mph [0-96.6 kph]	8.2 sec	9.5 sec	11.5 sec	6.4 sec	5.8 sec **(9% error)**
Accel. 50-70 mph [80.5-112.6 kph]	8.0 sec	8.0 sec	10 sec	3.2 sec	3.7 sec **(15% error)**
Braking 60-0 mph	43.7 m [143.4 ft]	43.7 m [143.4 ft]	54.8 m [180 ft]	40.2 m [132 ft]	25.3 m [82.9 ft] **(37% error)**

At the final competition of the 3rd year, the team's vehicle was able to compete as a fully functional PHEV, but the full functionality was intermittent due to motor "Resolver Not Connected" faults occurring just after an aggressive acceleration in hybrid mode – this fault then disabled the motor inverter until the next key cycle power

down/up of the vehicle. This fault occurred often enough to prevent the team from scoring what the WSU PTTR vehicle was fully capable of, for both the dynamic performance portion, and the energy consumption portion of the competition. An example of the inverter fault occurring during 0-60 mph & 50-70 mph acceleration event is shown in Figure 2-15.
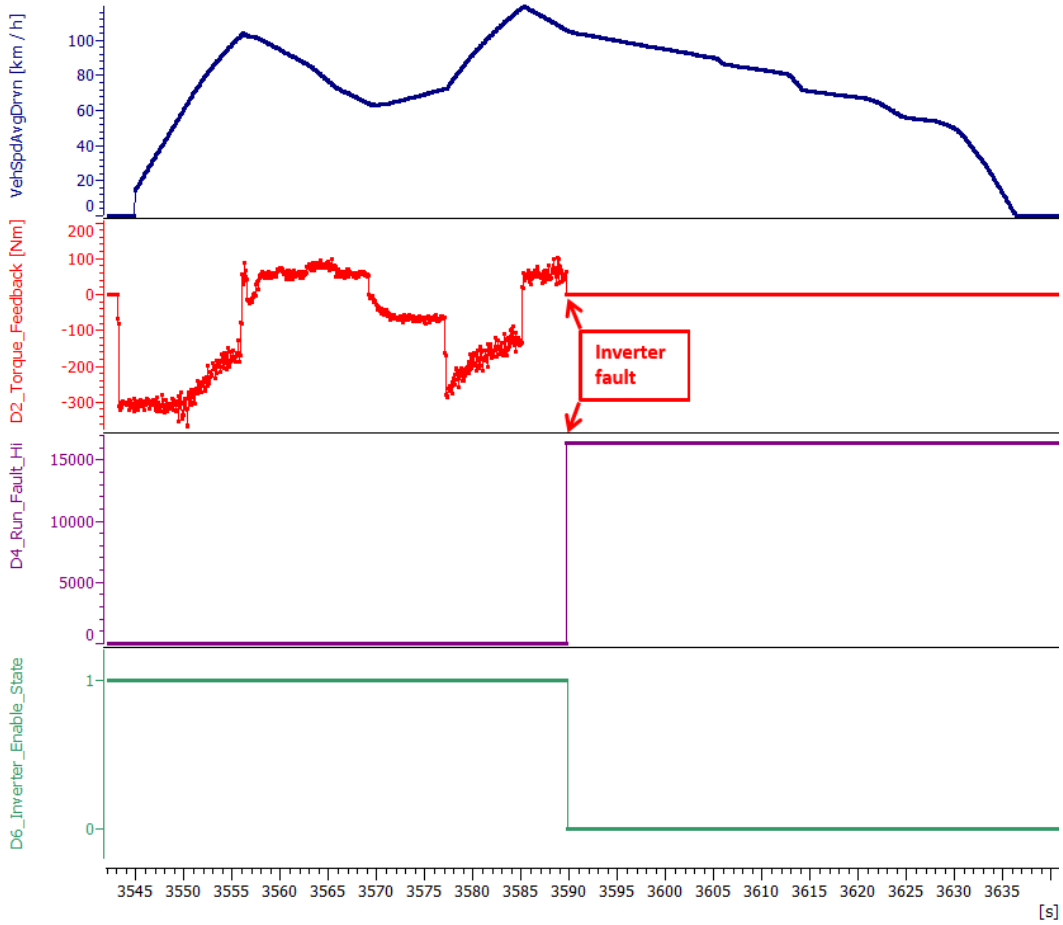
Figure 2-15. Inverter fault during 0-60 mph & 50-70 mph acceleration event.

The WSU PTTR modeling and simulation tool was developed by the team using MATLAB, Simulink, and StateFlow with a user interface shown in Figure 2-16.
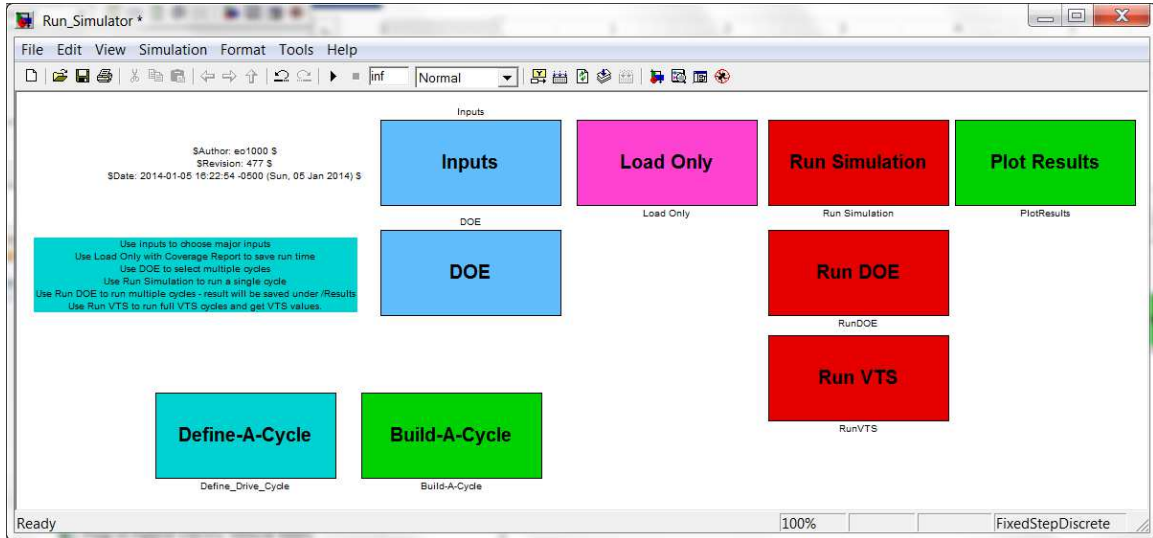
Figure 2-16. WSU PTTR modeling and simulation tool Graphical User Interface (GUI).

Clicking the "Inputs" button brings up a dialog box for the user to select the desired drive cycle, SOC, and other parameters, as shown in Figure 2-17.
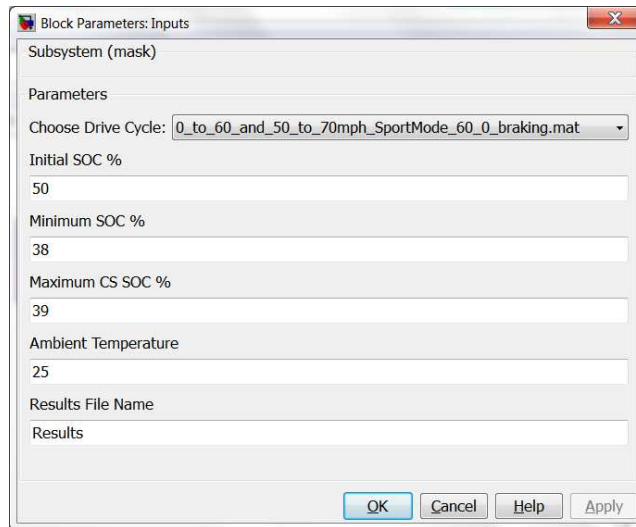
Figure 2-17. Selecting a dynamic performance drive cycle, initial SOC, and other parameters.

The WSU PTTR controls code has a "Sport Mode" to have more acceleration capability than the normal "eco" mode meant for lowest energy consumption (highest fuel economy). The Sport Mode is enabled by having the vehicle shift lever in Park and the propulsion on from a key crank, followed by 100% brake pedal, 100% accel

pedal, finally 100% brake pedal. This is achieved in the simulation by a 1 second speed pulse in the drive cycle

trace before the real speed trace has started. Figure 2-18 shows the simulation results with a Sport Mode enable

pulse at 7 seconds, the driving speed trace starting at 20 seconds for the 0-60, 50-70, and 60-0 events.
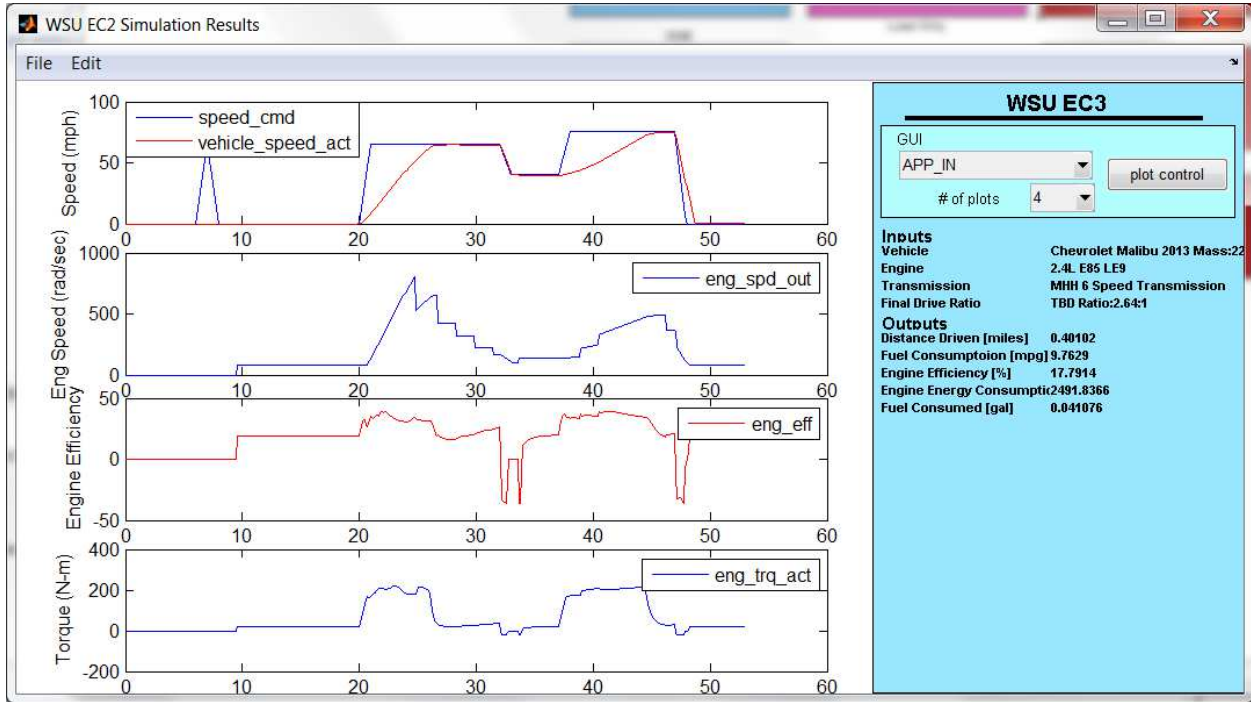
Figure 2-18. WSU PTTR simulation results for acceleration (0-60, 50-70) and braking (60-0), shows ICE efficiency below zero (not possible) during braking.

Close examination of the vehicle speed for the 0-60 mph phase shows that the vehicle could reach 65 mph,

but never does during this phase of the drive cycle. The Driver PI controller plant model has a problem with the

integral term, shown in Figure 2-19.
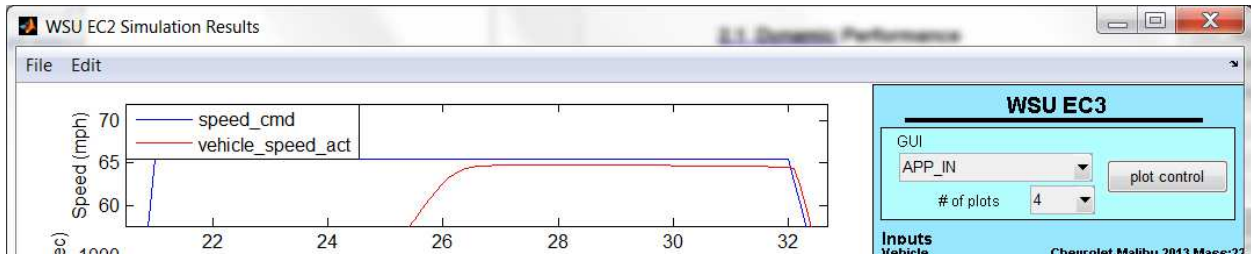
Figure 2-19. WSU PTTR simulation results show Driver model error for acceleration.

Close examination of the vehicle speed at the end, for the 60-0 braking distance phase shows that the vehicle never comes to a stop. Again the Driver PI controller plant model has a problem with the integral term, shown in Figure 2-20.
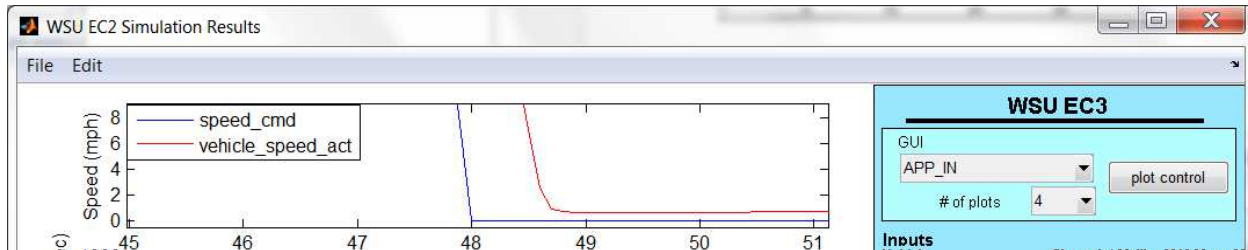
Figure 2-20. WSU PTTR simulation results show Driver model error for braking.

2.5. Energy Consumption

The energy consumption for the WSU PTTR PHEV included a mobile SEMTECH emissions instrumented trailer towed by the team's vehicle and the competition used the following metrics:

1. Total Vehicle Range (ESS + Fuel Tank)

2. Charge Depletion (CD) Range

3. CD Fuel Consumption

4. Charge Sustaining (CS) Fuel Consumption

5. Utility Factor (UF)-Weighted Fuel Energy Consumption

6. UF-Weighted AC Electric Energy consumption

7. UF-Weighted Total Energy Consumption

8. UF-Weighted WTW Petroleum Energy Use

9. UF-Weighted WTW GHG Emissions

10. Tailpipe Criteria Emissions *(not simulated, not a VTS requirement)*

Table 2-2 shows the Emissions & Energy Consumption (E&EC) comparison of the stock vehicle, the actual experimental data, and the WSU PTTR simulation results. The AC charging efficiency was updated from 87% (first EcoCAR competition population samples) to 73% for the WSU PTTR actual measured efficiency during competition.

Table 2-2. WSU PTTR simulation results for E&EC compared to experimental data.

EcoCAR 2 VTS - Emissions & Energy Consumption **"On-Road Competition"** Drive Cycle **with SEMTECH instumentation trailer**	Production 2013 Chevy Malibu (eAssist Hybrid) Experimental Data	WSU PTTR Y3 E85 Experimental Data	WSU PTTR Y3 E85 Simulation Prediction
Total Vehicle Range CD+CS (59.8 L [15.8 gal] stock tank, PTTR Y3 tank 34.2 L [9.04 gal])	606 km @ 59.8 L 383 km @ 37.9 L	243.3 km @ 34.2 L 151.2 mi @ 9.04 gal	363.5 km [225.9 mi] **(49% error)**
Charge-Depleting (CD) Range	N/A	48.7 km [30.3 mi]	54.1km [33.6 mi] **(11% error)**
Charge-Depleting (CD) Fuel Consumption	N/A	0	0
Charge-Sustaining (CS) Fuel Consumption	9.87 lge/100km	13.7 lge/100km	7.86 lge/100 km **(43% error)**
UF-Weighted Fuel Energy Consumption	9.87 lge/100km [842 Wh/km]	7.47lge/100km [665 Wh/km]	3.99 lge/100km **(47%** [356 Wh/km] **error)**
UF-Weighted AC Electric Energy Consumption	N/A	182 Wh/km	166 Wh/km*** **(9% error)**
UF-Weighted Total Energy Consumption	842 Wh/km	848 Wh/km	522 Wh/km **(38% error)**
UF-Weighted WTW Petroleum Energy (PE) Use	829 Wh PE/km	216 Wh PE/km	118 Wh PE/km **(45% error)**
UF-Weighted WTW GHG Emissions	279 g GHG/km	351 g GHG/km	201 g GHG/km **(43% error)**

*** Includes 73% actual efficiency measured for WSU PTTR charging system and battery for grid AC electricity

To run the WSU PTTR modeling and simulation tool for the E&EC drive cycle, clicking the "Inputs" button brings up a dialog box to select the desired E&EC drive cycle, and other parameters, as shown in Figure 2-21.
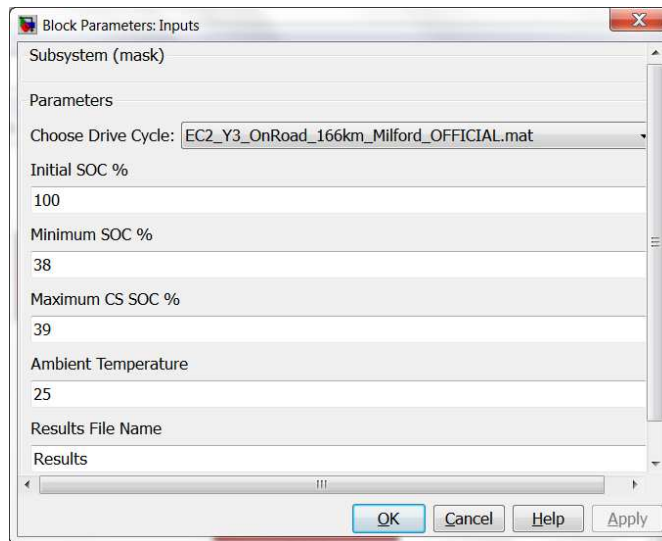
Figure 2-21. Selecting an E&EC drive cycle, initial SOC, and other parameters.

The Y3 On Road Competition Milford E&EC drive cycle contains 10 sections, shown in Figure 2-22:

- Section 1 – To Track (from garage to oval test track)

- Sections 2,3,4 – City Highway periods on the oval track, repeated 3 times (3 of 7 periods), designated by the red rectangles

- Section 5 – A vehicle off soak time of 18 minutes

- Sections 6,7,8,9 – City Highway periods on the oval track, repeated 4 times (4 of 7 periods), designated by the red rectangles

- Section 10 – From Track (from oval test track back to garage)
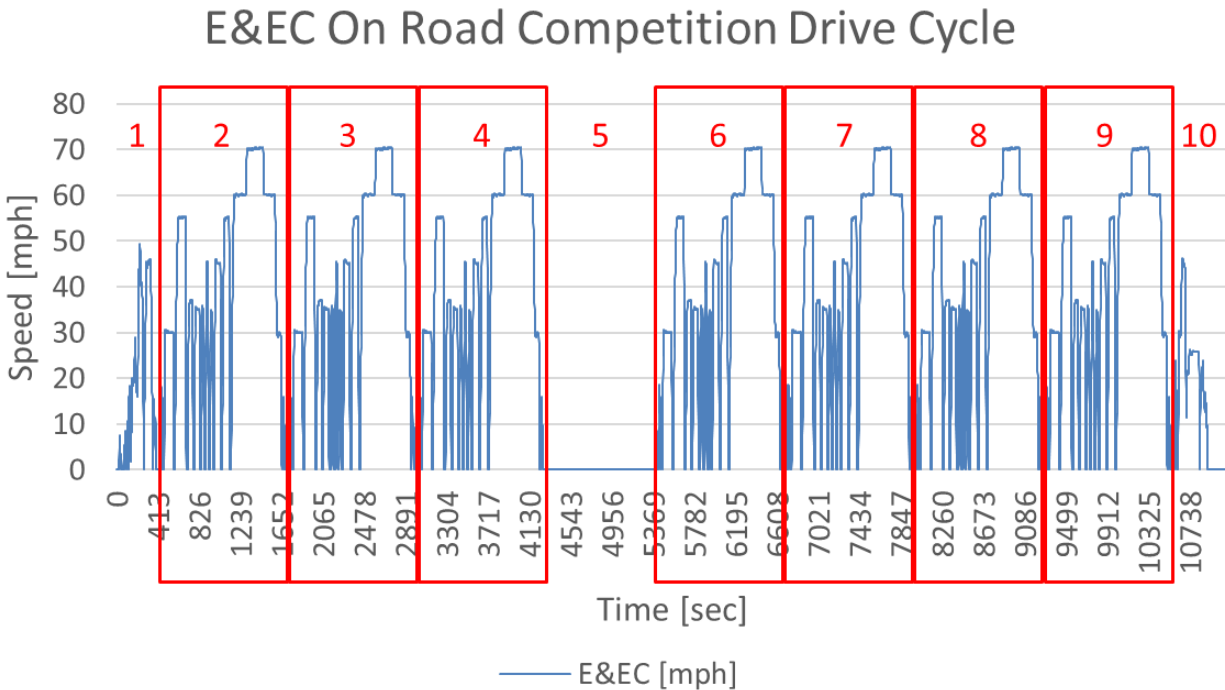
Figure 2-22. Emissions & Energy Consumption 103.7 mile drive cycle with 7 City Highway periods.

The Y3 On Road Competition Milford E&EC drive cycle was loaded into the WSU PTTR modeling and simulation tool and run with the inverter fault at the same time as when the team actually experienced it on the test track to produce the simulation results used for comparison in Table 2-2. The inverter fault in experimental data is shown in Figure 2-23 and the inverter fault in simulation results is shown in Figure 2-24.

- Inverter fault occurs at 7922 seconds into the E&EC drive cycle, during the 5th City Highway period out of 7 City Highway periods

- CD mode transitions to CS mode at:

  o 2986 seconds in experimental data at 20% SOC of the ESS (right after 2nd City Highway period ends)

  o 3773 seconds in WSU PTTR simulation at 37% SOC of the ESS (in the middle of the 3rd City Highway period)

- Distance driven for 103.7 mile E&EC drive cycle:

  o 101.5 miles driven in WSU PTTR simulation

    - 2.1% error distance driven from E&EC cycle

    - 1.2% error distance driven from experimental data

  o 102.7 miles driven in experimental data

    - 1.0% error distance driven from E&EC cycle
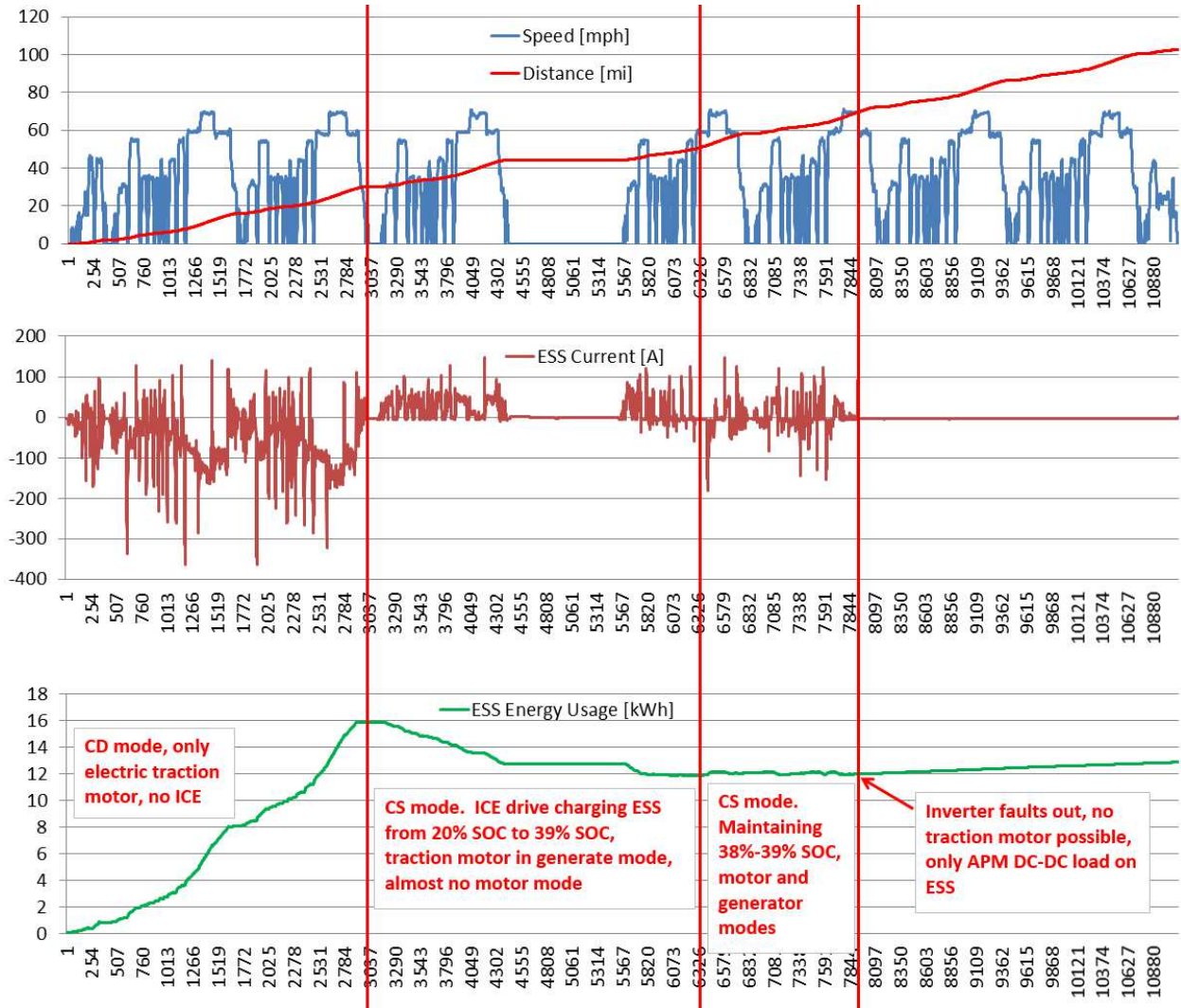
Figure 2-23. Experimental data for Emissions & Energy Consumption with Inverter Fault.

During the CD mode of electric only driving, 15.85 kWh of energy was discharged out of the ESS by the vehicle pulling the instrumentation trailer to drive 30.3 miles before switching to CS mode by turning the engine on. The experimental data shows an electric driving energy consumption of:

- 523.1 Wh/mi with the Instrumentation Trailer

- 434.7 Wh/mi vehicle only, no trailer (projection based on calculated road load difference)
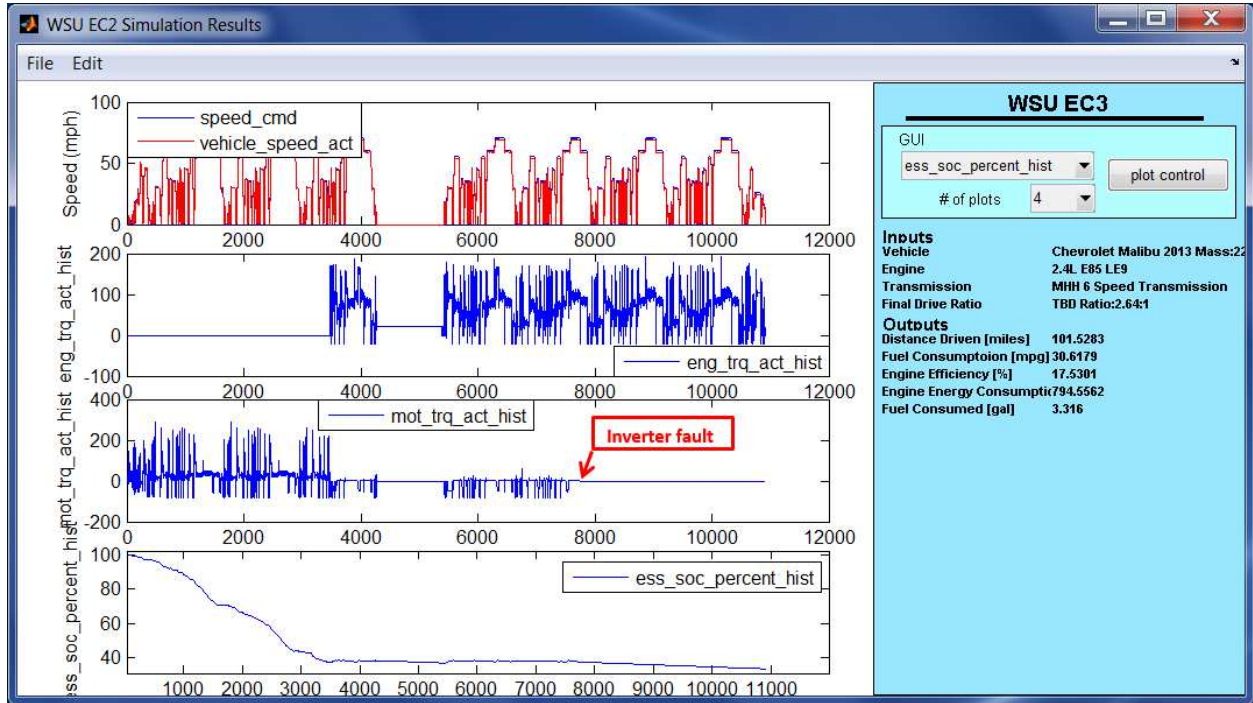
Figure 2-24. WSU PTTR simulation results for Emissions & Energy Consumption with Inverter Fault forced at same point as it occurred in the experimental data.

Figure 2-25 shows the experimental data of the E&EC drive cycle with the actual inverter fault occurrence. Zoomed in detail of the inverter fault is shown in Figures 2-26 & 2-27.
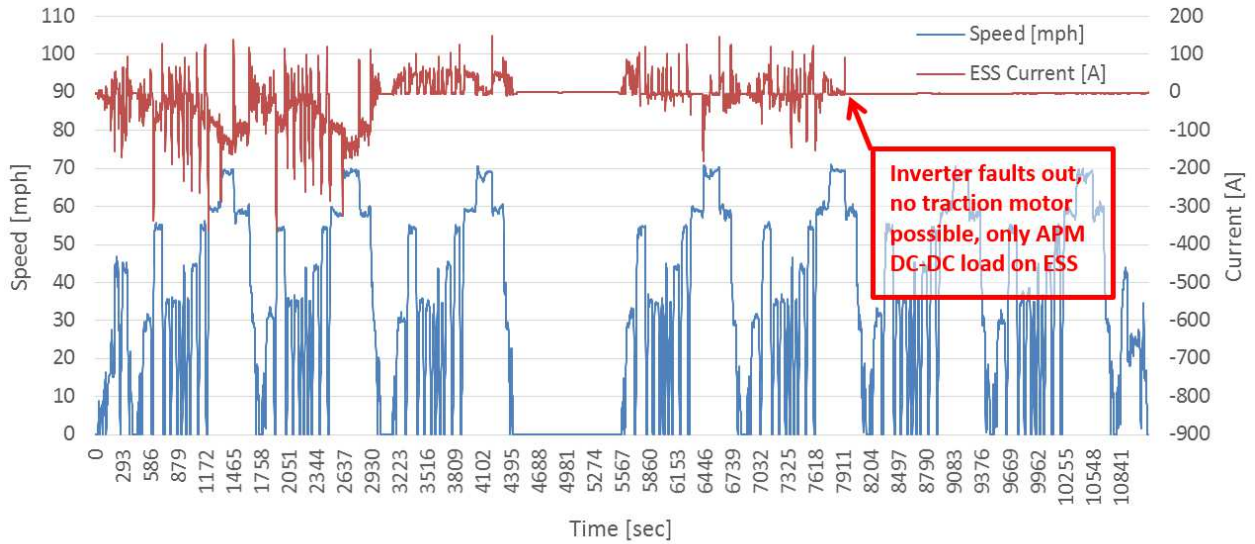
Figure 2-25. Experimental data showing the inverter fault during E&EC event.
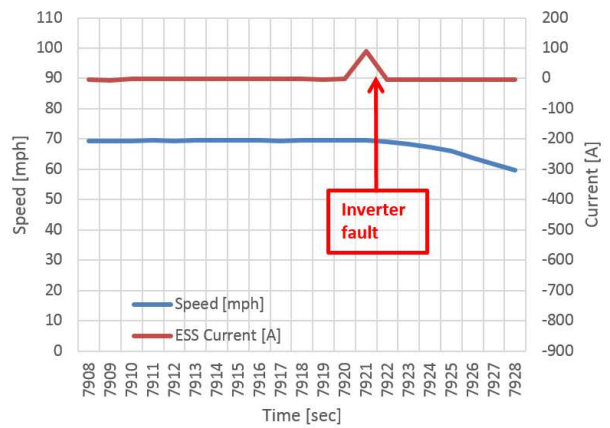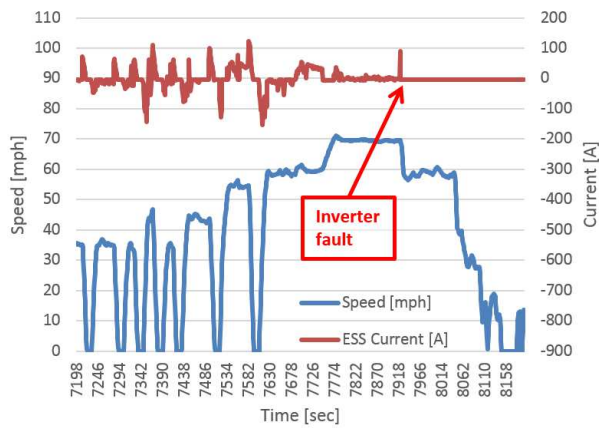
Figures 2-26 & 2-27. Experimental data showing zoomed in detail of the inverter fault during E&EC event.

WSU PTTR simulation results for the simulated vehicle speed versus E&EC drive cycle are shown in Figure 2-28.

- 10923 seconds (182 minutes) in the 103.7 mile Y3 Milford E&EC drive cycle

    o 8739 seconds (145.6 minutes) driving (80.0%)

    o 2184 seconds (36.4 minutes) stopped (20.0%)

        ▪ 1083 seconds (18 minutes) stopped with vehicle keyed off (9.9%)

- 7.5% trace missed by over 2 mph (658 out of 8739 seconds driving)
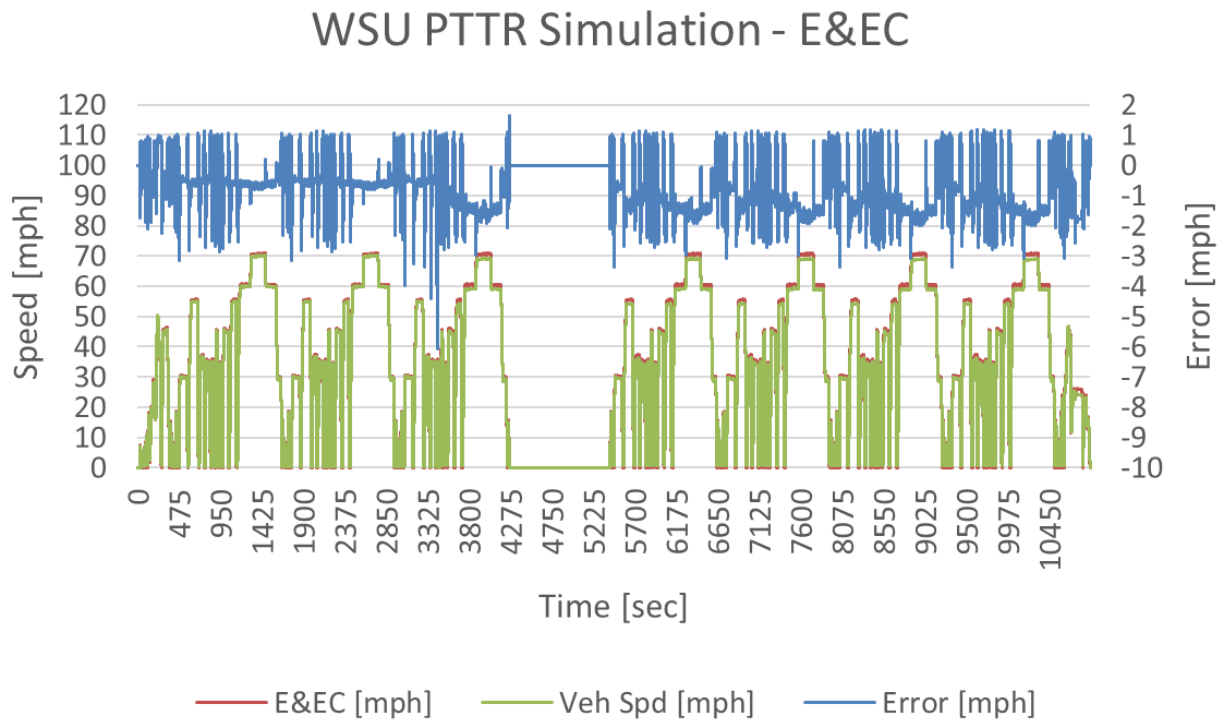
Figure 2-28. WSU PTTR simulation for E&EC for following the drive cycle.

To better visualize the simulation speed error, filtering was done by applying a rolling 200 second average across the trace results. The simulation results for CD mode (only electric traction motor), followed the drive cycle trace better than CS mode (motor plus engine), shown in Figure 2-29.

- 0.7 mph average absolute error in CD mode (without filtering)

- 1.3 mph average absolute error in CS mode (without filtering)
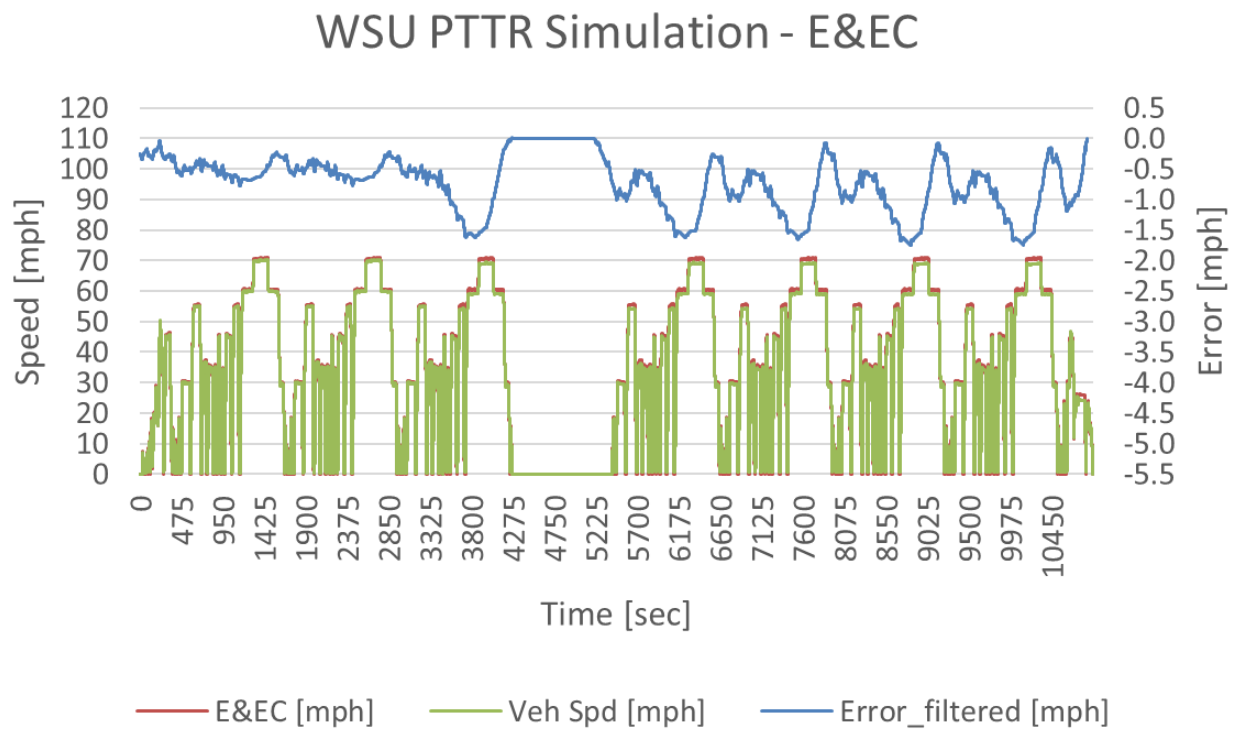
Figure 2-29. WSU PTTR simulation error filtered for E&EC for following the drive cycle.

Overlaying the E&EC experimental data with the simulation results showed that in the experimental data, the driver with a driver's aid on the oval track in the experimental data did not follow the start time of each City Highway to schedule, so some significant time shifting occurred and made it impossible to compare speed error results of the entire cycle, shown in Figure 2-30.
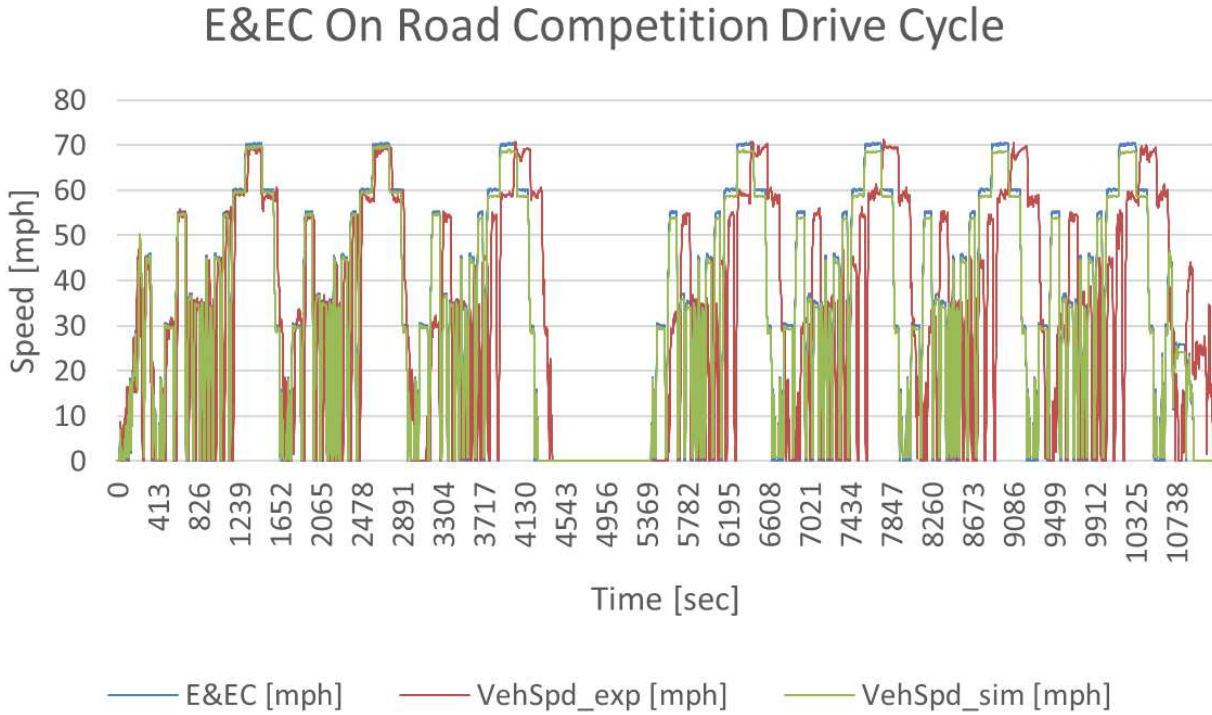
Figure 2-30. E&EC speed trace comparison between WSU PTTR simulation results and experimental data.

So time shifting for speed alignment was performed on the 1ˢᵗ City Highway period to directly compare WSU PTTR simulation results to experimental data, shown in Figure 2-31.

- Simulation Results: 7.6% trace missed by over 2 mph (99 out of 1299 seconds driving)

- Experimental Data: 46.7% trace missed by over 2 mph (606 out of 1299 seconds driving)
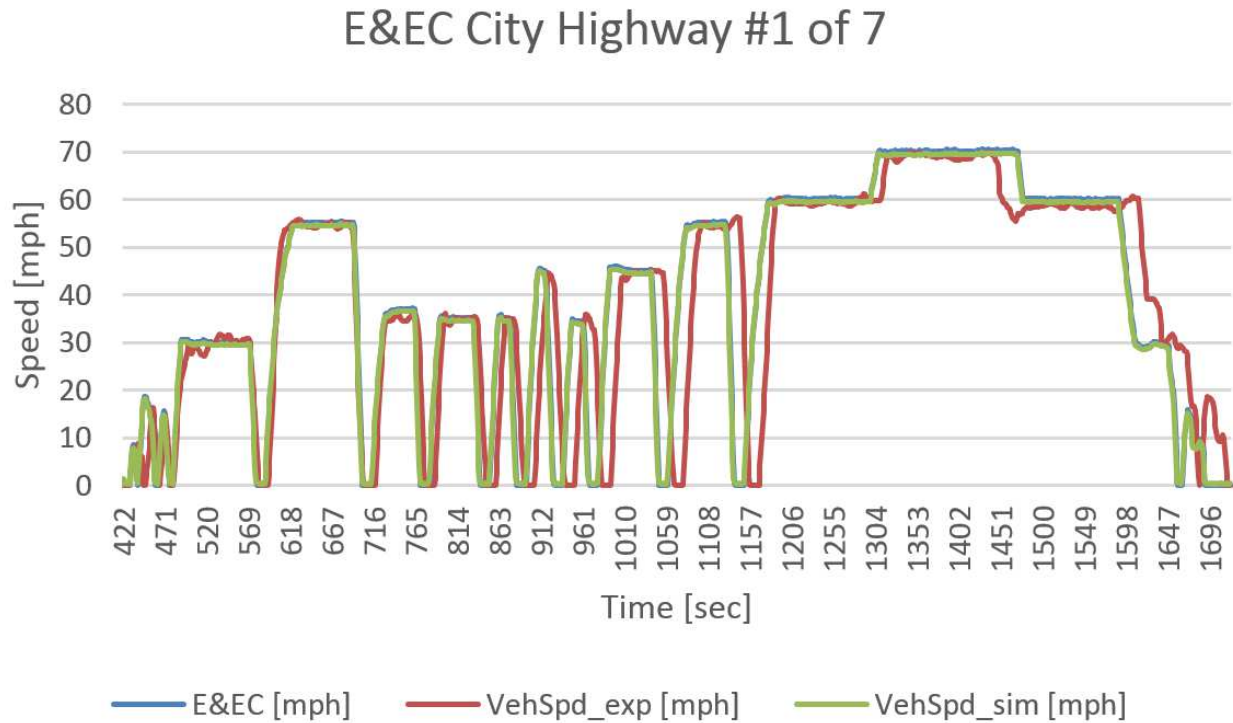
Figure 2-31. E&EC 1ˢᵗ City Highway comparison between WSU PTTR simulation and experimental data.

Even with time shifting the 7th City Highway, there was more trace miss in both the simulation results and the experimental data once the vehicle transitioned from CD mode to CS mode, shown in Figure 2-32.

- Simulation Results: 9.5% trace missed by over 2 mph (123 out of 1294 seconds driving)

- Experimental Data: 53.1% trace missed by over 2 mph (687 out of 1294 seconds driving)
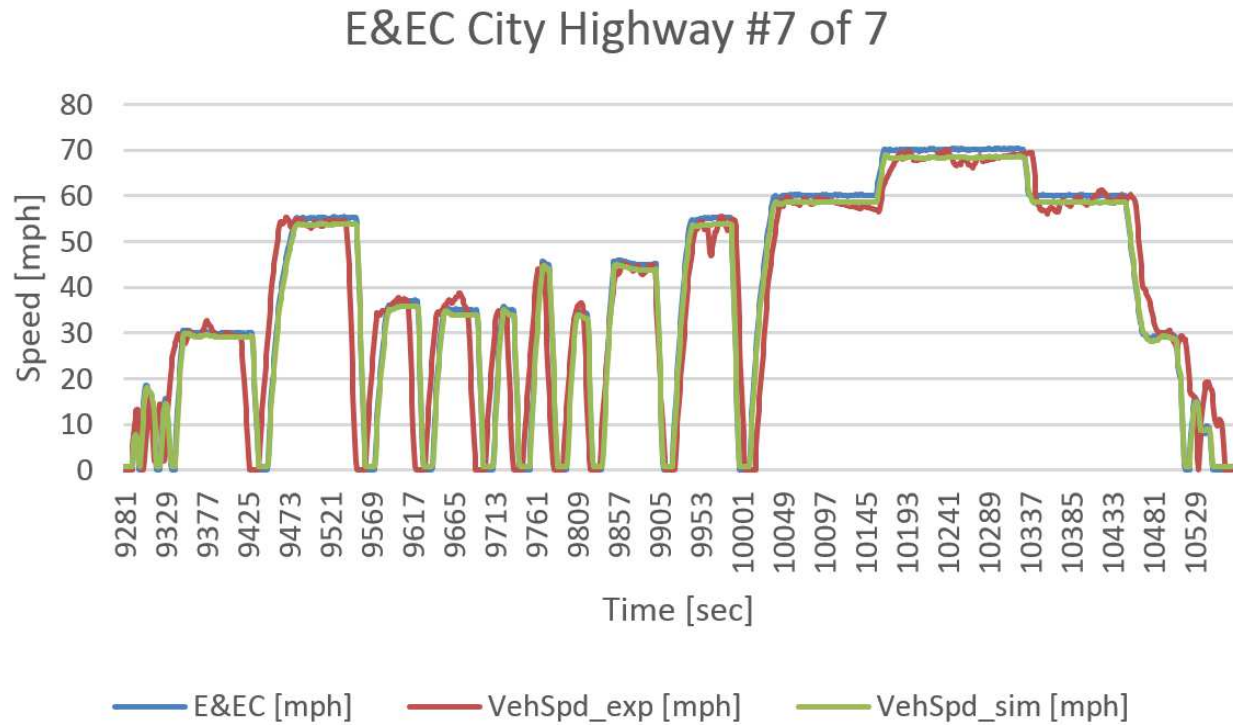
Figure 2-32. E&EC 7th City Highway comparison between WSU PTTR simulation and experimental data.

CHAPTER 3. VEHICLE PLANT MODEL ADVANCEMENT

Before plant models can be advanced from experimental data, the experimental data should be validated to another reference source, where practical/possible. After validation of experimental data to another reference source, the plant models can be validated with higher confidence when using the experimental data. The error between the simulation results and the experimental data needs to be analyzed and determined if there is problem in the equations of the model or if the problem is in the input parameter assumptions of the model.

3.1. Experimental Data Validation: Component Test Benches

The team performed bench testing for functionality of the component, troubleshooting (controller IO interfaces, Controller Area Network (CAN) messages, controls logic, wiring harness), and component characterization (determining the input parameters for the component models). The following components were bench tested:

1. Engine Controller for power up & CAN messages transmitted

2. Transmission Controller for power up & CAN messages transmitted

3. Transmission Internal Model Switch (IMS) for controller IO interfaces, controls logic, wiring harness

4. APM DC-DC Converter for power up & CAN messages transmitted

5. APM Blower Fan for controller IO interfaces, controls logic, wiring harness

6. High Voltage Air Conditioning Compressor Module (ACCM) for power up & CAN messages transmitted

7. Water Ethylene Glycol (WEG) coolant pumps for controller IO interfaces, controls logic, wiring harness

3.2. Experimental Data Validation: HIL Test Bench

The Hardware-In-the-Loop (HIL) test bench was used for IO testing between the Hybrid Control Unit (HCU) supervisory controller and the simulated vehicle. The digital IO ended up being relatively much less work than the analog IO and CAN communication. The accelerator pedal control designed ended up with the vehicle's accelerator pedal dual analog outputs wired to the HCU supervisory controller. The HCU supervisory controller then had dual analog outputs wired to the engine controller. This design was tested in the HIL bench before testing in the vehicle. Noise on the analog IO was the first time the team was dealing with "real world" signals, rather than perfectly ideal signals from SIL testing. Figure 3-1 shows the Year 1 HIL bench with the dSPACE mid-sized HIL

vehicle simulator on the far right and the MicroAutoBoxII HCU supervisory controller in the middle between the laptop and the vehicle simulator.

Figure 3-1. Year 1 HIL test bench.

Year 2 improvements to the HIL bench included relocation to a more suitable test area and a larger monitor, seen in Figure 3-2.

Figure 3-2. Year 2 HIL test bench.

Year 3 HIL additions shown in Figure 3-3 include a second laptop, second external monitor, a Vector VN8910 as 4 channel CAN gateway, and the team's Freescale based Power Driver system. Still present, but not visible in Figure 3-3: the dSPACE mid-sized HIL vehicle simulator on far left with MicroAutoBoxII HCU supervisory controller.

Figure 3-3. Year 3 HIL test bench

3.3. Experimental Data Validation: Component on Dynamometer (Dyno)

Ideally, the team would have been able to test the engine on an engine dyno and then test the engine and transmission on a transmission dyno. The same testing sequence repeated for the electric traction motor drive train: test the electric motor on a motor dyno and then test the motor and gear reducer on a transmission dyno. The team was not able to do all four cases, but was able to test the electric traction motor on a motor dyno.

In Year 3 the team gained access to a 20 kW motor dyno stand that had a UQM Technologies motor as the original Device Under Test (DUT), shown in Figure 3-4.

Figure 3-4. Motor dyno stand with 20 kW induction AC motor (painted black, on left) for dyno load. The UQM Technologies motor (on right) was the original Device Under Test (DUT).

The 20 kW motor dyno stand torque and speed capability could handle 80 Nm of torque from 0 to 2400 rpm, then torque decreasing to 42 Nm at 4500 rpm max speed [29]. The original UQM Technologies motor was removed and the team's Remy motor was installed after modifying the stand's motor adapter plate and fabricating a thin aluminum spacer plate. The mounted Remy as the new DUT is shown in Figure 3-5.
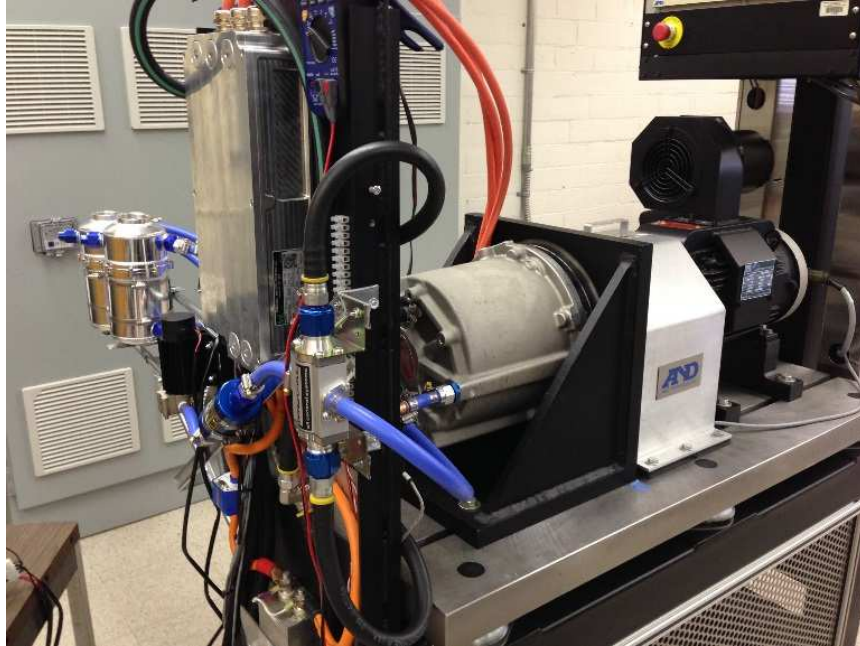
Figure 3-5. Remy motor as the new DUT (middle of the figure).

Even though the motor dyno stand capability at 20 kW was much less than the 115 kW capability of the Remy/Rinehart motor/inverter, the following motor/inverter integration work was accomplished:

1. Calibrated motor resolver delay [30]

2. Calibrated motor resolver offset with dyno spinning the freewheeling motor at 1000 rpm [30]

3. Calibrated inverter current offsets at zero current [30]

4. Motor phase cables swapped to get the correct motor behavior [31]

5. Inverter Phase C current fault discovered at startup (returned inverter unit to manufacturer for repair)

6. Debug motor lack of torque - motor type parameter corrected [31]

7. Finally, the inverter's calculated torque was typically within 10% of the dyno stand's measured torque for motoring (positive torque) and typically within 20% for generating (negative torque) at tested constant speeds of 1000 rpm and 2000 rpm, with torque ranging from -70 Nm to +70 Nm. See Figures 3-6 through 3-13.
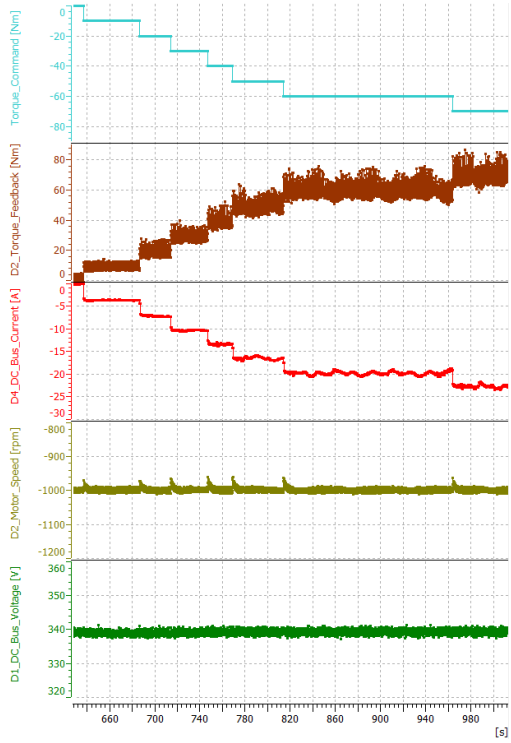
Figure 3-6. Motor Torque 0 to +70 Nm at 1000 rpm.
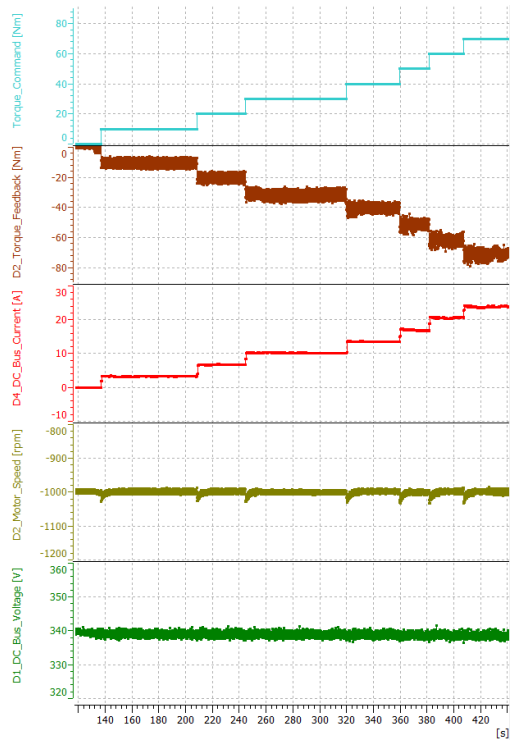
Figure 3-7. Motor Torque 0 to -70 Nm at 1000 rpm.
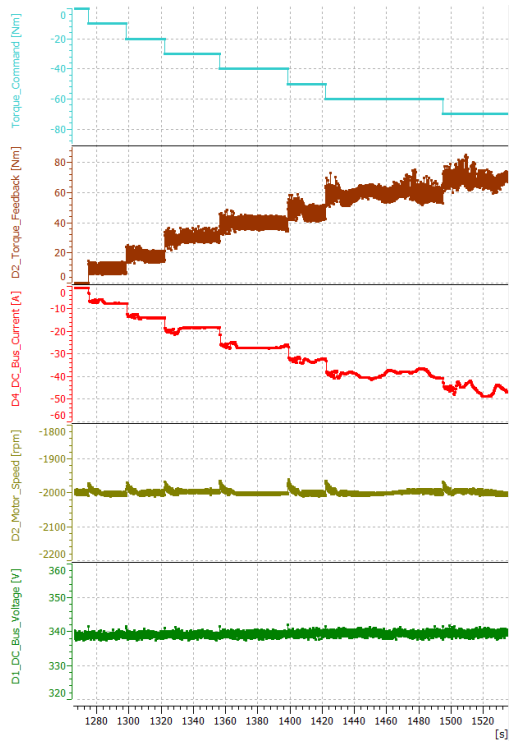
Figure 3-8. Motor Torque 0 to +70 Nm at 2000 rpm.
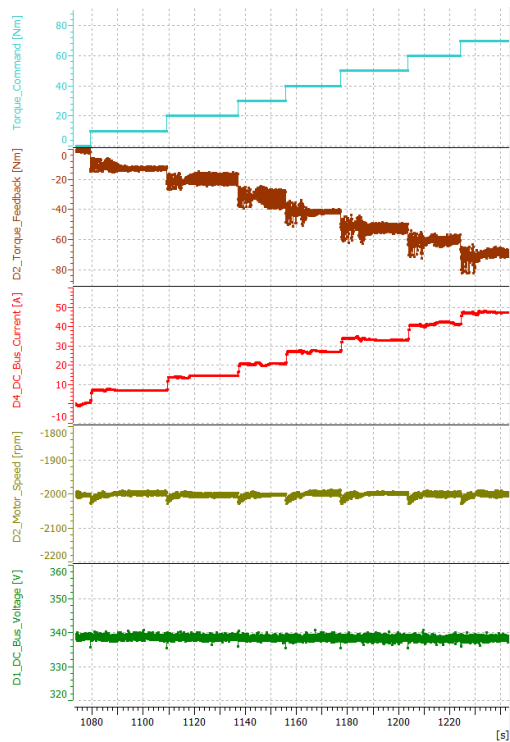
Figure 3-9. Motor Torque 0 to -70 Nm at 2000 rpm.

Dyno speed control	HCU Torque Command [Nm]													
1000 rpm	-70	-60	-50	-40	-30	-20	-10	10	20	30	40	50	60	70
MCU Trq Fdbk [Nm]	68.9	59.4	49.2	39.1	29.4	19.3	9.3	-10.9	-20.6	-31.2	-40.5	-51.1	-61.6	-70.8
Dyno Trq Fdbk [Nm]	-75.9	-65.5	-54.8	-44.4	-33.8	-22.9	-11.8	11.6	22.5	33.2	43.5	54.2	64.6	74.0
Error [%]	-10%	-10%	-11%	-14%	-15%	-19%	-27%	-6%	-9%	-6%	-7%	-6%	-5%	-5%

Figure 3-10. Motor Torque error at 1000 rpm.

Dyno speed control	HCU Torque Command [Nm]													
2000 rpm	-70	-60	-50	-40	-30	-20	-10	10	20	30	40	50	60	70
MCU Trq Fdbk [Nm]	68.1	58.8	47.8	40.0	29.6	18.2	10.0	-12.2	-20.0	-31.6	-41.7	-52.3	-61.0	-70.0
Dyno Trq Fdbk [Nm]	-75.9	-65.5	-54.8	-44.4	-33.8	-22.9	-11.8	11.6	22.5	33.2	43.5	54.2	64.6	74.0
Error [%]	-11%	-11%	-15%	-11%	-14%	-26%	-18%	5%	-13%	-5%	-4%	-4%	-6%	-6%

Figure 3-11. Motor Torque error at 2000 rpm.

Dyno speed control	HCU Torque Command [Nm]													
1000 rpm	-70	-60	-50	-40	-30	-20	-10	10	20	30	40	50	60	70
MCU DC Crnt [A]	-22.7	-19.8	-16.5	-13.4	-10.3	-7.1	-3.6	3.3	6.8	10.2	13.5	16.9	20.6	23.9
Power Elect [kW]	-7.70	-6.71	-5.59	-4.54	-3.49	-2.41	-1.22	1.12	2.31	3.46	4.58	5.73	6.98	8.10
Power Mech [kW]	-7.22	-6.22	-5.15	-4.09	-3.08	-2.02	-0.97	1.14	2.16	3.27	4.24	5.35	6.45	7.41
Efficiency [%]	94%	93%	92%	90%	88%	84%	80%	102%	94%	94%	93%	93%	92%	92%

Figure 3-12. Calculated combined motor/inverter efficiency at 1000 rpm.

Dyno speed control	HCU Torque Command [Nm]													
2000 rpm	-70	-60	-50	-40	-30	-20	-10	10	20	30	40	50	60	70
MCU DC Crnt [A]	-45.5	-38.8	-32.8	-26.8	-18.8	-13.8	-7.2	7.1	14.4	20.6	27.1	33.3	41.3	47.3
Power Elect [kW]	-15.42	-13.15	-11.12	-9.09	-6.37	-4.68	-2.44	2.41	4.88	6.98	9.19	11.29	14.00	16.03
Power Mech [kW]	-14.26	-12.32	-10.01	-8.38	-6.20	-3.81	-2.09	2.56	4.19	6.62	8.73	10.95	12.78	14.66
Efficiency [%]	92%	94%	90%	92%	97%	81%	86%	106%	86%	95%	95%	97%	91%	91%

Figure 3-13. Calculated combined motor/inverter efficiency at 2000 rpm.

The calculated combined motor/inverter efficiency exceeded 100% at 10 Nm due to measurement error of current by the inverter and/or measurement error of torque by the dyno stand torque transducer.

Motor speed reported by the inverter from the motor resolver SIN & COS signals are compared to the dyno at a fixed steady state speed. Motor speed validation shown in Figures 3-14 & 3-15.

- 3.5 rpm speed average error @ 1000 & 2000 rpm

- 0.4% speed average error @ 1000 rpm, all error is within +/- 1.5%

- 0.2% speed average error @ 2000 rpm, all error is within +/- 0.7%
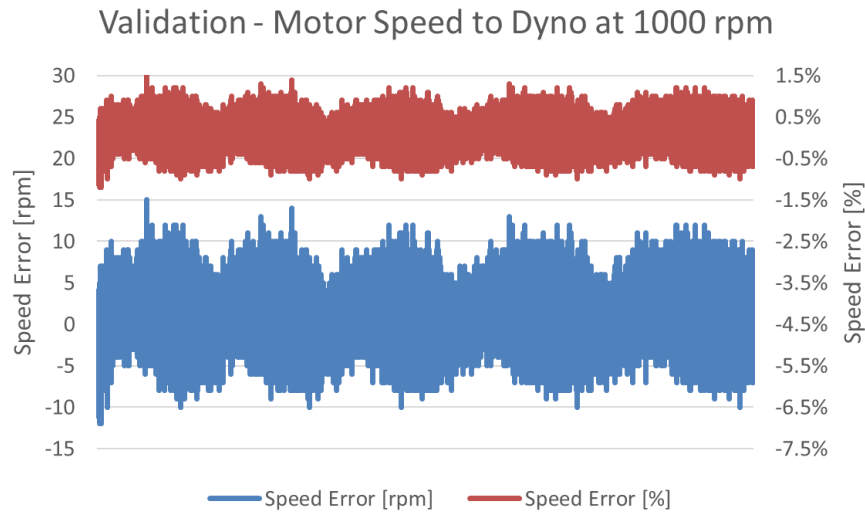
Figure 3-14. Motor speed validation to dyno speed at 1000 rpm.
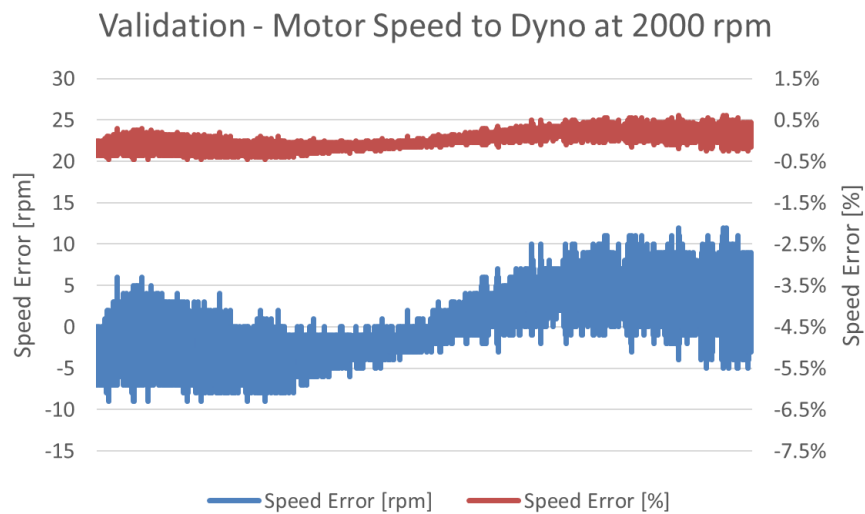
Figure 3-15. Motor speed validation to dyno speed at 2000 rpm.

The dyno stand only needed a WEG cooling loop as the original UQM Technologies motor and inverter were both WEG cooled. To add the required oil cooling loop for the Remy motor, the same components the team planned to use for the vehicle were used for the dyno stand. This allowed some initial thermal system testing in an open, stationary test environment to easily correct obvious problems. The thermal system schematic created for vehicle installation is shown in Figure 3-16, only three components were different between the stand and the vehicle: WEG radiator, WEG reservoir, and WEG pump.
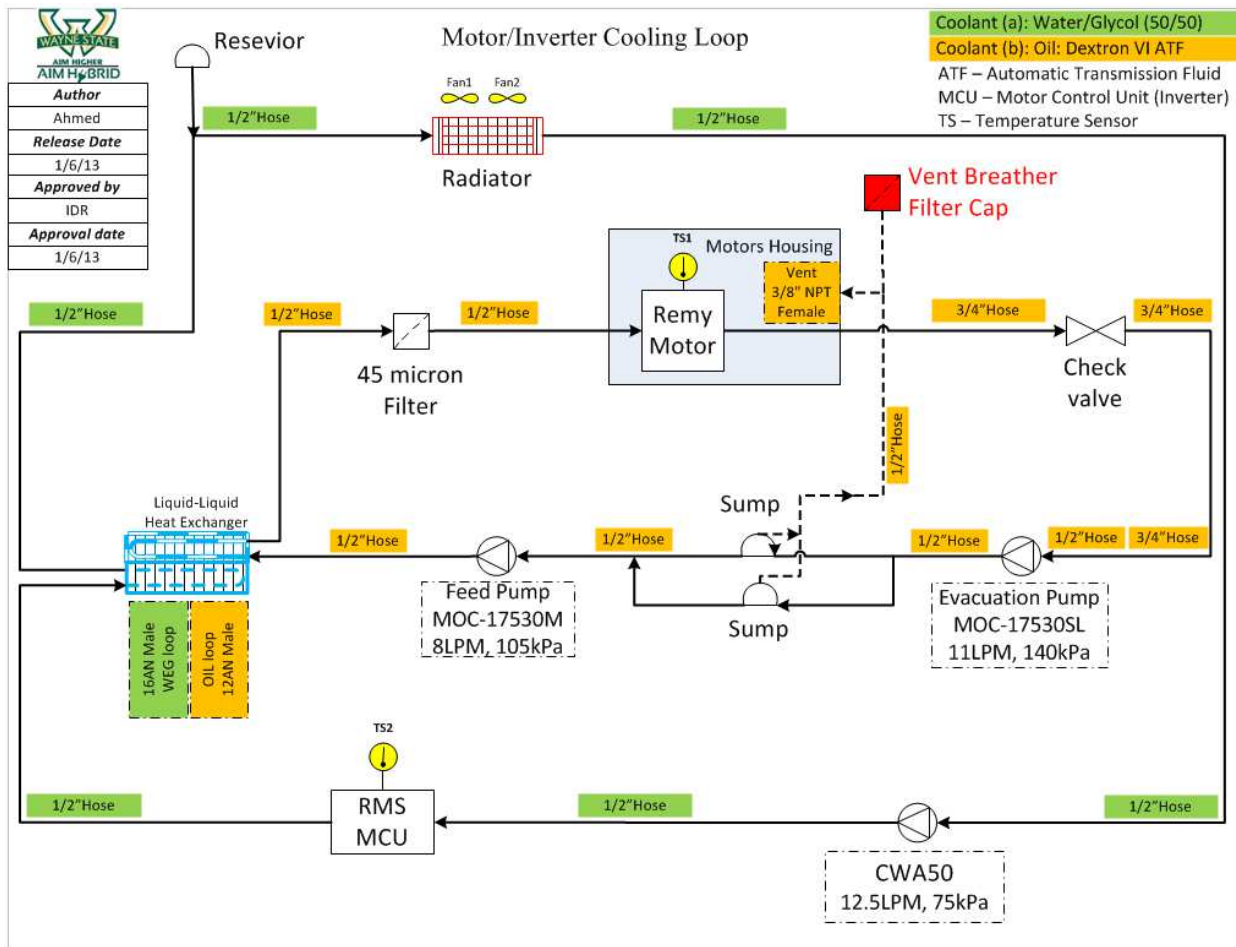
Figure 3-16. Motor and motor inverter thermal system.

To create the thermal system loops for the dyno stand specific installation arrangement, dyno stand specific mounting brackets and supports were fabricated to mount the two oil pumps, dual oil sumps, oil filter, and liquid to liquid heat exchanger (oil to WEG), shown in Figure 3-17.
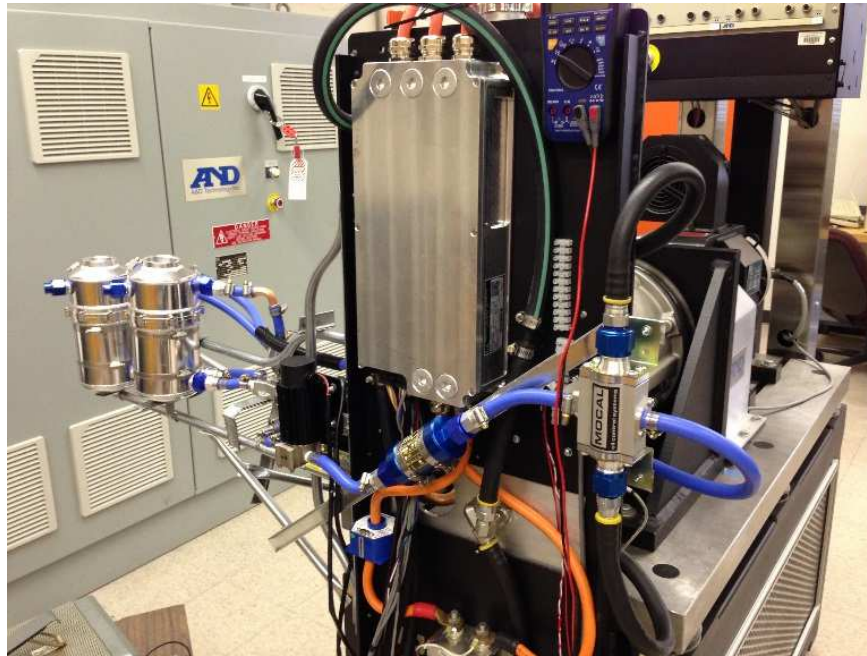
Figure 3-17. Rinehart motor inverter and the motor thermal system mounted on the dyno stand. Blue tubing is the oil loop, black rubber hose (with or without green stripe) is the WEG loop.

After filling the dyno stand thermal loops with WEG and oil, the oil scavenge and feed pumps were run at various speeds with a variable voltage laboratory DC power supply. The team's HCU supervisory controller with the power driver system was also tested for running the pumps at various speeds by varying the PWM commands. This was the first time the team tested the power driver PWM speed control of these 12 Vdc oil pumps. The oil feed pump installed on the dyno stand, running, and leaking is shown in Figure 3-18.
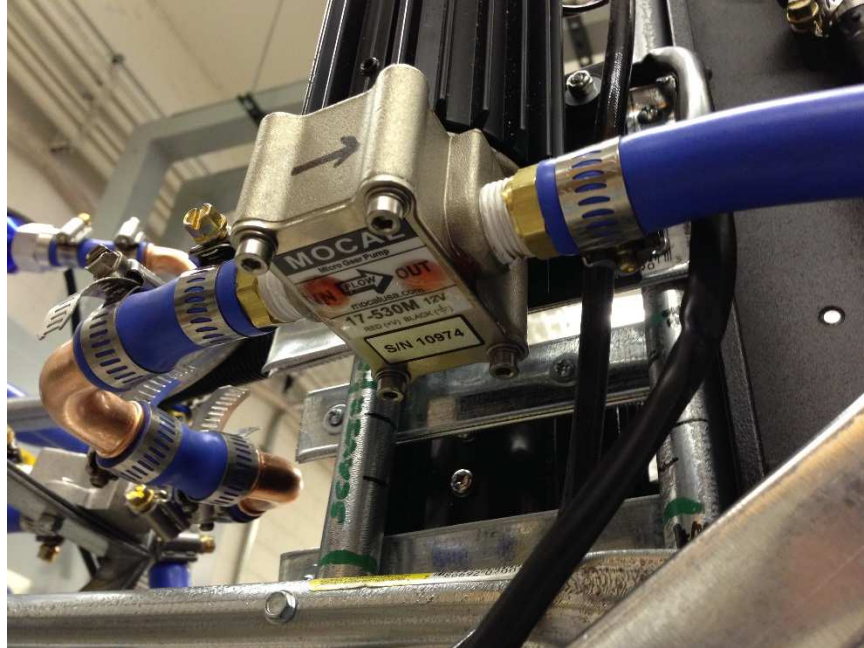
Figure 3-18. Oil feed pump on dyno stand with oil leaking from feed pump cover plate.

Oil coolant pumps were bench tested for component characterization for Accessory Load loss accounting while installed on the motor dyno as a part of the motor thermal system and lubrication loop. Both oil pumps shown new out of their packing box in Figure 3-19.

- Oil scavenge pump current draw: 1 A @ 6 Vdc   2 A @ 12 Vdc

- Oil feed pump current draw: 3 A @ 6 Vdc   6 A @ 12 Vdc

Figure 3-19. Oil feed pump on left and oil scavenge pump on right.

3.4.   Experimental Data Validation: Vehicle on Dyno

All 15 teams competing in EcoCAR 2 were able to test their own team's vehicle on a chassis dyno in Year 3 at an Emissions Test Event in the competition, about 2 months before the Year 3 Final Competition. The first supervisory controls bug discovered from chassis dyno testing was that the PRNDL shift lever position was in Drive position, but the shift lever position display to the Driver went blank intermittently, see Figure 3-20.
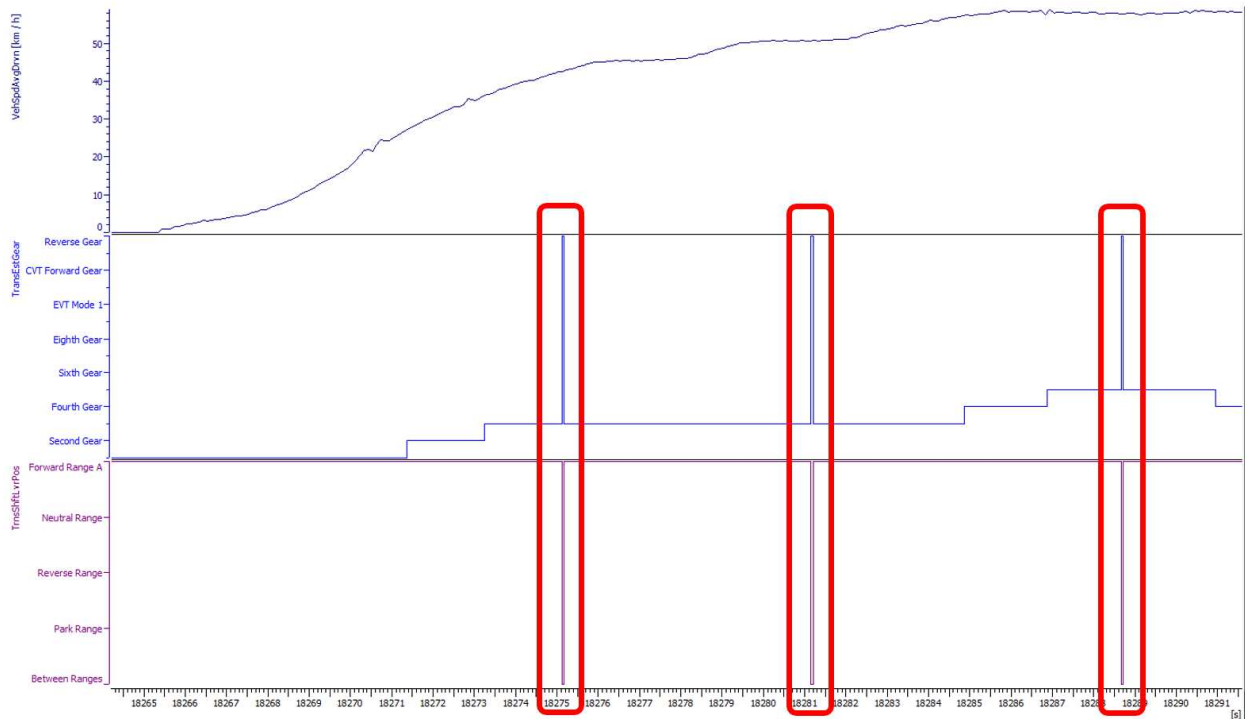
Figure 3-20. While driving on chassis dyno, a bad calibration in the supervisory code sends erroneous state to the IMS switch so the TCM reports Trans Gear which toggles to Reverse (middle trace) causing the shift lever position toggle to no gear (bottom trace) due to the position state of "Between Ranges" [32].

The team's added wiring overrides to the transmission IMS had accompanying voltage limit threshold calibrations in controller I/O for determining switch state (open/closed) and the voltage calibration for switch state had to be changed from 0.1 V to 2.5 V on a 12 V logic level, due to the initial 0.1 V calibration turning out to be unrealistic for the noise level on signals in the vehicle environment.

The second supervisory controls bug discovered from dyno testing was that the AccActPos (Accel Pedal) analog output from Supervisory controller to ECM, has excessive variation in certain situations, see Figure 3-21.
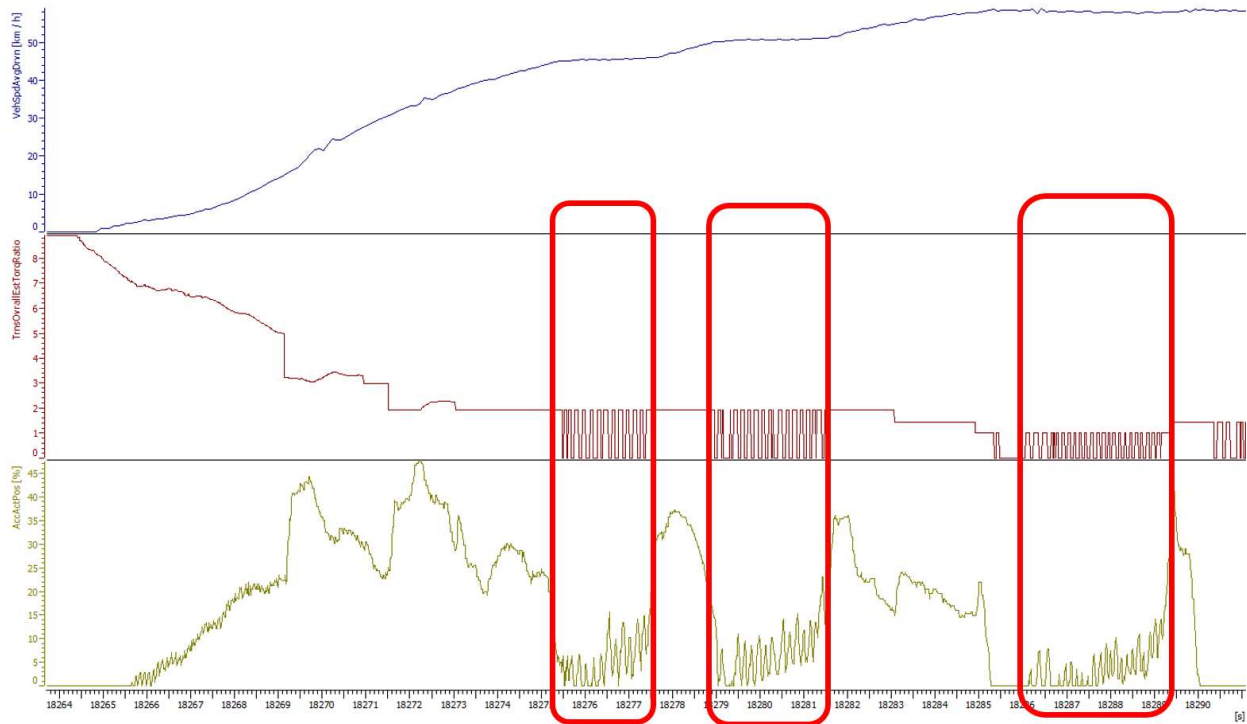
Figure 3-21. While driving on the chassis dyno, the TCM reports Trans Torque Ratio (middle trace), which sometimes toggles to a ratio of zero while actually still in gear, this toggling input to the supervisory controller cascades to a toggling HCU output torque request to the ECM (bottom trace) [32].

The team's HCU supervisory controls utilized the TCM's transmitted TrnsOvrallEstTorqRatio as an input to the team's calculation of a driver axle torque demand. The TCM sometimes sent an invalid value of "0" for torque ratio when truly in a gear in Drive ("0" is really only valid for Park/Neutral). The team had to add filtering to the TrnsOvrallEstTorqRatio input to ignore "0" when in Drive or Reverse. The technician driver at the Year 3 Emissions Test Event immediately noticed the improved vehicle drivability on a dyno retest after the fix to add filtering.

The third supervisory controls bug discovered from dyno testing was that the traction motor regen braking command was toggling on/off at low vehicle speed, around 3-4 kph, as vehicle approaches a stop, see Figure 3-22.
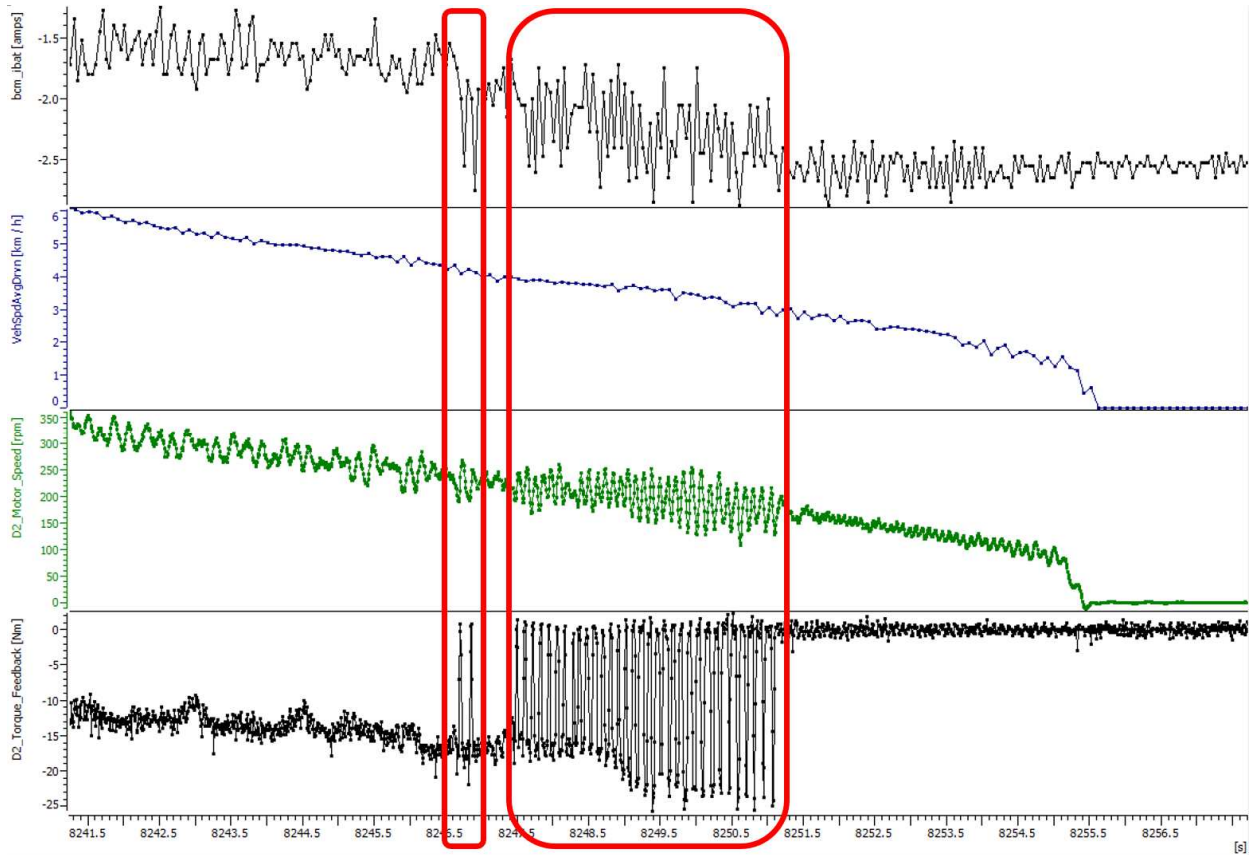
Figure 3-22. While driving on the chassis dyno, the inverter disables regen torque (4th trace) when motor speed (3rd trace) drops below 200 rpm, but without hysteresis capability in the inverter, the regen is toggling between enabled and disabled during deceleration to a stop [32].

The motor inverter has a cutoff below 200 rpm motor speed for disabling regen, but the inverter controller does not have hysteresis capability on regen, so the team added a 200 rpm hysteresis by adding code to the team's HCU supervisory controller to require 400 rpm motor speed for re-enabling regen.

3.5. Experimental Data Validation: Vehicle On Road

All 15 teams competing in EcoCAR 2 were able to test their team's vehicle on a proving ground test track at the Year 2 Final Competition in Yuma, AZ and then for the second and final time on a proving ground test track at the Year 3 Final Competition in Milford, MI. With many Electronic Control Units (ECU's) in modern vehicles, there is a tremendous amount of data for engineering analysis available from the CAN communication networks connecting all the ECU's together.

3.5.1. Vehicle Speed

The competition organizers collected GPS data during the Year 3 Final Competition's 103.7 mile "On Road Competition" drive cycle for the Emissions & Energy Consumption event which was compared against the vehicle's speed reported from CAN, shown in Figure 3-23 & 3-24.

- 0.6 mph average error, within +/- 1 mph when at steady state speeds

- 3.3% average error
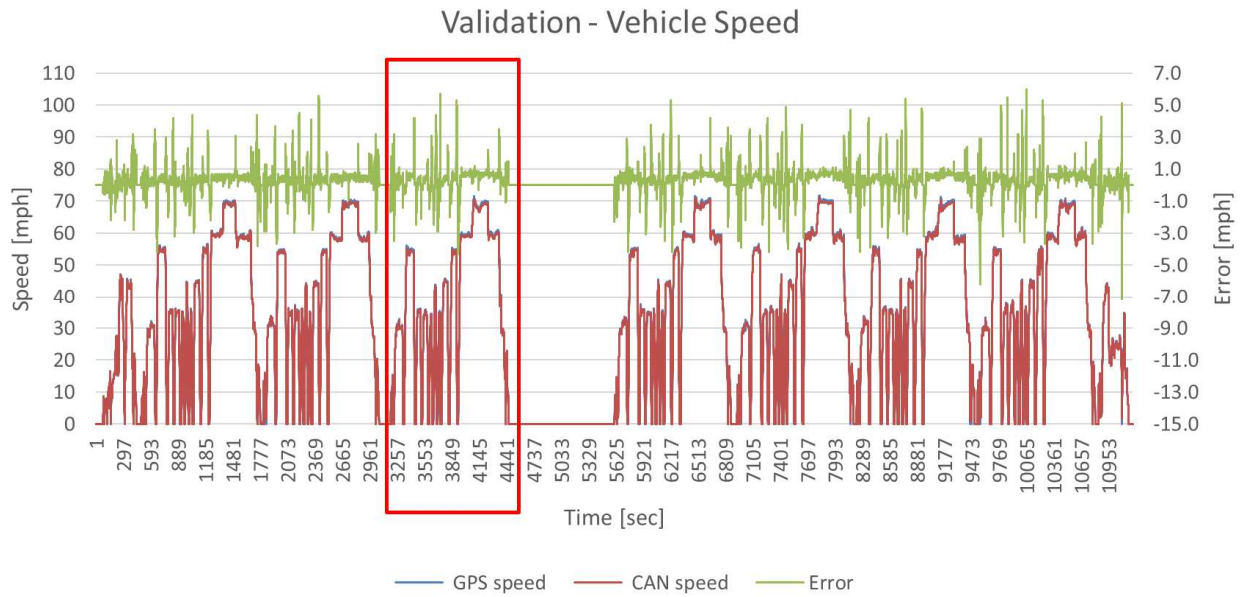
Figure 3-23. Vehicle's speed from CAN data validated by GPS measured speed from E&EC drive cycle.
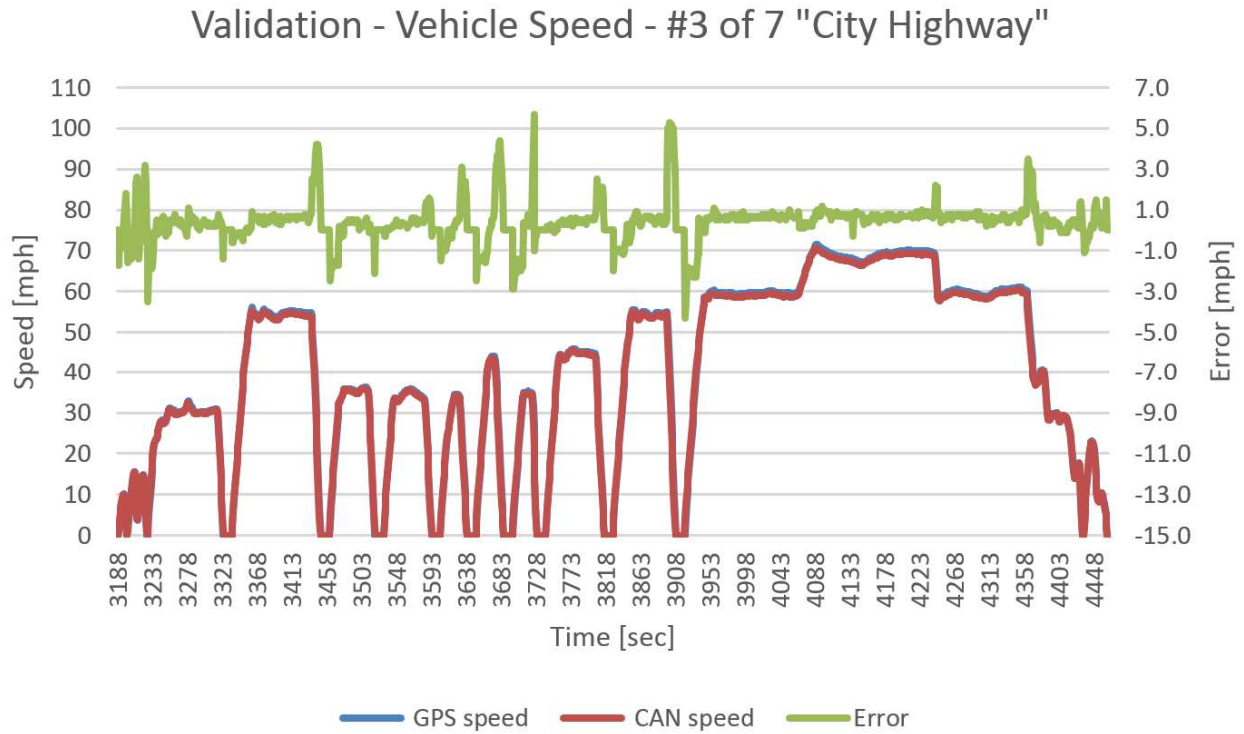
Figure 3-24. Detail view of #3 of 7 City Highway periods for validating vehicle speed.

3.5.2. Motor Speed and Torque

Validation of electric traction motor speed and torque was done only with 0-60 acceleration dynamic performance data because the detailed CAN logger data was lost from the Emissions & Energy Consumption "On Road Competition" 103.7 mile drive cycle. Motor speed validation shown in Figure 3-25.

- 5439 rpm Motor speed at 60 mph from experimental data

- 5285 rpm Motor speed at 60 mph from simulation

- 2.8% error in Motor speed at 60 mph
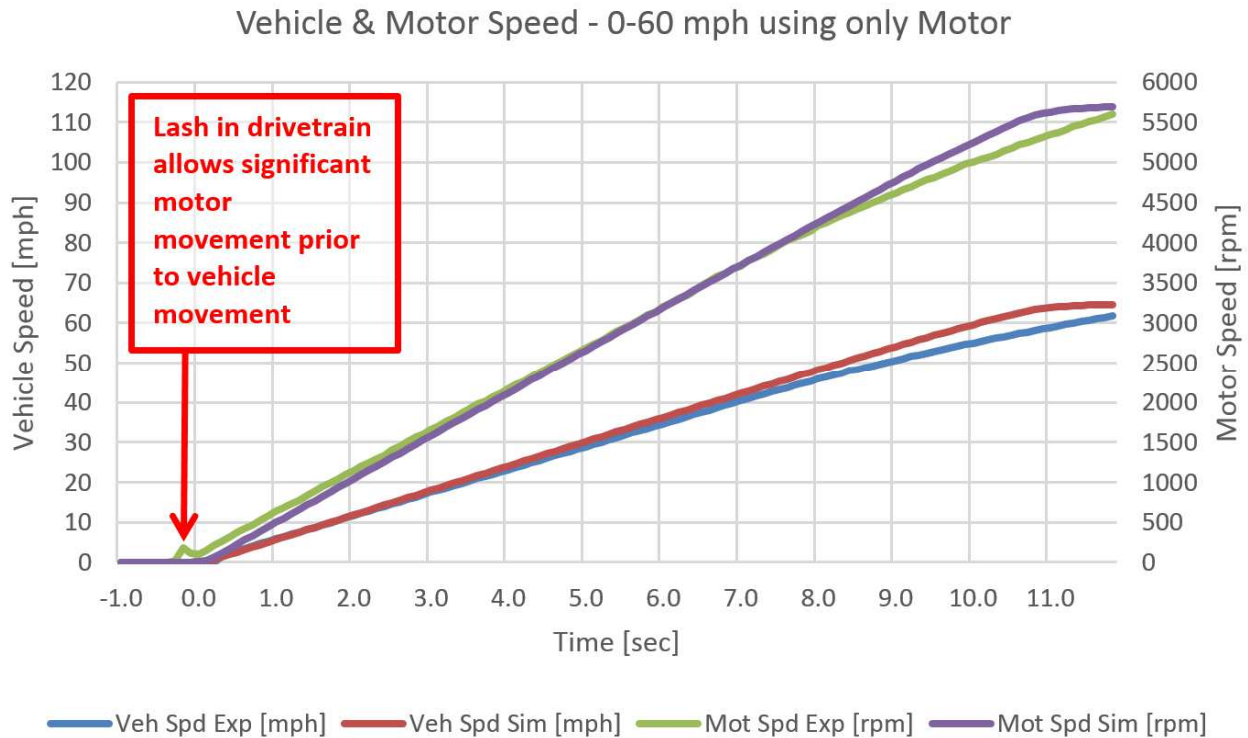
Figure 3-25. Motor speed - validation of simulation results to experimental data.

There was more lash in the drivetrain than desired which required the team to tune shudder compensation in the motor inverter to reduce NVH at low vehicle speeds. Lash sources on the RWD that contributed to motor movement without vehicle movement:

- Motor shaft to coupling

- Coupling to gear reducer pinion gear shaft

- Pinion gear to main gear in reducer

- Main gear shaft to coupling

- Coupling to differential input shaft

- Differential input shaft pinion gear to ring gear

Also, there is torsional shaft twisting, especially of the half shafts that connect the wheels to the differential output and significant tire flex under large torque loads. Drivetrain lash was not simulated, as it is a transient and not a significant factor in energy consumption/fuel economy. Motor speed to vehicle speed ratio shown in Figure 3-26.

- Ratio of 90.7 rpm to 1 mph (at 60 mph from experimental data)

- Ratio of 88.1 rpm to 1 mph (at 60 mph from simulation)

- 2.9% Error at 60 mph from simulation results to experimental data

Ratio - Motor Speed to Vehicle Speed - 0-60 mph using only Motor
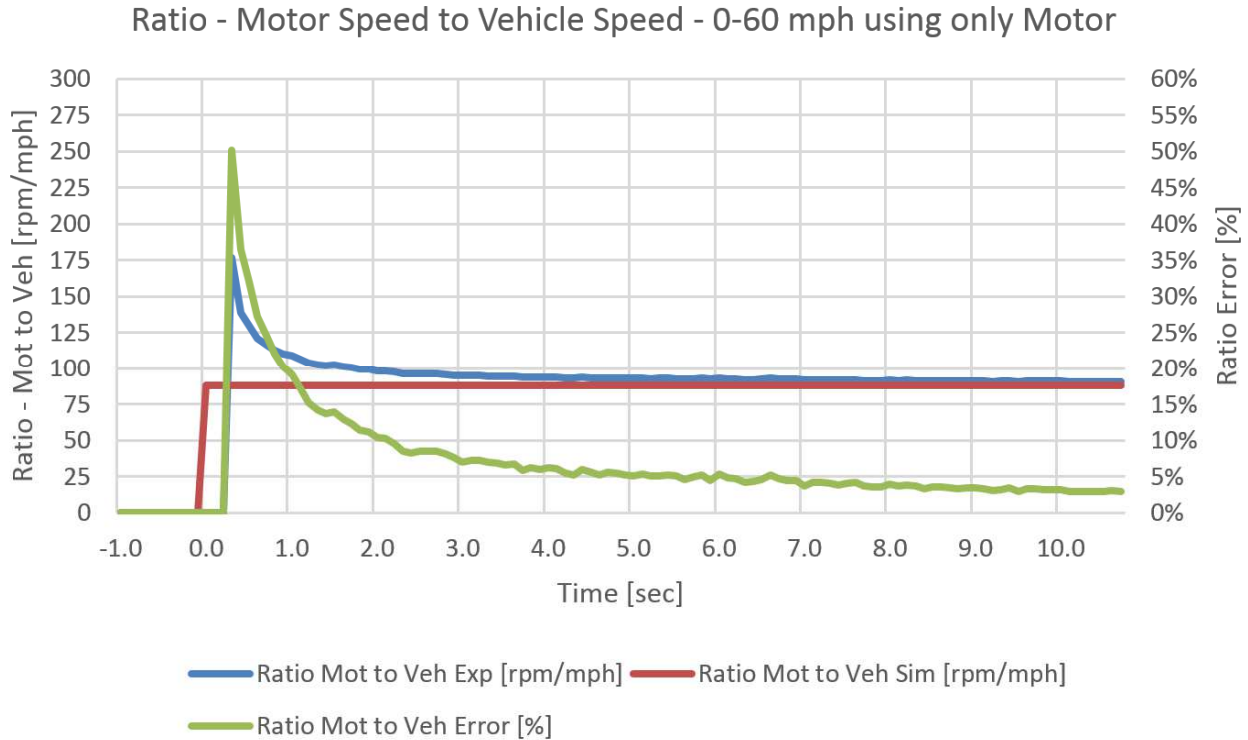
Figure 3-26. Ratio of motor speed to vehicle speed - validation of simulation results to experimental data.

Motor torque validation produced surprising results and helped explain why 0-60 mph simulation results are very different than experimental data (9.4% error in 0-60 time). The simulation's torque model had higher torques than seen in the experimental data of torque feedback reported by the motor inverter. Motor torque validation failure is shown in Figure 3-27.

- 5% - 21% Motor torque error for max peak torque

- 18% - 38% Motor torque error for max continuous torque
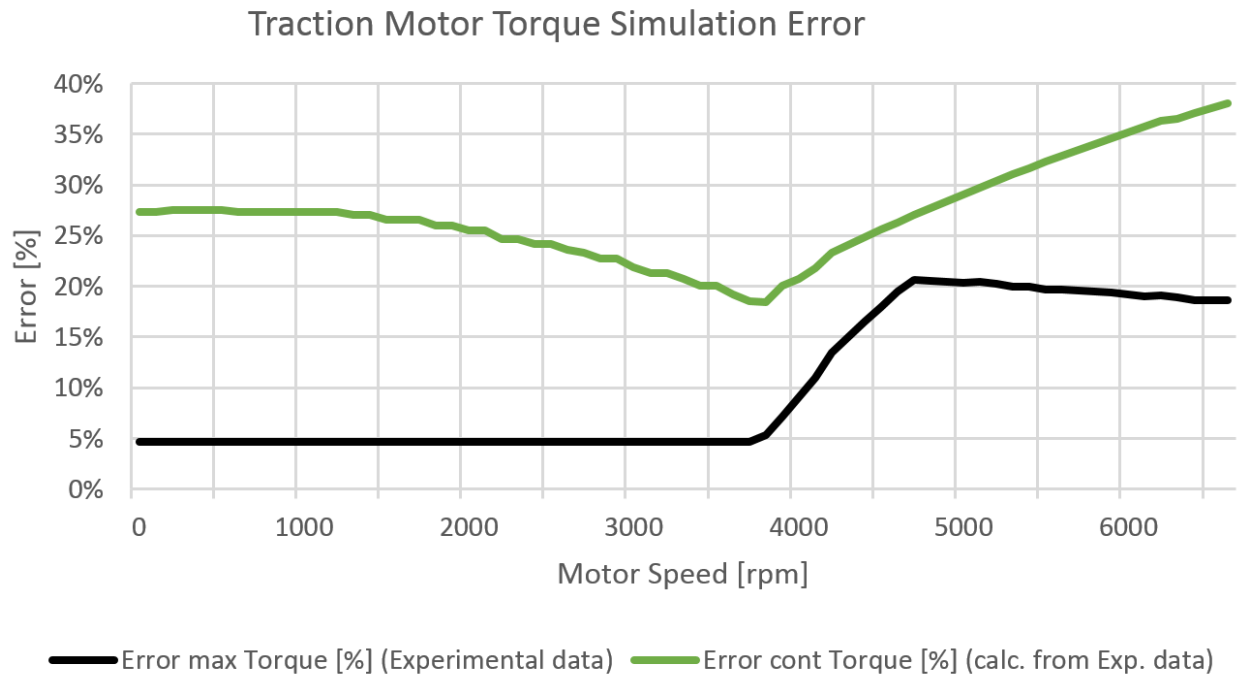
Figure 3-27. Motor torque - validation failure of simulation results to experimental data.

3.5.3. Motor Inverter Voltage and Current

Validation of electric traction motor inverter voltage and current was done with only the 0-60 acceleration dynamic performance (due to lost team's data logger detailed data from E&EC event). The experimental data for the motor inverter voltage was validated to the experimental data for the ESS, shown in Figures 3-28 & 3-29.

- Motor inverter voltage from experimental data reported over CAN appears to be an unfiltered signal (see Figure 3-28) compared to the ESS voltage, so a 21 sample moving average was used as a simple filter (see Figure 3-29)

- In Figure 3-28, the unfiltered motor inverter voltage was under 1% error to the ESS for the first half

- In Figure 3-28, the unfiltered motor inverter voltage was became 3-4% error to the ESS for the second half, as the motor mode switched from constant torque mode to constant power mode

- In Figure 3-29, the filtered motor inverter voltage was 0.2% to 0.9% error to the ESS with an average of 0.5%
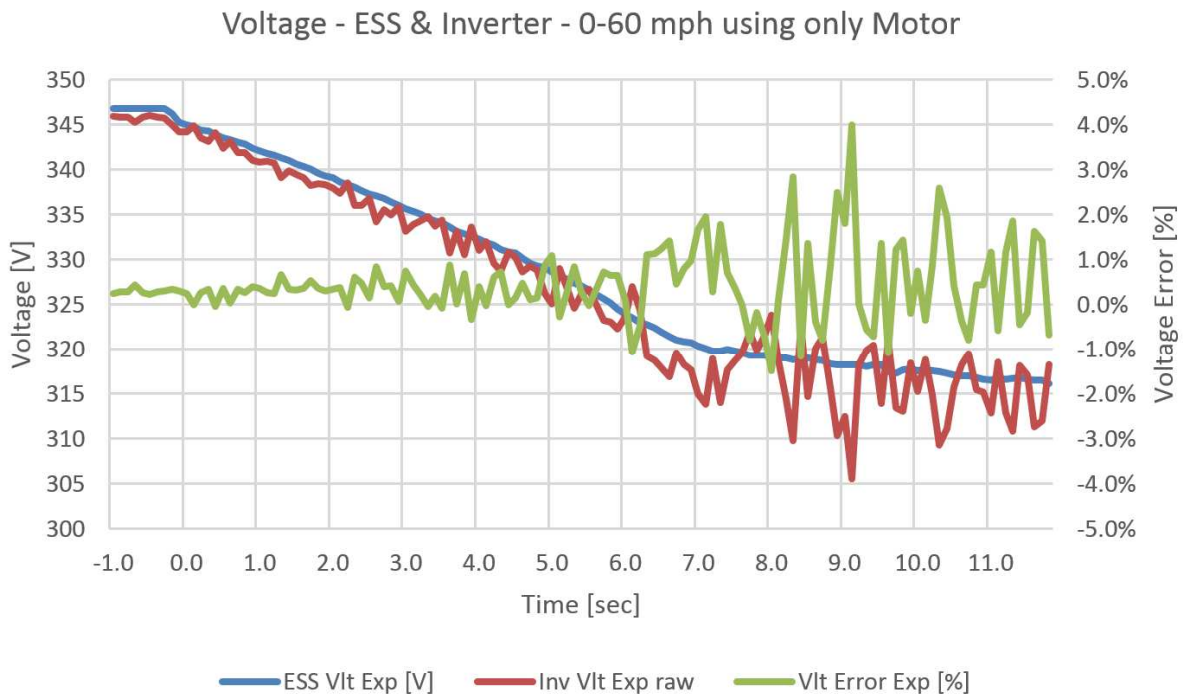
Figure 3-28. Validation between ESS voltage and Motor Inverter voltage using experimental data.
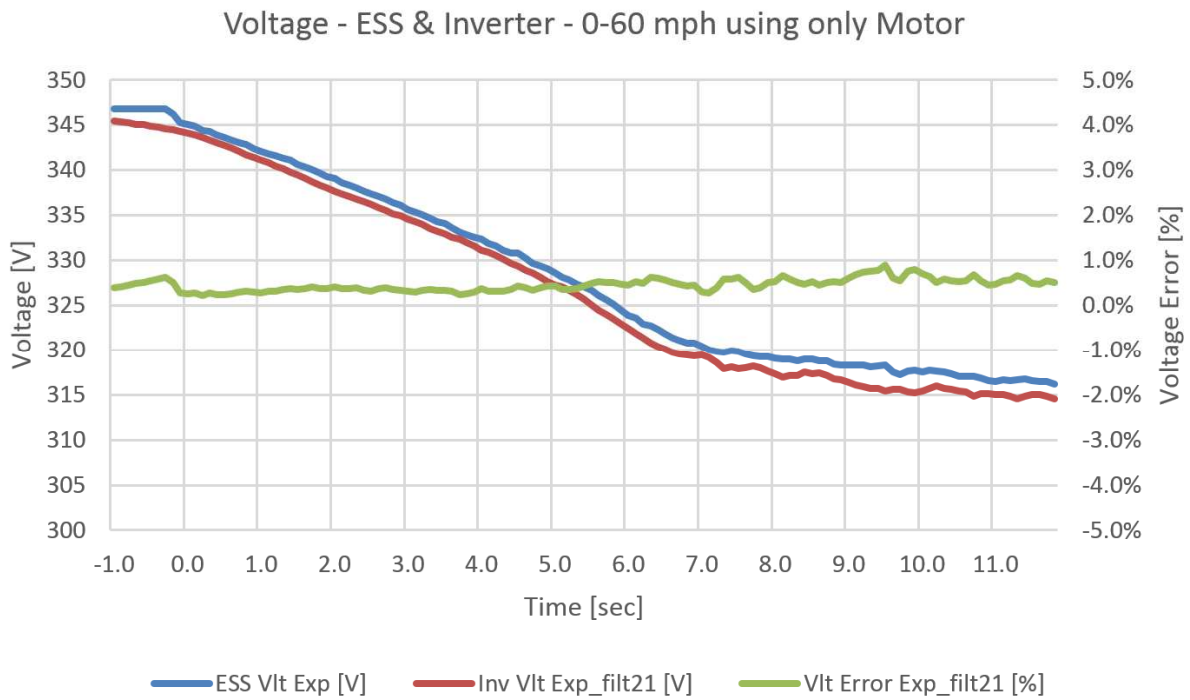
Figure 3-29. Validation between ESS voltage and Motor Inverter voltage (filtered) using experimental data.

Next, the motor inverter voltage from simulation results was validated to the experimental data with 0-60 acceleration dynamic performance, shown in Figure 3-30.

- Error ranged from -0.4% to +0.7% for simulation motor inverter voltage

- Absolute error average was 0.1% for simulation motor inverter voltage
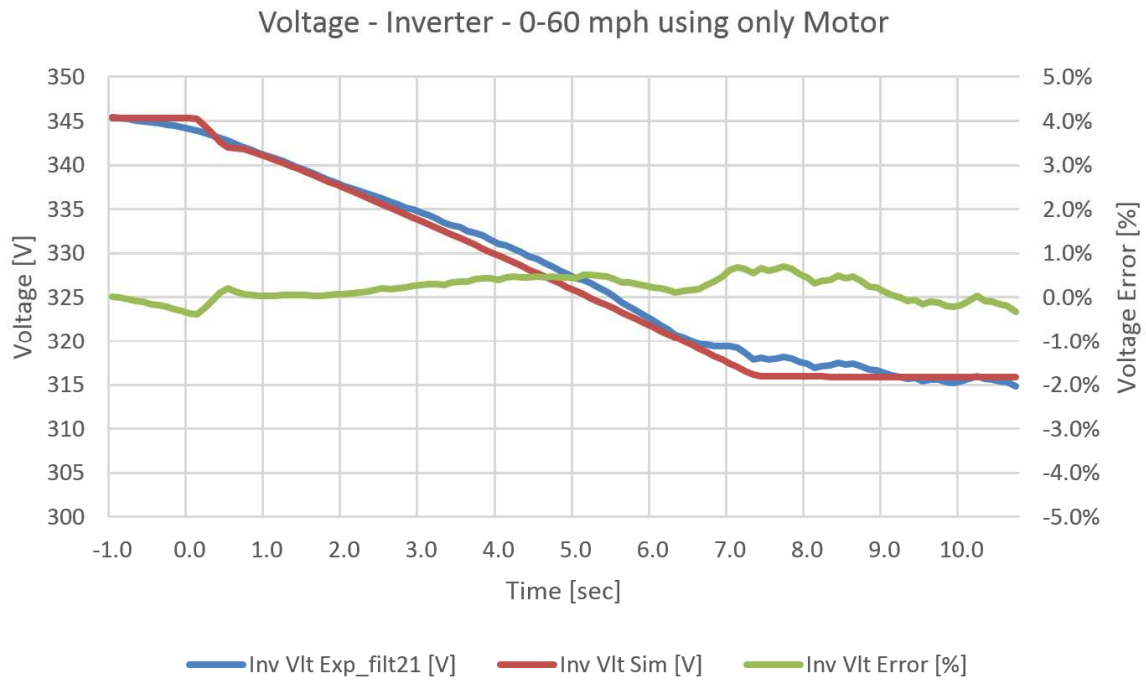
Figure 3-30. Motor Inverter voltage - validation of simulation results to experimental data.

The experimental data for the motor inverter current was validated to the experimental data for the ESS, shown in Figure 3-31.

- 100% error before 0.0 seconds because there is the additional accessory load current of 2.2 A that is only present on the ESS (this error can be ignored for validating current of motor inverter to ESS)

- 74% error at 0.0 seconds: current is flowing from ESS (33.6 A reported), through the motor inverter (8.6 A reported) and into the motor, producing motor torque causing the motor to rotate, taking up the lash of the drivetrain and the vehicle is about to start moving

- 10.7% error on average from 2.0 seconds through 12.0 seconds when motor is no longer operating at low speed (under 1000 rpm)
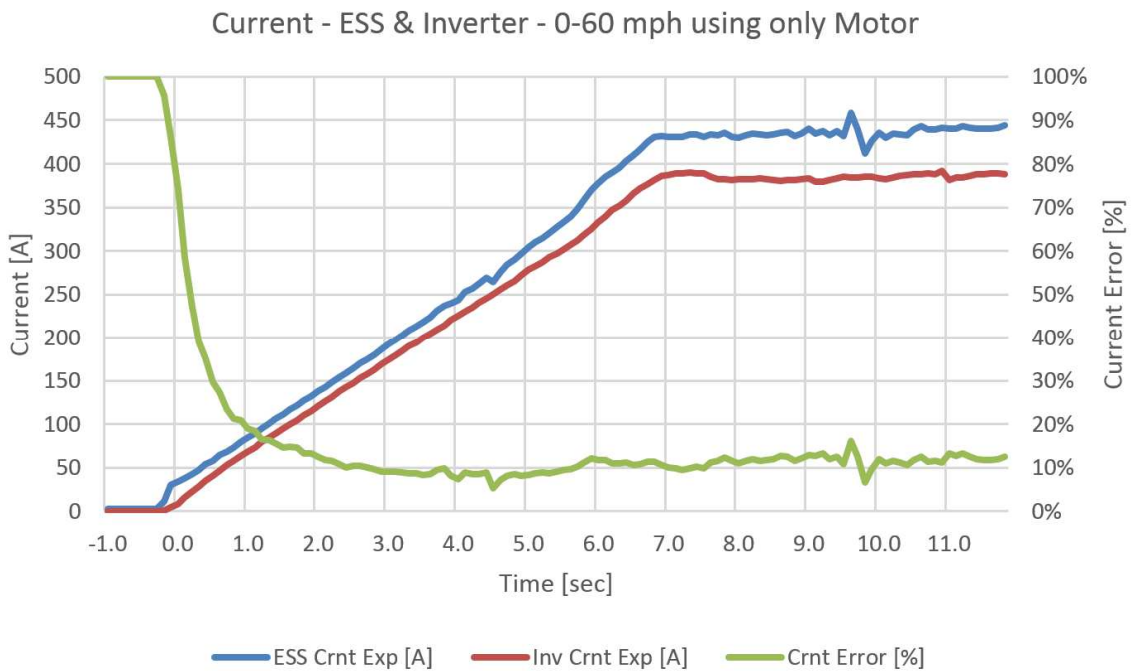
Figure 3-31. Validation between ESS current and Motor Inverter current using experimental data.

Motor inverter current from simulation results was validated to the experimental data with 0-60 acceleration dynamic performance, shown in Figure 3-32. The largest errors were due to a brief time in the initial wheel movement where the simulation motor inverter current was lagging the experimental data motor inverter current and then was leading.

- Error ranged from -25% to +100% for simulation motor inverter current

- Absolute error average was 12.3% for simulation motor inverter current
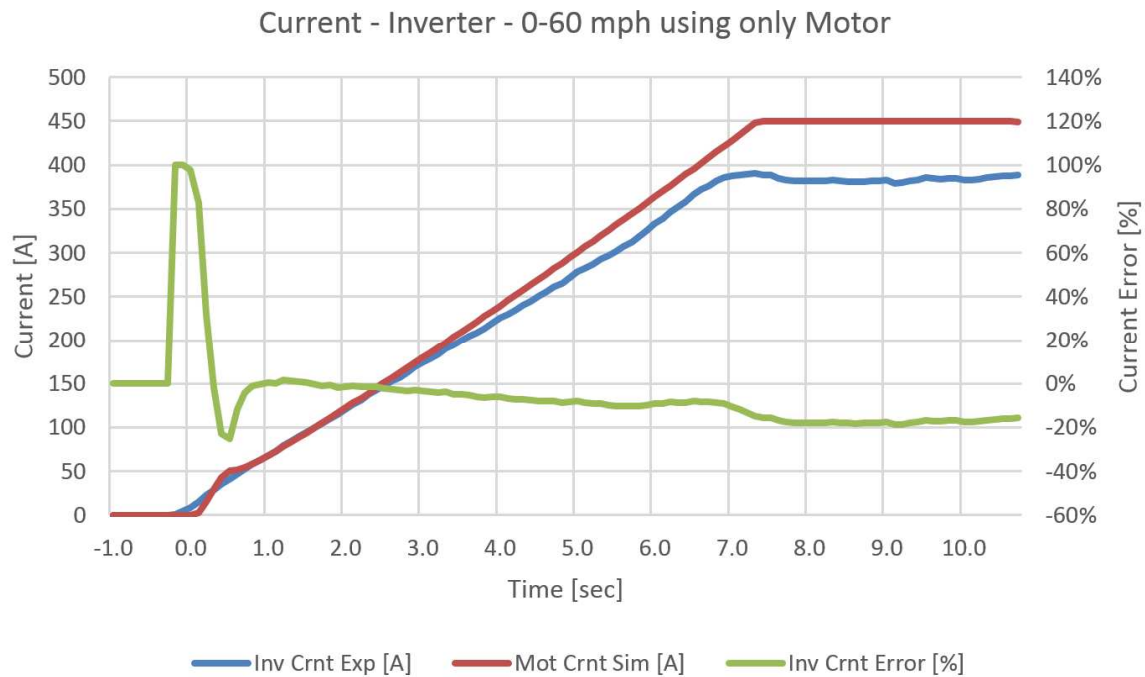
Figure 3-32. Motor Inverter voltage - validation of simulation results to experimental data.

3.5.4. ESS Voltage and Current

The ESS voltage from the simulation results was validated to the experimental data with 0-60 acceleration dynamic performance, shown in Figure 3-33.

- Error ranged from -0.1% to +1.3% for simulation ESS voltage

- Absolute error averaged 0.1% for simulation ESS voltage
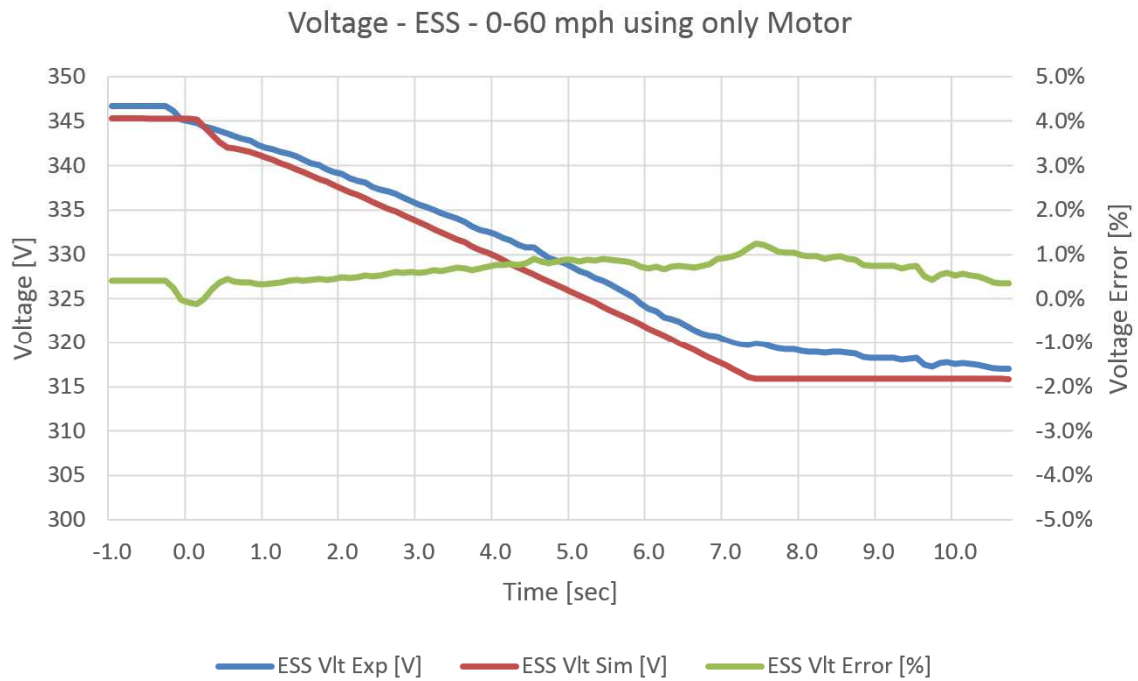
Figure 3-33. ESS voltage - validation of simulation results to experimental data.

ESS current from simulation results was validated to the experimental data with 0-60 acceleration dynamic performance, shown in Figure 3-34. The largest errors were due to a brief time in the initial wheel movement where the simulation ESS current was lagging the experimental data ESS current.

- Error ranged from -31% to +91% for simulation ESS current

- Absolute error average was 10.2% for simulation ESS current
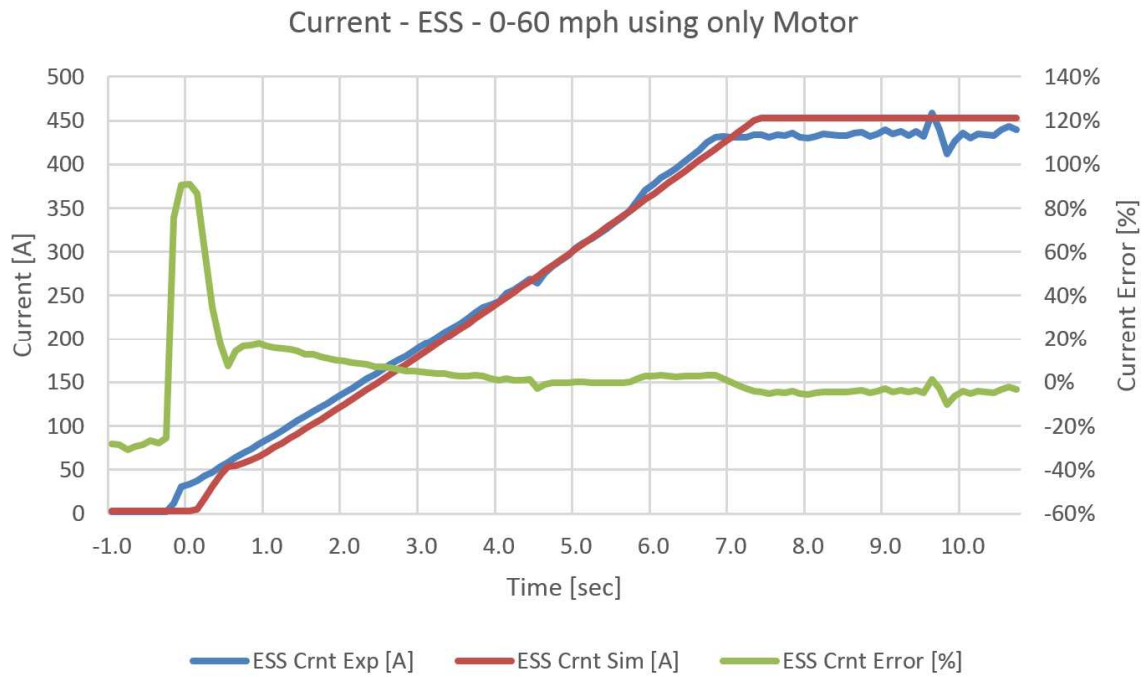
Figure 3-34. ESS current - validation of simulation results to experimental data.

3.5.5. ESS State of Charge (SOC)

ESS current from simulation results was validated to the experimental data with 0-60 acceleration dynamic performance, shown in Figure 3-35.

- Error ranged from -0.53% to +0.63% for simulation ESS SOC

- Absolute error average was 0.24% for simulation ESS SOC
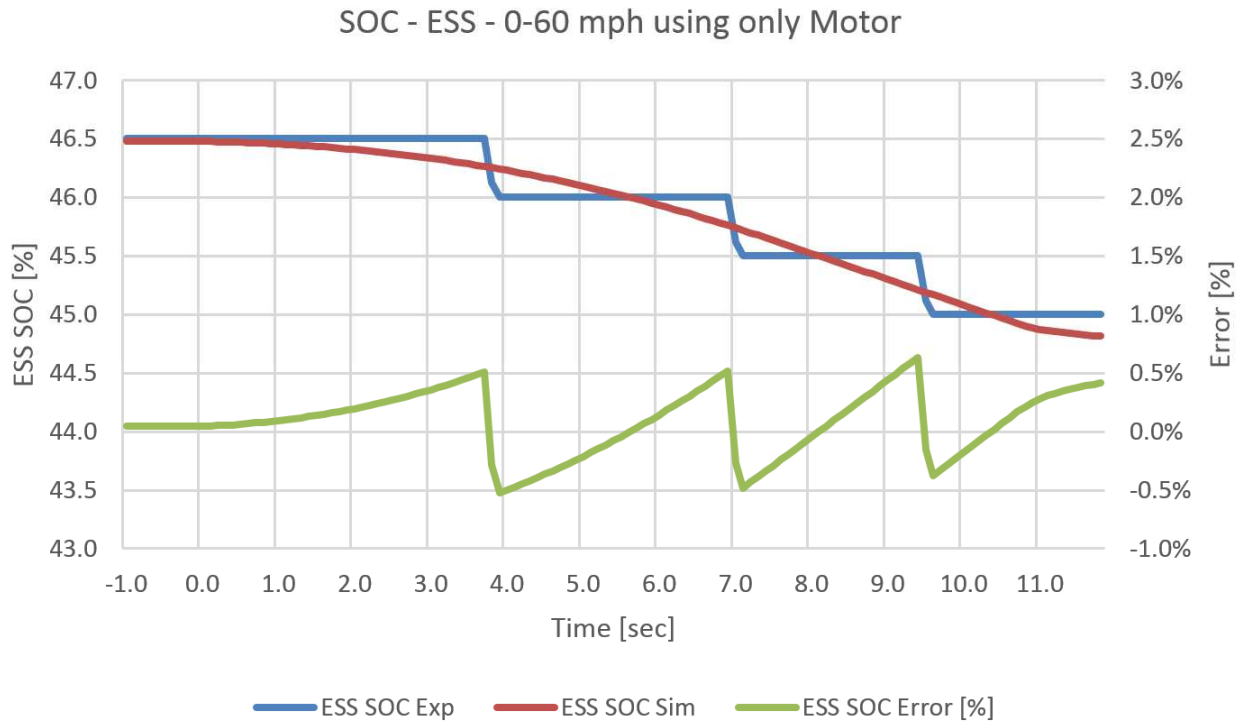
Figure 3-35. ESS SOC from 0-60 - validation of simulation results to experimental data.

Validation of ESS SOC during the E&EC drive cycle is more important than the 0-60 validation, but lacking the detail CAN logger data, there was electrical energy consumption detail from the competition organizer's data log so ESS SOC was reconstructed from the competition's organizer's 1 Hz log file and is shown in Figure 3-36.
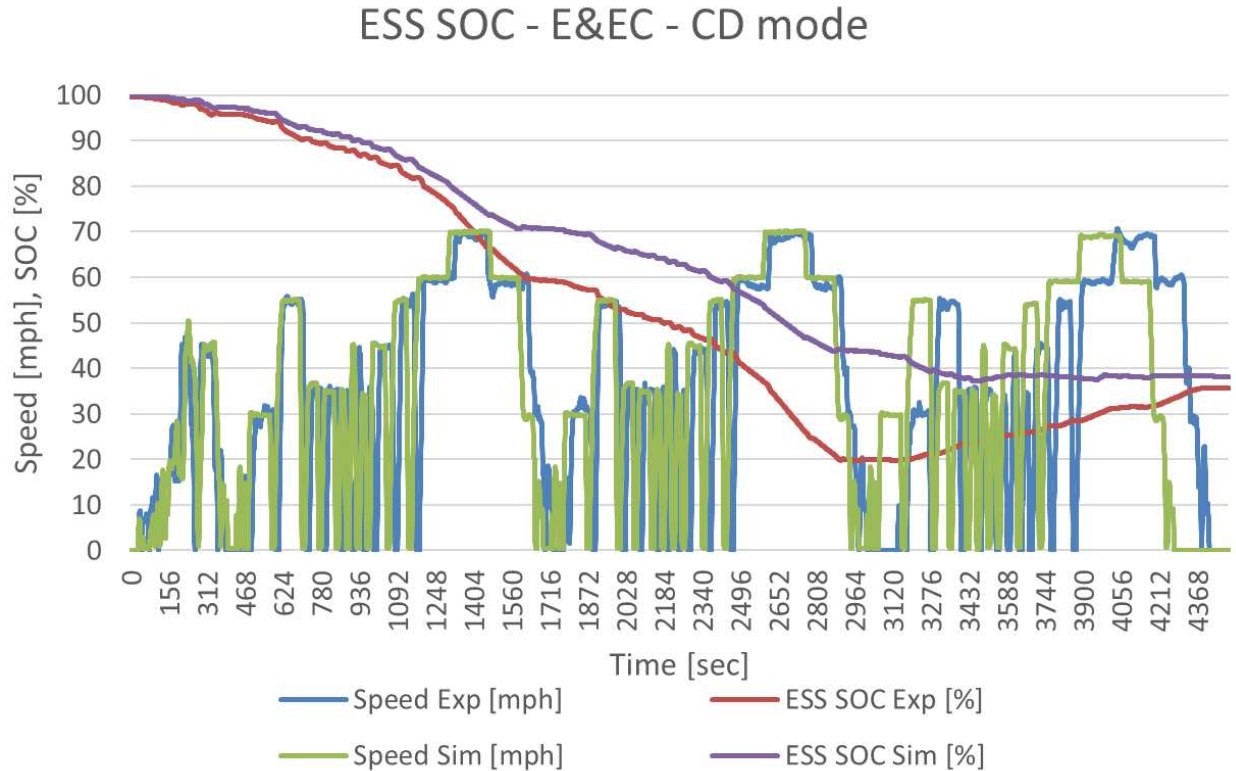
Figure 3-36. ESS SOC from E&EC - validation failure of simulation results to experimental data.

As previously discussed in Section 2.5 (see Figure 2-30), the driving on the oval test track for the experimental data did not strictly follow the timing of the E&EC drive cycle, as the experimental data is time shifted by various amounts throughout the entire 103.7 mile drive cycle. Because of the time shifting, direct comparison and validation is not possible on the E&EC cycle as a whole, so direct comparison was done on individual City Highway periods. The first two City Highway periods are compared individually after time shifting to speed align the data, shown in Figures 3-37 & 3-38.

- 28% error for SOC used in 1st City Highway

- o 26.6% SOC used in simulation results

- o 36.9% SOC used in experimental data

- 31% error for SOC used in 2nd City Highway

  - o 26.9% SOC used in simulation results

  - o 38.9% SOC used in experimental data
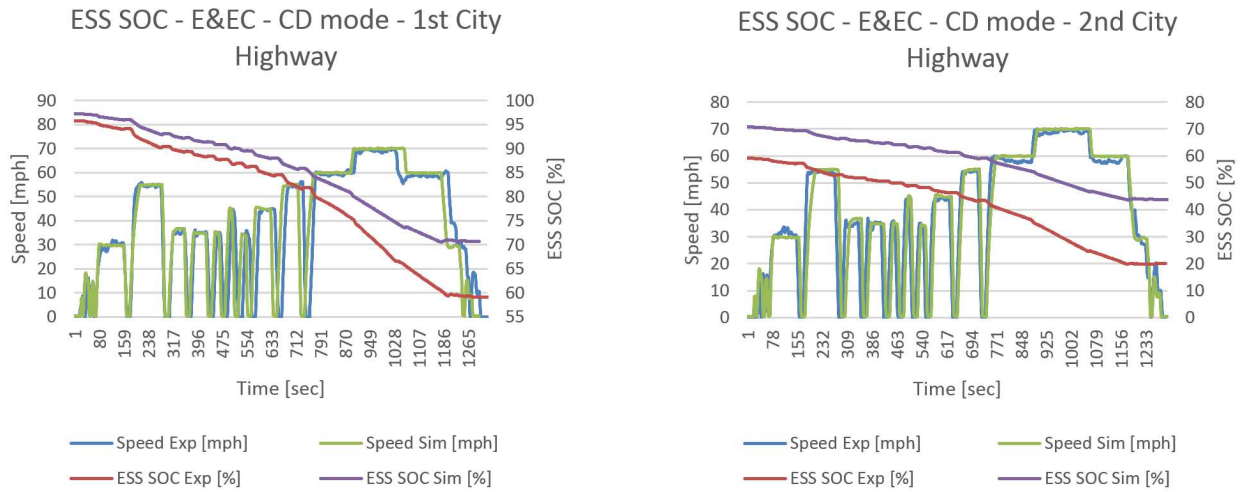
Figures 3-37 & 3-38. First two City Highway's speed aligned with ESS SOC compared by drive cycle trace.

The same two speed aligned City Highway periods are compared with ESS current in place of speed, shown in Figures 3-39 & 3-40. There is an ESS current error in the transient spikes that shows up in the E&EC City Highway that was not present in the 0-60 acceleration validation, part of this is explained by more aggressive accelerations by the driver in the experimental data. Both simulation results and experimental data have 100% accelerator pedal position for the duration of the 0-60 event, so there was no difference in aggressiveness between simulation and experimental data for the 0-60 event.
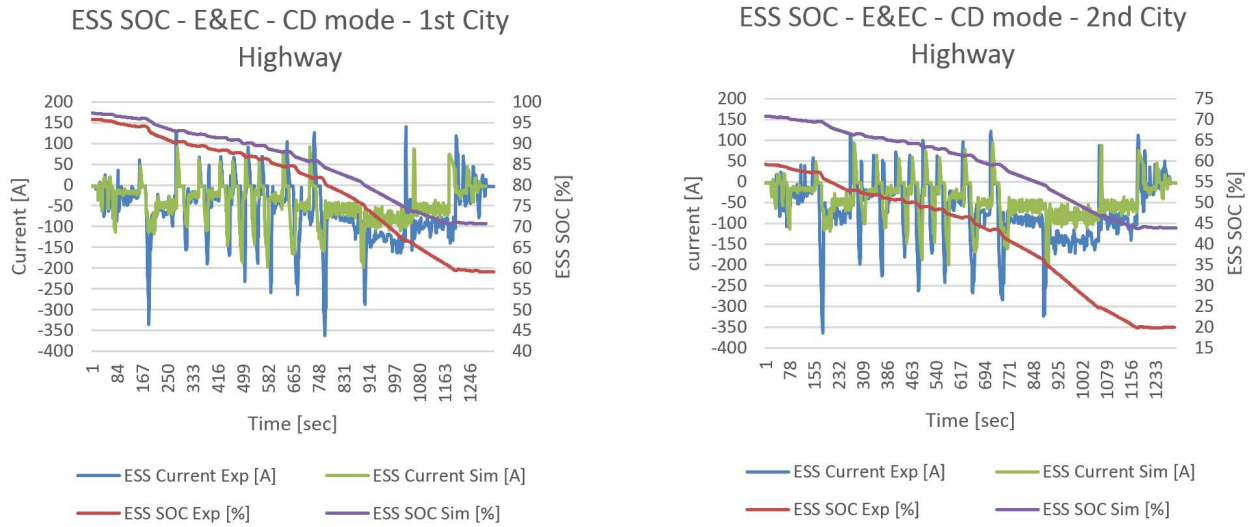
Figures 3-39 & 3-40. First two City Highway's speed aligned with ESS SOC compared by ESS current.

The same two speed aligned City Highway periods are compared with ESS power (filtered) in place of speed, shown in Figures 3-41 & 3-42. The largest differences in SOC slope occur when the filtered power was 15 kW or more (corresponding to areas of 50 A or more current, 40 mph or more speed).
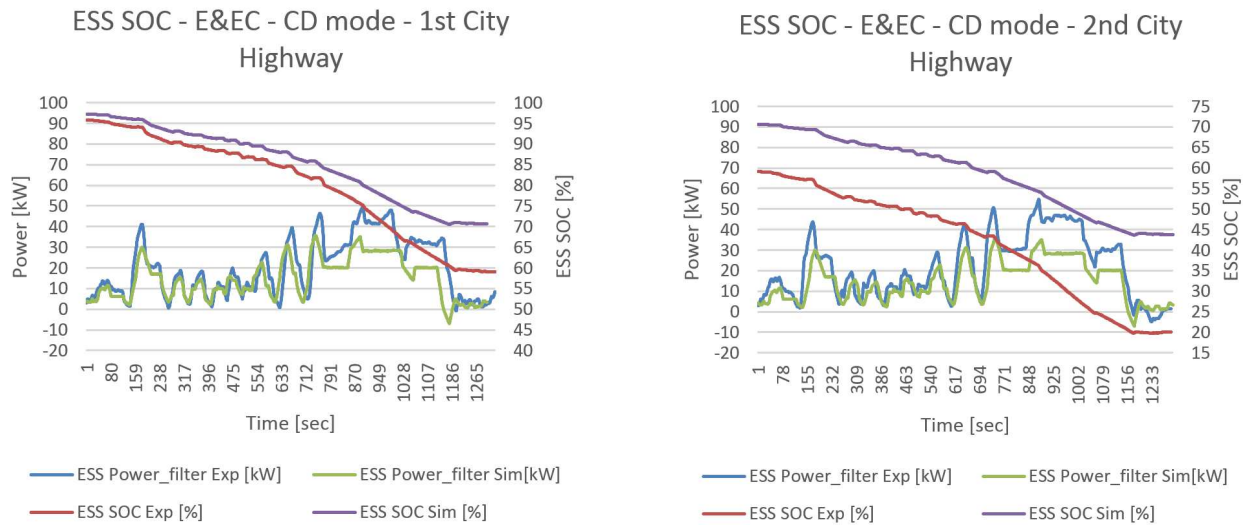
Figures 3-41 & 3-42. First two City Highway's speed aligned with ESS SOC compared by ESS power.

3.6. Chassis, Brakes, and Driver Plant Model Advancement

Advancement of the WSU PTTR plant models started with the driver PI controller, then the vehicle chassis, and worked back through the FWD & RWD powertrains to the torque sources (combustion engine, electric traction motor). It was an in-depth investigation of:

- Where the significant errors are between the simulation results and experimental data

- Why there are errors (typo, omission, bad assumption, formula error, over simplification, etc.)

- Solution(s) to reduce/fix the errors

3.6.1. Driver PI Controller

The Driver PI controller was completely overhauled because of problems seen in the simulation results, with some of the problems shown earlier in Figures 2-19 & 2-20. To make the Driver PI plant model closer to actual driver behavior, several problems were addressed.

Problem #1 fixed: Integral gain was being reset to zero whenever speed command went to zero (I_gain_sum x Req_Speed = 0, whenever Req_Speed = 0) which prevented vehicle from ever coming to a stop, at every stop in drive cycle. Original Driver PI control shown in Figure 3-43 with red boundary outline around integral gain reset problem. This was fixed by removing the original integral gain reset and adding a new integral gain reset for any time the vehicle was stopped, shown in Figure 3-44.
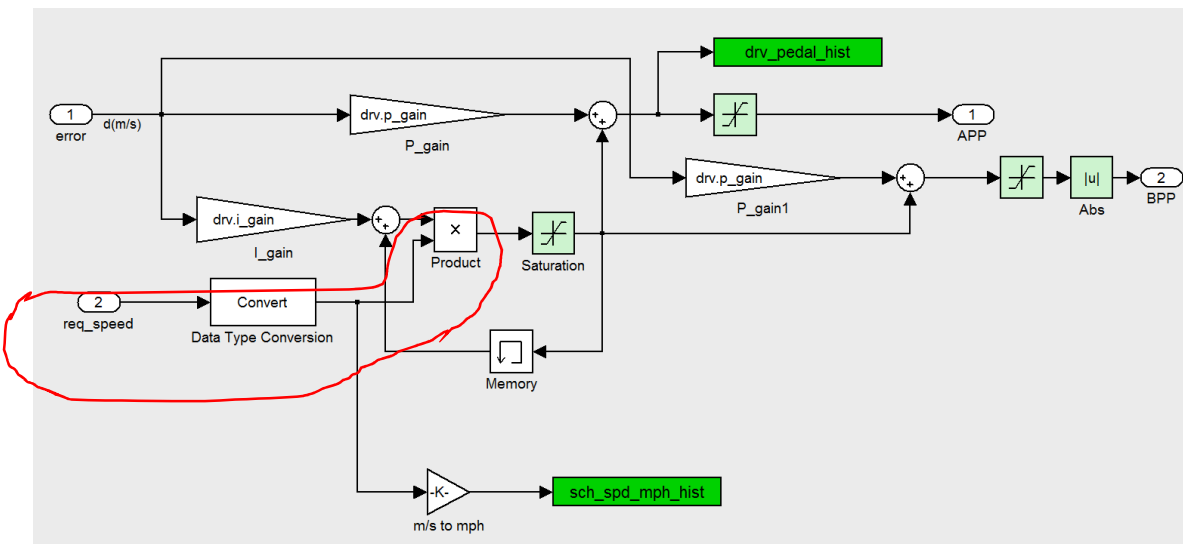
Figure 3-43. Original Driver PI control plant model.

This now allowed the integral gain to be effective during a braking event where the vehicle had to come to a stop. The reset of the integral gain was deemed important so as to not have a delay in launching from a stop due to a large integral gain accumulation (windup). The only issue with this solution was that as soon as the vehicle stopped, the integral would be reset. This was addressed by the next fix.
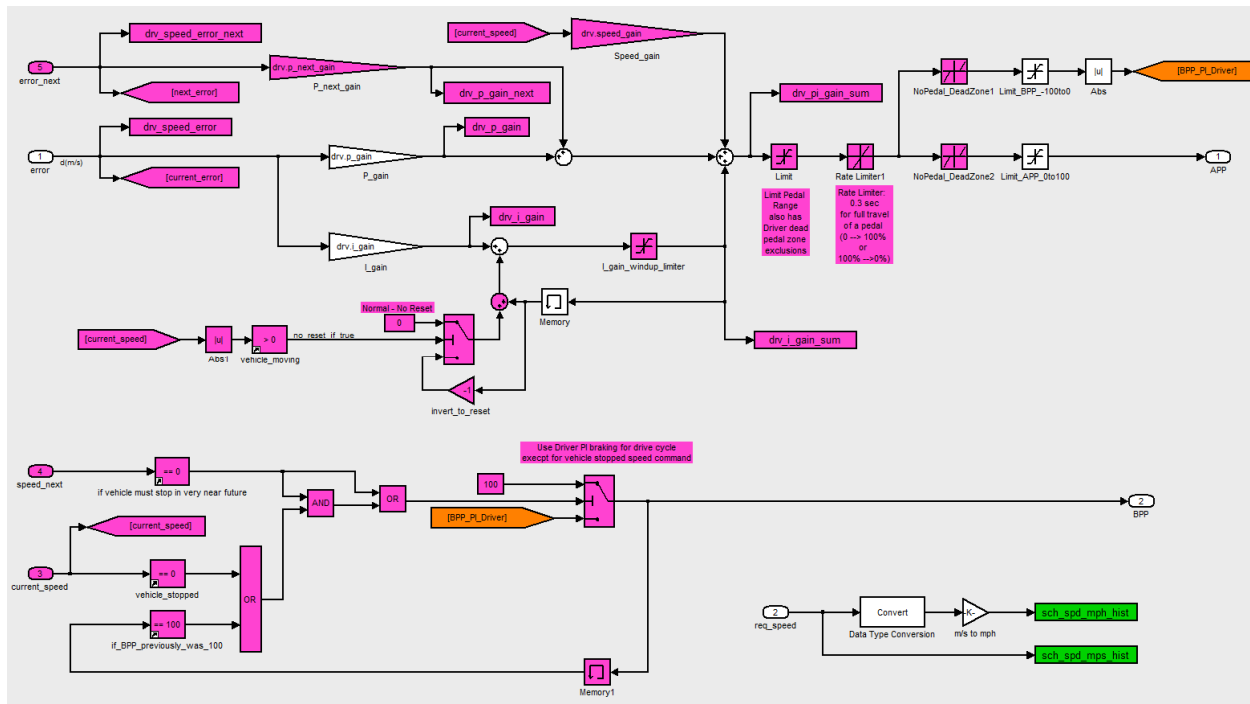
Figure 3-44. Newly overhauled Driver PI control plant model (magenta color blocks are new).

Problem #2 fixed: Brake Pedal not sufficient to bring vehicle to complete stop and hold vehicle at a stop. This was fixed with a bypass of the PI controller once both of the following conditions were met:

1. Driver PI controller has pressed brake pedal to 100%

2. The vehicle must stop (drive cycle speed command is zero/stopped 0.35+ seconds into the future)

Problem #3 fixed: PI gain combination not large enough for vehicle speed to reach target speed (Figure 2-19). Fixed by increasing proportional gain and adding the other proportional type gains described later in Problem #5 & #7 fixes.

1. 130+% increase in proportional gains 65 → (50 + 100 + (1.1 x VehSpd[m/s]))

2. 70% decrease in integral gain 1 → 0.3

Problem #4 fixed: Accel Pedal & Brake Pedal transitions were too fast (Figures 3-45 & 3-46). The simulation Driver PI controller would fully press a pedal 3 times faster than a human could actually press a pedal, based on engine controller and brake controller data collected from the vehicle's CAN bus.

- Experimental data shows ~0.3 seconds for full travel

- Simulation results have full travel in 0.1 seconds

- Thesis simulation results have full travel in ~0.3 seconds now
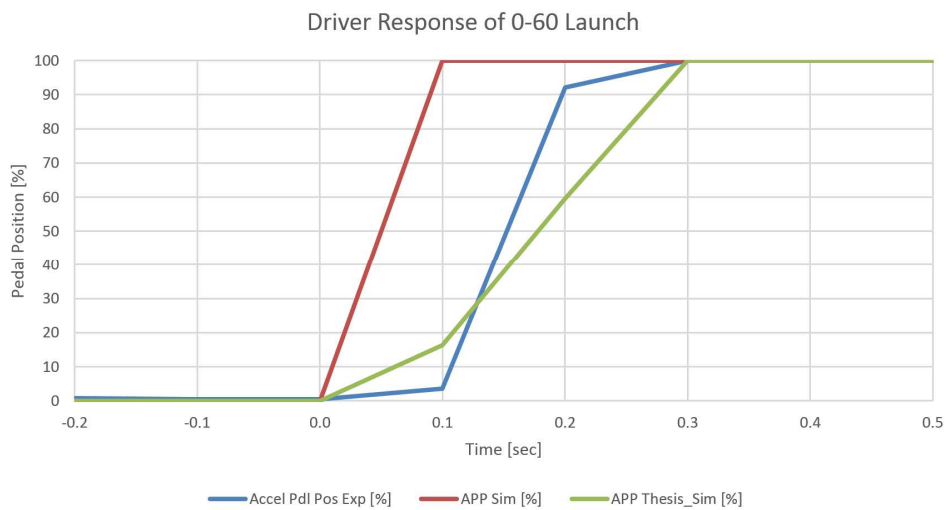
Figure 3-45. Driver plant model advancement: Accelerator Pedal full scale travel time duration.
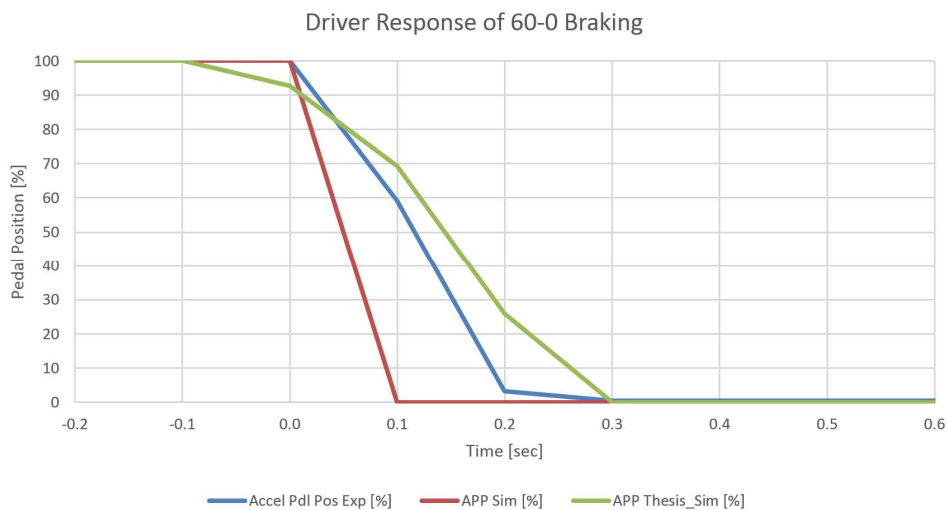
Figure 3-46. Driver plant model advancement: Brake Pedal full scale travel time duration.

Problem #5 fixed: PI controller was purely reactive, not proactive/anticipatory. An actual driver following a speed trace will see the upcoming speed change and start reacting slightly ahead of the actual point in time of the speed change in order to do the best at following the trace. The driver does this because they have learned that there are response times through themselves and the vehicle's systems. To add a similar proactive feature to the Driver PI controller, another proportional gain was added which also helped counter the effect of slowing down the Accel & Brake Pedals response.

- Added a future looking proportional gain (0.35 seconds into the future)

Problem #6 fixed: Oscillations between Accel Pedal & Brake Pedal when speed error is very small. A dead zone from -1% to +1% was implemented that kept both pedals at 0% to eliminate the oscillations between Accelation and Braking when the speed error is very small.

Problem #7 fixed: Integral windup (summation of the integral gain) was large enough to delay a change from acceleration to braking or vice versa, even though it was limited to +/-100%. The proportional gains were increased to reduce the need of large integral summation gain. This allowed the integral windup limit to be changed to +/-50%, but this still caused too much delay when changing from one pedal to the other pedal. Finally, a speed gain was added in parallel to the proportional and integral gains. The speed gain is like a modified proportional gain, as it takes the vehicle's current speed through a gain multiplier (speed[m/s] x 1.1 gain) to create an Accel pedal position (0-100%) that is close to what is needed to maintain the current speed. The speed gain allowed the integral windup limit to be reduced to +/-15% which then had an acceptable response time when changing from one pedal to the other. The speed gain will be a problem as implemented for any drive cycles that have negative speed (vehicle driving in reverse), but so far EPA certification cycles and EcoCAR competition cycles do not have vehicles driving in reverse for any portion of the drive cycles.

The results of the 7 fixes are seen in Figures 3-47 through 3-50. Figures 3-47 & 3-48 show that the thesis simulation Driver PI controller now accelerates to the target speed, with slight overshoot – compared to the WSU PTTR simulation Driver PI controller which never reaches the target speed.
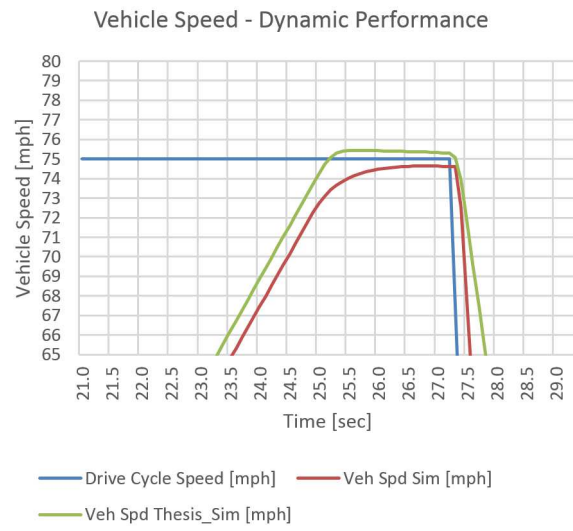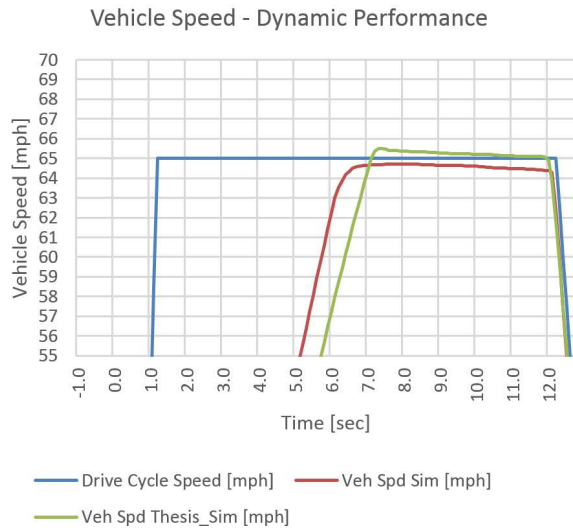
Figure 3-47 & 3-48. Thesis simulation fixes for Driver PI controller for 0-60 accel and 50-70 accel.

Figures 3-49 & 3-50 show that the thesis simulation Driver PI controller now succeeds in stopping the vehicle and is closer to target speed – compared to the WSU PTTR simulation Driver PI controller which never stops the vehicle, continuing to drive at a very slow 0.7 mph.
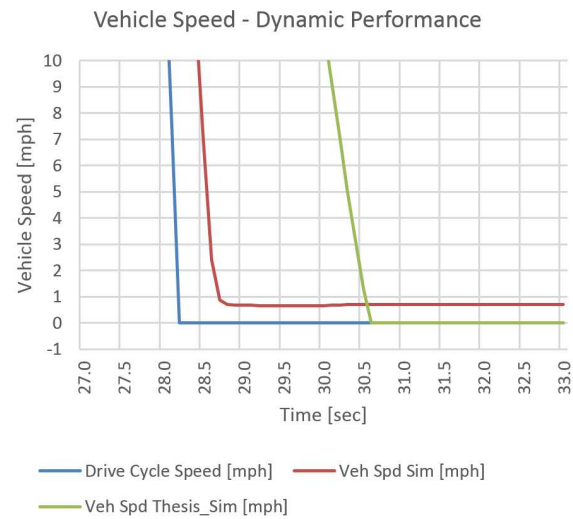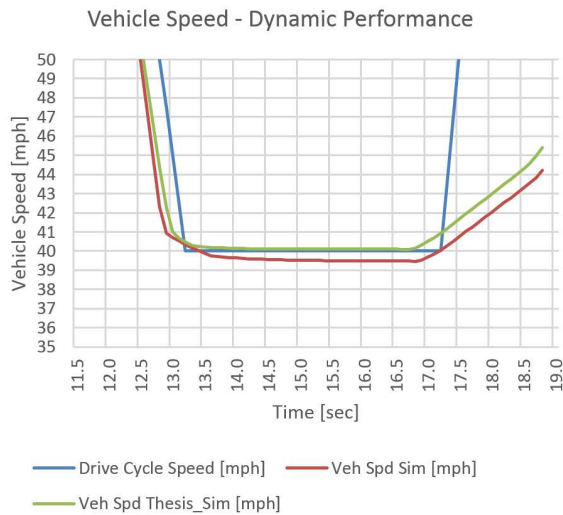
Figures 3-49 & 3-50. Thesis simulation fixes for Driver PI controller for decel and stop.

3.6.2. Vehicle Chassis

The chassis parameters for the PTTR PHEV remained unchanged except for mass which was increased by 10 kg (0.4% increase) to be at the vehicle's actual GVWR of 2250 kg based on the measured curb weight of 2072 kg then plus two male adults (estimated 180 kg more, totals 2252 kg).

- Vehicle mas 2240 kg → 2250 kg (0.4% increase)

3.6.3. Wheel Effective Radius and Rolling Resistance

The stock tires on the WSU team's vehicle were P225/55R17 Goodyear "Assurance Fuel Max" mounted on 17" alloy rims. The wheel effective radius is dynamic and has multiple values depending on the state of the wheel:

- Free State - vehicle on lift with wheels off the ground

- Static Loaded State - vehicle on ground and stationary

- Effective Radius – vehicle is moving, Effective Radius will be somewhere in between the Free State and the Static Loaded State when following a fuel economy drive cycle on a smooth road

A steady state period (5.5 seconds) in the highway gradeability drive cycle was used for determining the effective radius for the front and rear wheels. The steady state period chosen was when the transmission was in 5th gear (1.0:1 ratio) and the torque converter was fully locked up (no slip), shown in Figures 3-51 & 3-52. The averages of the front/rear wheels, engine speed, and motor speed were calculated and used to determine the effective wheel radius.
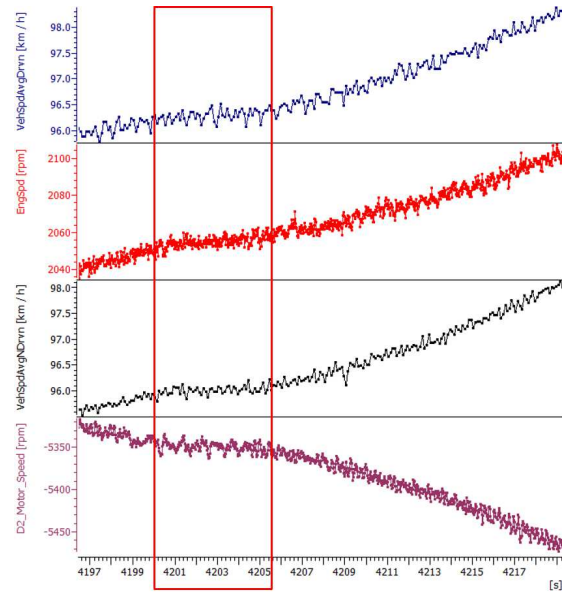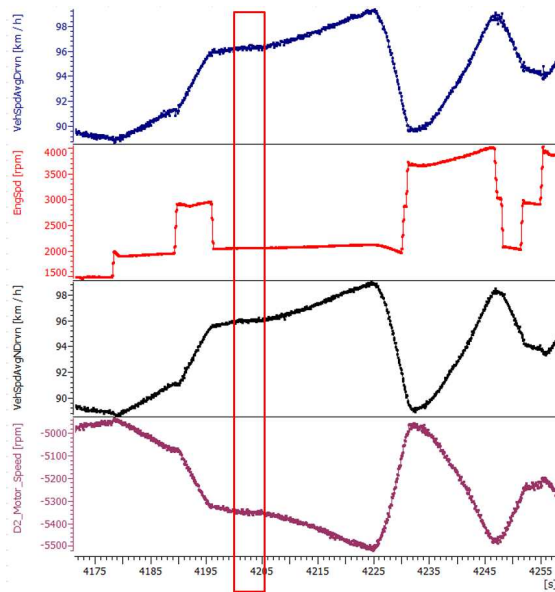
Figures 3-51 & 3-52. Experimentally determining the wheel effective radius from steady state driving.

The wheel speed sensor reported speeds from CAN showed a 0.3% difference in wheel speed between the front and the rear wheels. The rear wheels are loaded 24% heavier with 1148 kg axle load compared to the front wheels with 924 kg axle load. The rear tires were pressurized to 45 psi, 12.5% more than the front tires at 40 psi, to help compensate for the higher axle load.

- 0.3397 m nominal radius in the Free State (un-mounted tire or vehicle on lift with wheels off the ground)

- 0.3281/0.3262 m front/rear wheel Effective Radius

  - 0.6% smaller wheel effective radius at rear (tire is compressed more in rear than front)

  - 11.55 kg/psi for each of the front tires (axle load divided by tire pressure by each tire)

  - 12.76 kg/psi for rear tires (axle load divided by tire pressure by each tire)

- 0.3180 m radius in Static Loaded State for front wheels (visually estimated with tape measure)

The wheel radius in the plant model was updated:

- Front Wheel effective radius: 0.343 m → 0.3281 m   (4.3% decrease)

- Rear Wheel effective radius: 0.343 m → 0.3262 m   (4.9% decrease)

Wheel rolling resistance was left unchanged at $\mu_{roll} = 0.01$. This is reasonable estimate assuming a smooth paved road (concrete or asphalt) as a sampling of other publications shows Ehsani suggests 0.013 [24], Larminie suggests 0.005-0.015 [22] for a range of special electric vehicle tires to standard automotive tires, and Husain suggests 0.004 – 0.020.

3.6.4.   Wheel, Tire, Brake Rotational Inertias

The initial assumption of 1.2 kg m^2 of rotational inertia for an assembled tire and wheel was increased based on weighing the assembled tire and wheel and measuring their external dimensions. The rotational inertia was then calculated using an online rotational inertia calculator tool [33] and resulted in 1.51 kg m^2, but it was realized that the brake disc inertia should be included too, so the brake disc was weighed, dimensionally measured, and the resulting calculated rotational inertia was 0.09 kg m^2. The total assembly rotational inertia is now 1.60 kg m^2 which was checked for reasonableness with another team's experimental data based calculation of 1.346 kg m^2 for rotational inertia [34] (but they had no mention of brake disc inclusion). The online rotational inertia calculator tool and the reasonableness check both indicate that the initial assumption of 1.2 kg m^2 of rotational inertia was too low.

- Wheel assembly rotational inertia: 1.2 kg m^2 → 1.6 kg m^2 (33% increase)

3.6.5. Braking Force

The brake system plant model was updated in several areas. First, a major error in braking force was discovered as a unit conversion error - brake force was not converted to brake torque before sending to the wheel plant models, shown in Figure 3-53. The wheel plant model input was brake torque, so the braking force was incorrect by a factor of 3 (1/wheel_radius = 1/0.327), shown previously in Figures 2-7 & 2-12.
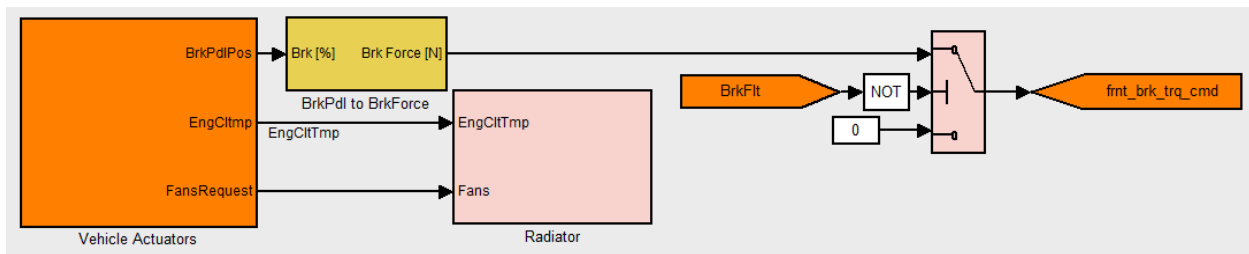
Figure 3-53. WSU PTTR brake system plant model.

The brake force error was corrected by adding a multiplication of the wheel radius before sending to the wheel plant models, shown in Figure 3-54.
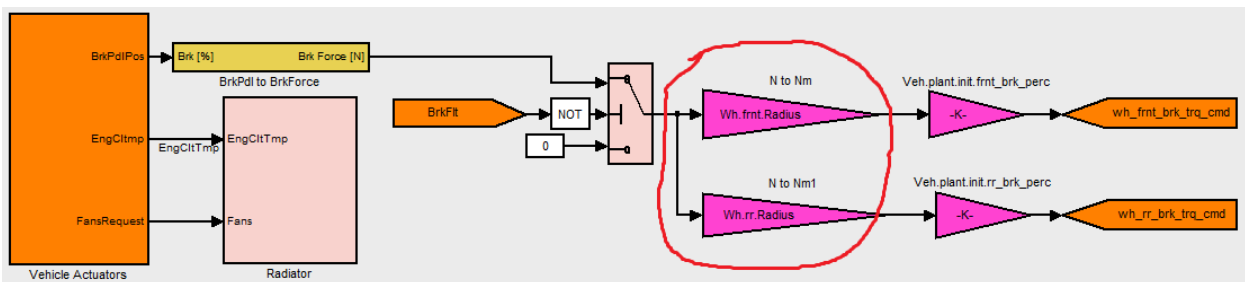
Figure 3-54. Thesis brake system fix for brake torque sent to wheel plant models.

Next, the brake force needed updating based on experimental data. From the stock vehicle braking distance testing, the braking force was calculated to be 15,600 N. The team upgraded all four disc brakes which retained the same pistons in the calipers, but the calibers were pushed radially out by 10%, creating a 10% increase in the radius of the brakes, so a 10% increase in brake torque for the same hydraulic force of the brake system. However, increasing the braking force 10% from 15,600 N to 17,200 N was not reflective of the experimental data. The

addition of 478 kg (1053 lbs) to the rear of the vehicle altered the Center of Gravity (CG) and lowered the rear of the vehicle such that the rear was lower than the front (vehicle not level), affecting the weight transfer effect during braking. The end result was to recalculate the braking force based on the experimental data after the weight gain and it was determined that the new brake force was 20,300 N.

- Brake force: 15,600 N $\rightarrow$ 20,115 N   (29% increase)

The original WSU PTTR braking model had 100% of the braking force going to the front wheels and 0% to the rear wheels. The thesis model was advanced to split the braking force between the front and rear, with 60% going to the front and 40% going to the rear. The assumption of 60% for the front brake force portion is reasonable based on an example from Husain (64% front) [20] because the team's vehicle had more rear weight bias, although the team's CG height was not known. Figure 3-55 shows the model code addition of splitting the braking force between the front and rear wheels.
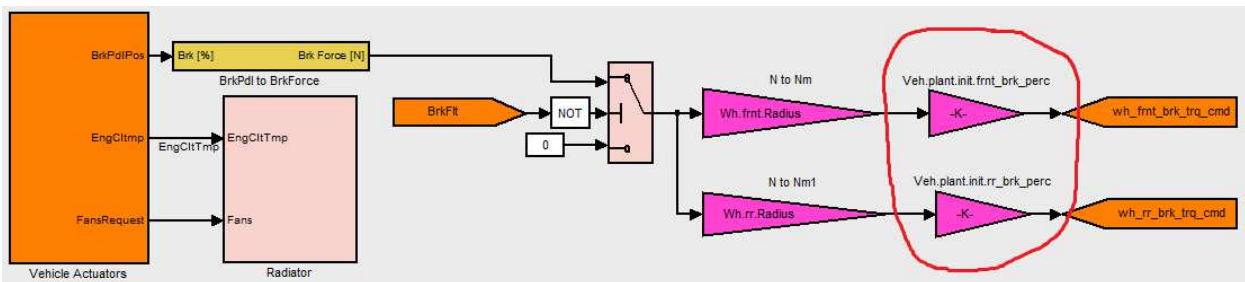
Figure 3-55. Brake system plant model advancement with brake force split front/rear addition.

The simulation results changed in some unexpected ways with the plant model advancements. One such change was that on some hills in E&EC, the engine speed gets frozen and never increases enough to upshift, so vehicle has large trace miss, but other hills are just fine. Problem was with the wheel slip model, it was now detecting wheel slip after thesis modifications and during wheel slip, the model was producing unrealistic vehicle behavior. The unrealistic behavior was complete and sustained trace miss, rather than a short and small trace miss, shown in Figure 3-56.
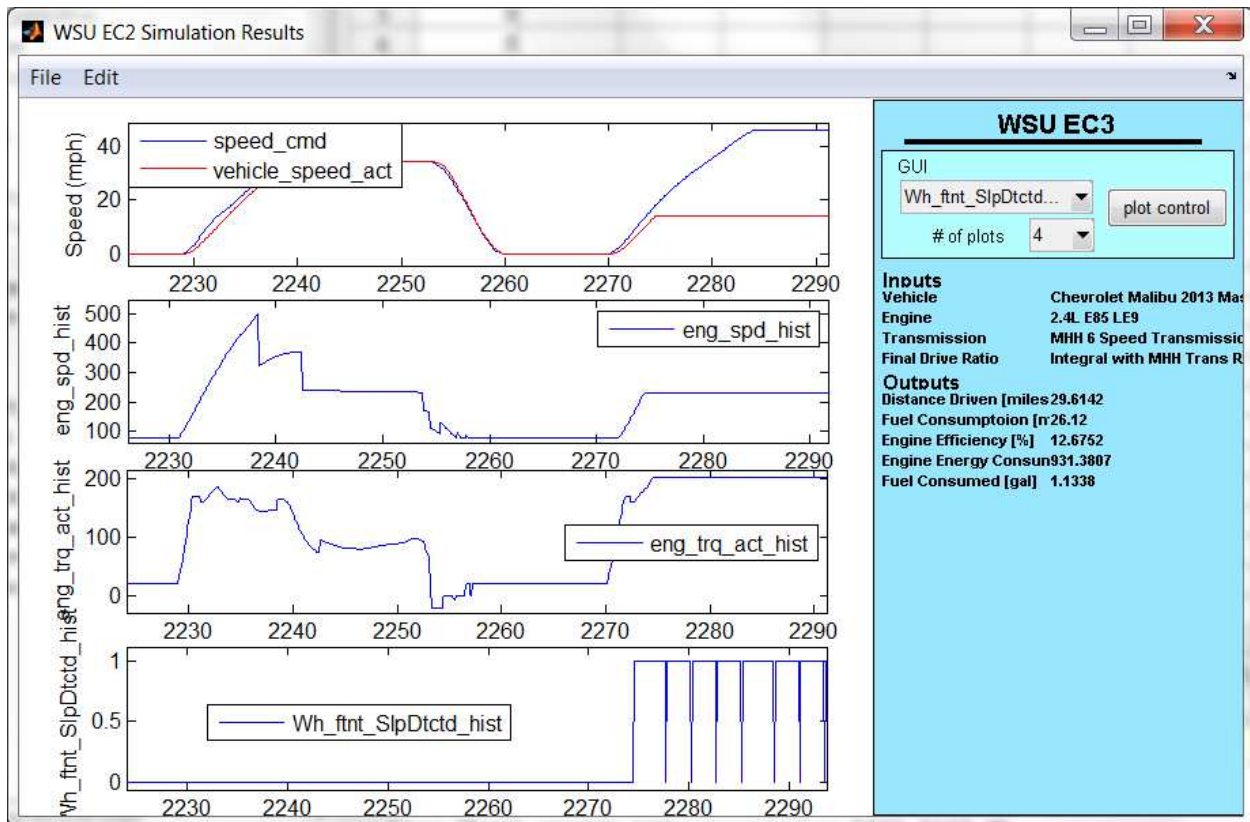
Figure 3-56. Wheel slip model producing complete and sustained trace miss (top graph).

Fixing the wheel slip behavior ended up being outside the scope of the thesis, but it would involve a adding a remedial action back to the propulsion torque source (engine, motor, or both) for a large reduction of torque until wheel slip stopped. As a temporary fix, the wheel slip model was disabled, shown in Figure 3-57. This was a reasonable short term fix as the experimental data from the competition events does not show any known wheel slip issues.
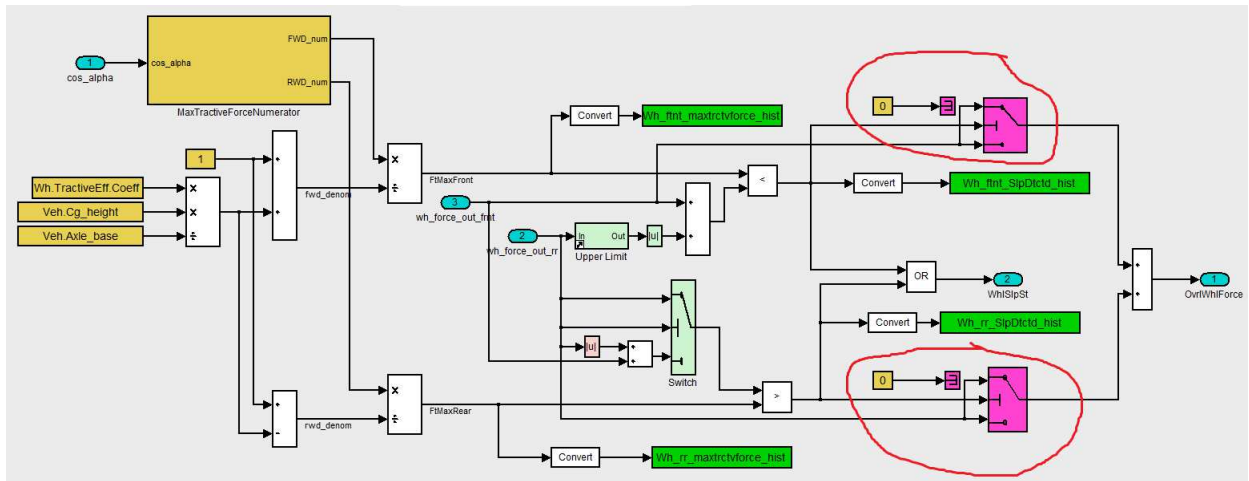
Figure 3-57. Wheel slip model disabled as short term fix for resuming driving of cycle traces.

3.6.6.   Trailer

Two mistakes were found in the trailer road load of the chassis plant model: a typo on the trailer mass and the trailer mass had been completely omitted from the vehicle inertia term. Figure 3-58 shows the addition of the missing trailer mass in the vehicle inertia term. Plant model updates:

- 334 kg → 344 kg trailer mass   (3.0% increase in trailer mass, 0.4% increase of total static mass)

- 2250 kg + 0 kg → 2250 kg + 344 kg   (15.3% increase of total static mass by including the trailer)
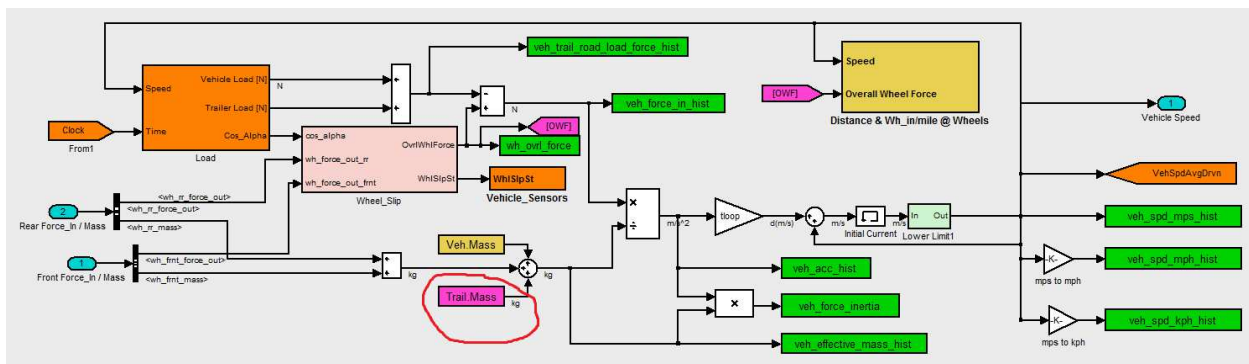
Figure 3-58. Added the missing trailer mass to the vehicle inertia term in the chassis plant model.

3.7. Electric Powertrain Plant Model Advancement

3.7.1. Energy Storage System (ESS) Efficiency

ESS efficiency calculated from energy flow addition (see Table 5-1 in Chapter 5) was marginally high based on manufactures application manual examples [28], so either the cell resistance tables could be modified to have slightly higher resistance (decrease ohmic efficiency) or coulombic efficiency could be decreased. The simplest update was to decrease coulombic efficiency from 100% to 99%. The 1% increase in ESS loss is added to the ESS plant model in Figure 3-59.
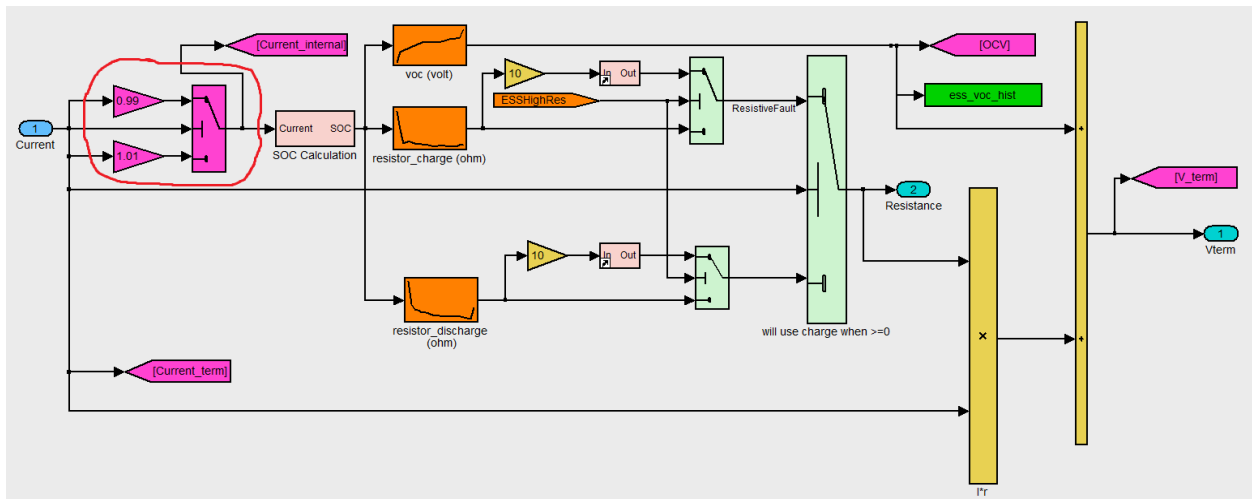
Figure 3-59. ESS plant model updated by adding a 1% coulombic loss to slightly increase ESS loss.

3.7.2. Motor Torque

The motor plant model was updated to match the reported motor torque from the experimental data. The error between original simulation torque model and the experimental data was shown back in Section 3.5.2, specifically in Figure 3-27. The largest part of the error was due to a significantly different base speed between simulation model and experimental data. Figure 3-60 is a different, but similar motor that serves as an example of the reduction of motor torque available for propulsion if the base speed is shifted significantly [23].
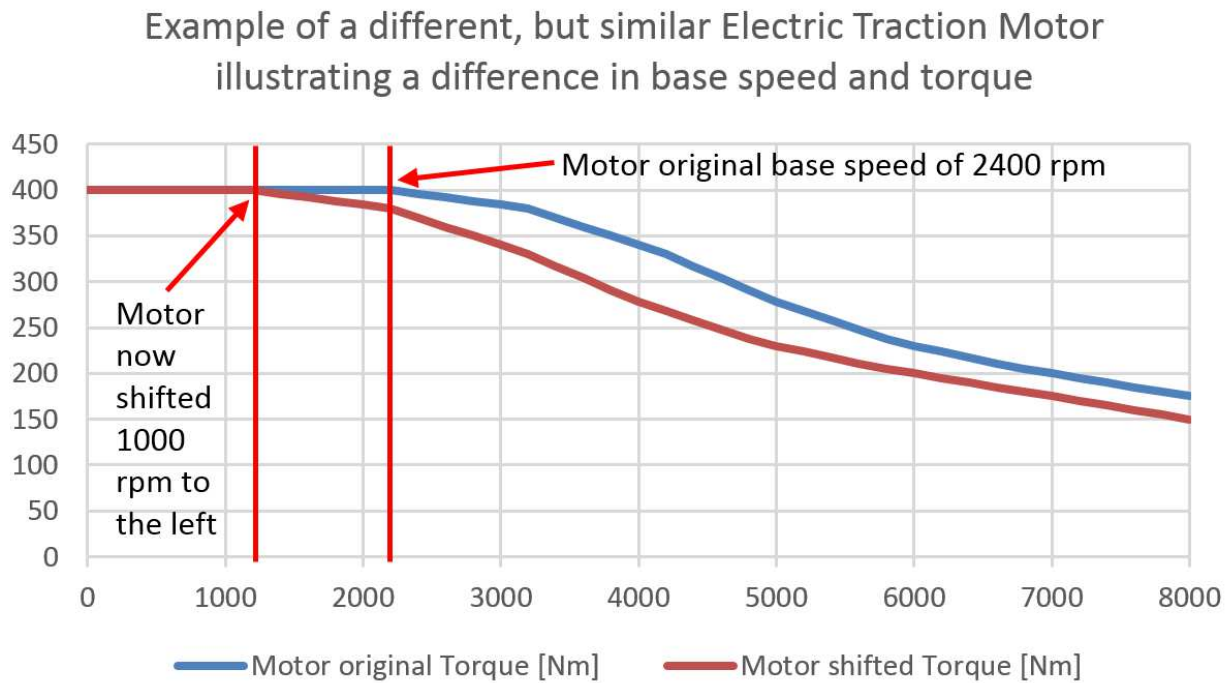
Figure 3-60. An illustrative example from a different, but similar motor from Autonomie on how a base speed difference creates a torque difference that results in different vehicle performance [23].

Reviewing the Remy motor family application manual (manufacturer's data), a set of peak and continuous motor torque and power was found and used to update the simulation model. Not enough data was available to update the efficiencies, so some manual overall adjustment of the existing simulation model efficiency table done to get the simulation results closer to the experimental data – a simple scalar factor of 0.92 was applied to the efficiency table to reduce the motor efficiencies. Also the motor inverter efficiency was reduced from the initial assumption of constant 97% to constant 92% at the same time from simulation iterations of E&EC drive cycle for electrical energy consumption during charge depletion. Figure 3-61 shows the updated 0-60 using only the electric traction motor - all of the updates from all of the thesis sections are applied to the model in this simulation.

- 10.6% error of original simulation (10.1 seconds simulation, 11.3 seconds experimental data)

- 0.9% error of thesis simulation (11.4 seconds simulation, 11.3 seconds experimental data)
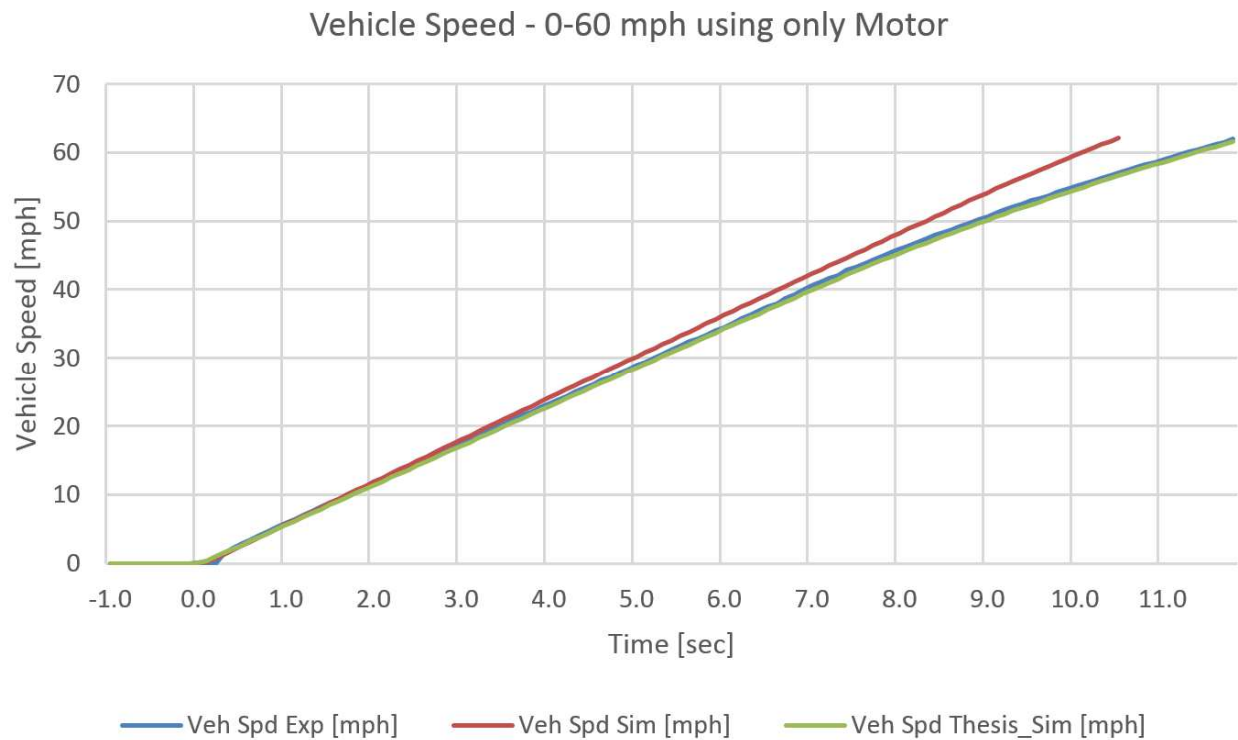
Figure 3-61. Motor plant model advancement: 0-60 acceleration using only electric motor.

3.7.3. Motor Rotational Inertia

The motor rotational inertia was found in manufacturer's application manual and updated in the motor plant model. This updated resulted in a 38% increase in rotational inertia from the initial estimated value. The manufacturer's data for the rotational inertia was more reasonable than the WSU's team's initial estimated rotational inertia, as the 38% increase to the manufacturer's rotational inertia was closer to the 0.1 kg m^2 used by another team modeling and simulation for a similar sized motor [34].

- 38% increase of motor rotational inertia in motor plant model

3.7.4. Motor Inverter

A problem was found with the motor inverter losses – the generating losses were being subtracted from the motoring losses, so the total losses were being underreported. To fix this problem, an absolute value function was added to the motor plant model, shown in Figure 3-62. Now all losses are accumulative, nothing can reduce any accumulated loss.
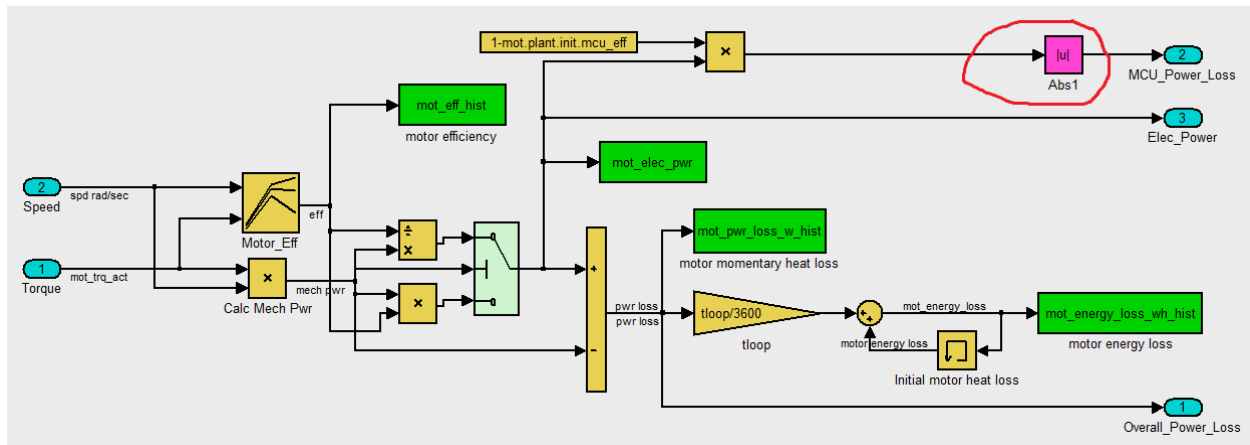
Figure 3-62. Motor plant model advancement: motor inverter loss problem fixed.

3.7.5. Motor Thermal

After the losses were increased in the motor and motor inverter, the thermal portion of the plant model became a problem and prevented following a drive cycle trace. The increased losses meant that the components had more waste heat than before and so the component temperatures increased more than before. The increased temperature in simulation was enough to trigger degraded performance and eventually a shutdown of the electric motor and inverter. The degradation is seen in Figure 3-63 in City Highway #2 and the shutdown seen in City Highway #3 continuing for the rest of the cycle.
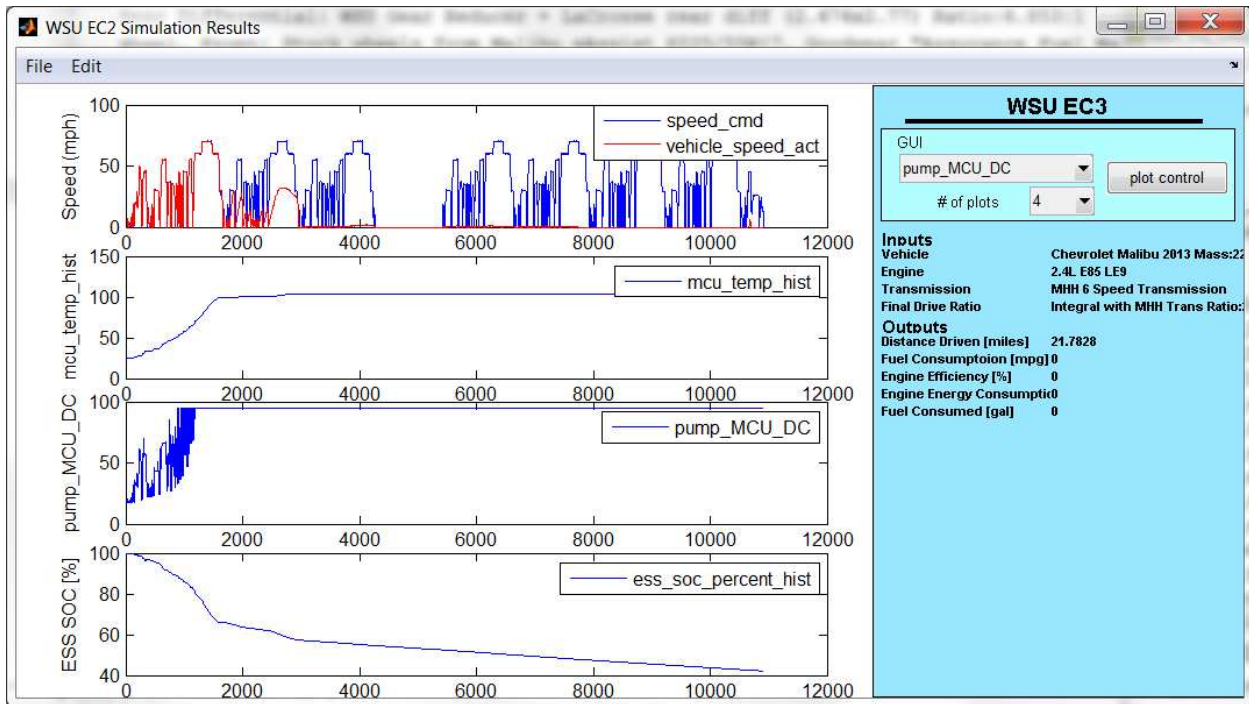
Figure 3-63. Motor thermal model of the inverter (MCU – Motor Control Unit) overheating and shutting down.

The motor thermal model is a very simple model where all motor and inverter losses become heat that raises the temperature of both those components. Only heat conduction to coolant is used to transfer heat out of the component, no radiation and no convention heat transfer. Even the conduction is simplistic where: (a) if the pump runs, then (b) heat is removed without regard to how much heat the coolant and heat exchange surfaces can really transfer for the unknown coolant flow rate with only knowing the pump speed. This is workable for the purposes of

the team's controls code modeling and simulation, as the main objective of the thermal portions of the plant models is to test controls code, not to simulate a vehicle's cooling system for thermal performance for various drive cycles.

The controls code testing needs to have the component heat up from losses so that the controls testing verifies that the controls code turns on fans and pumps and increases their speed as component temperatures increase. Also, the testing needs to show that if the fans and pumps do not turn on or do not increase in speed that the component will overheat and shutdown depending on the drive cycle demands. An accurate thermal heat transfer model is not needed for this type of testing of controls code. If a heat transfer model was implemented that had some accuracy, it would have to be balanced with the resulting increase in simulation time. A 30% increase in simulation time may be acceptable, but at 300% increase in simulation time is probably not acceptable.

Thermal heat transfer model accuracy is needed for capacity sizing thermal system for vehicle testing on hot desert grades (up a mountain), or hot desert trailer towing, or both. Fuel economy drive cycles do not contain desert mountain grades or trailer towing, so no heat transfer accuracy is needed for fuel economy modeling and simulation.

However, there was an error in the thermal portion of the motor plant model – the motor was being cooled by both of the oil pumps: feed pump and scavenge pump, see Figure 3-64. This is not the case, the motor is cooled by the feed pump providing cooled oil to the motor stator windings, rotor shaft, and rotor bearings. The scavenge pump does not provide any cooled oil to the motor, it only evacuates the hot oil and air bubbles from the bottom of the motor to keep the oil level from rising up and flooding the spinning rotor.
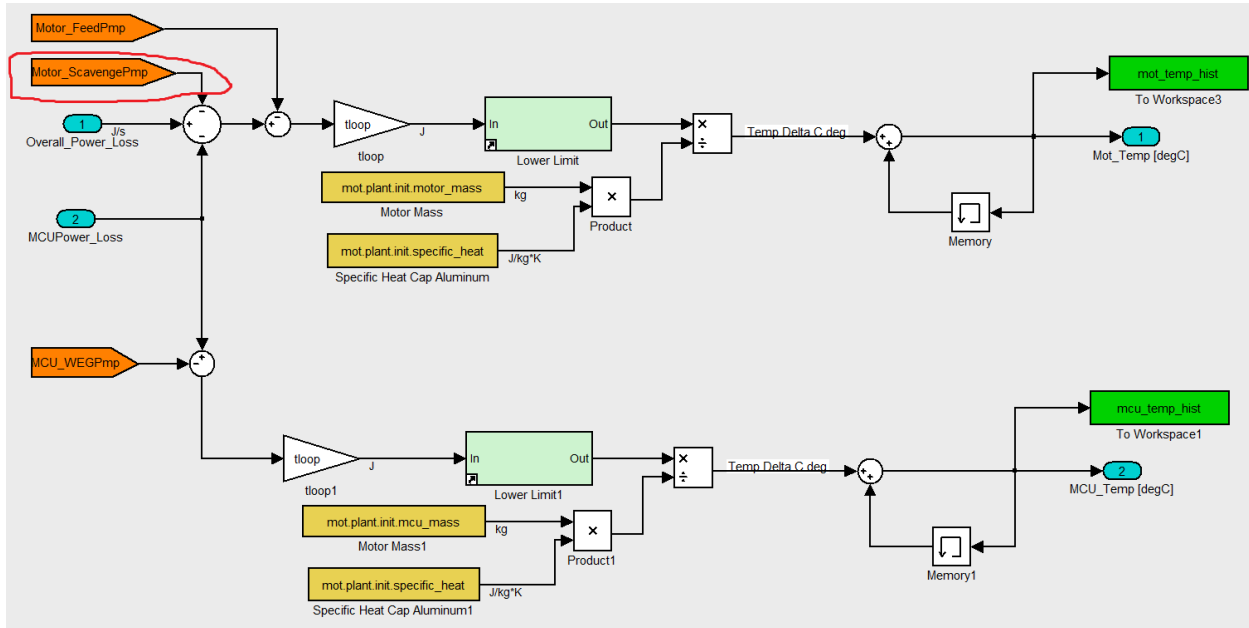
Figure 3-64. Motor thermal model with error of scavenge pump providing motor cooling.

Figure 3-65 shows the deletion of the scavenge pump and additions of coolant pump gains for increasing the cooling flow rate so that the components no longer overheat as long as the controls code increases pump speed and fan speed to maximum speed. This is valid because the vehicle never did suffer from a component overheating and shutdown during the competition events. Also shown in Figure 3-65 are newly added lower temperature bounds for the components that are adjustable to keep the component from ever cooling all the way down to ambient air temperature. This is overly simplistic, but directionally closer to reality than allowing the components to be completely cooled back down to ambient air temperature during a drive cycle.
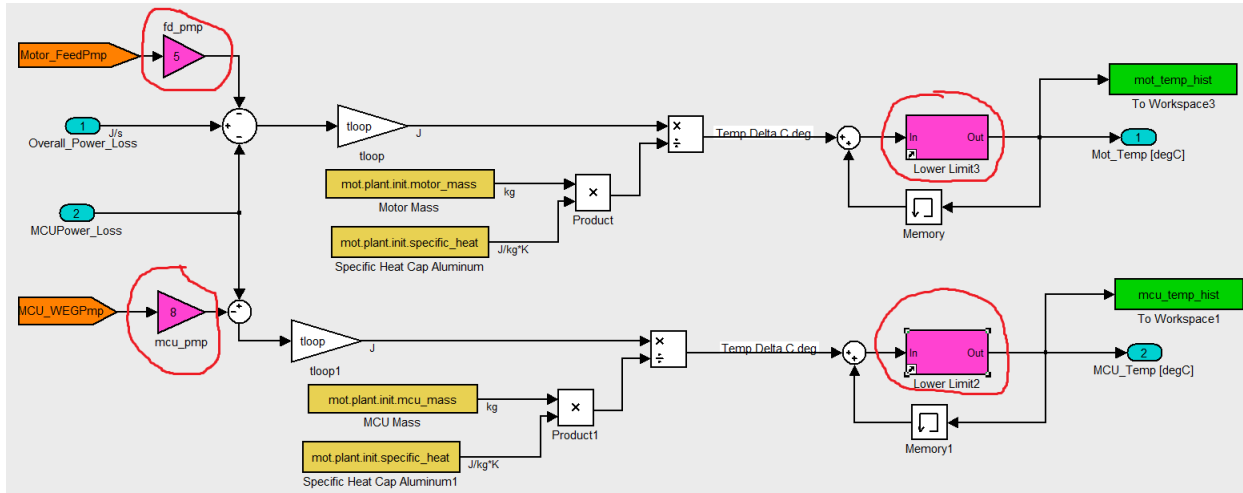
Figure 3-65. Motor thermal model advancement: scavenge pump deleted, added component lower temp limits, added gains to cooling pumps to change cooling rate.

The updated plant model now shows components no longer overheating and shutting down during the E&EC drive cycle. The new pump speeds and updated component temperature responses are shown in Figures 3-66 & 3-67.
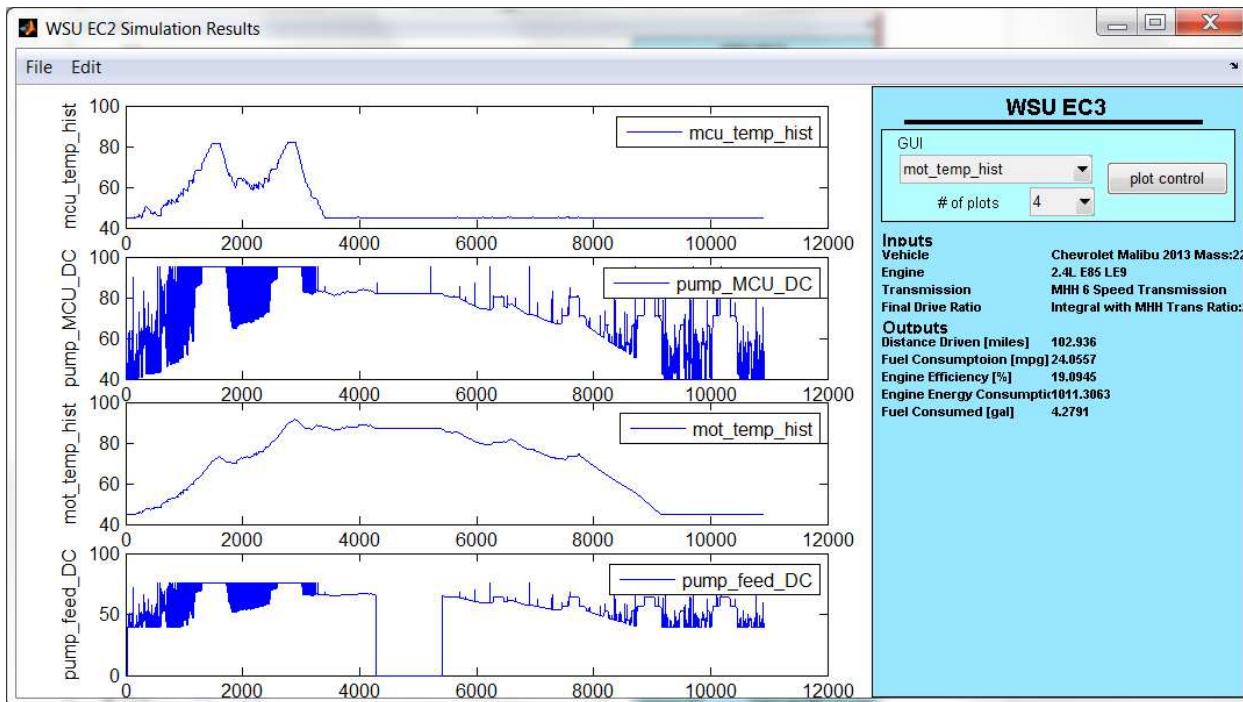
Figure 3-66. Motor thermal model advancement: coolant pump speed command Duty Cycle (DC).
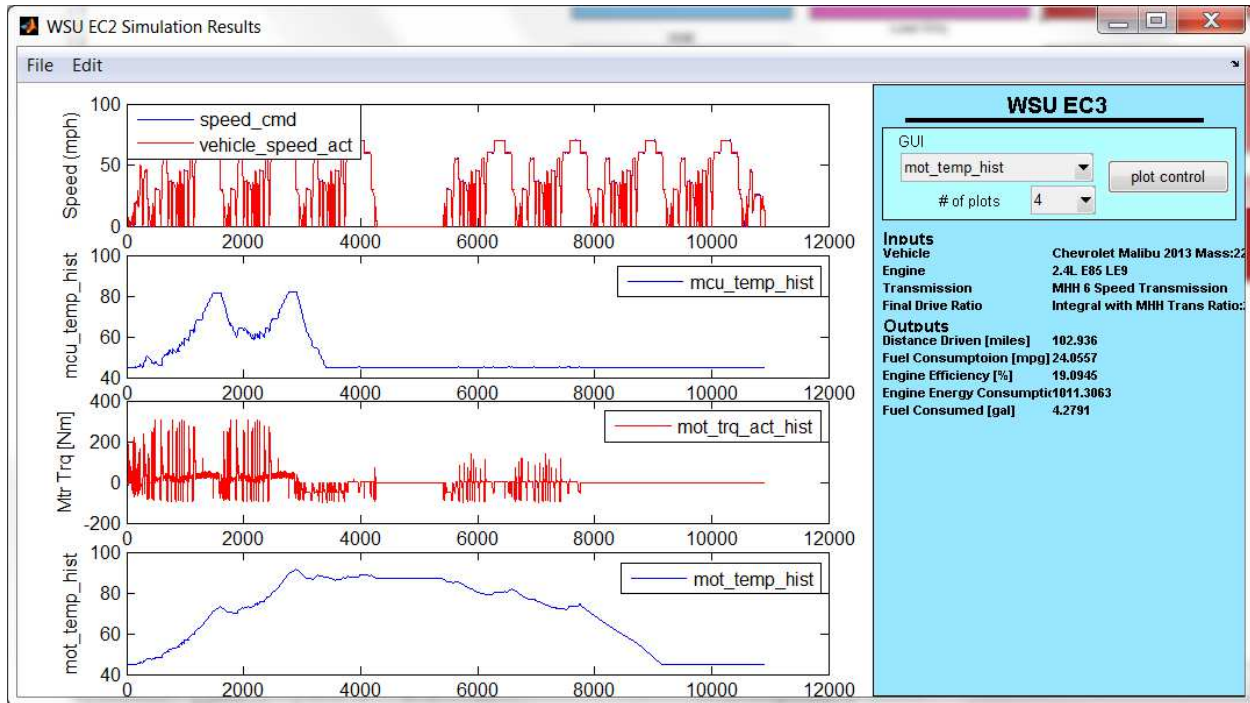
Figure 3-67. Motor thermal model advancement: component temperatures now directionally closer to reality (no longer overheating).

The radiator fan speed is more complicated than the cooling pumps speed that varies from 10% to 100% Pulse Width Modulated (PWM) Duty Cycle (DC) command. The radiator fan control consists of 2 Digital Outputs (DO) controlling 2 relays that provide 4 states:

1. Both fans off

2. Both fans low speed (low airflow)

3. One fan full speed, the other fan off (medium airflow)

4. Both fans full speed (full airflow)

The radiator fan control in Figure 3-68 shows that states 2-4 are used for the E&EC drive cycle. Signal saving blocks were added to the model in Figure 3-69 to save the radiator fan relay commands.

Figure 3-68. Motor thermal model advancement: radiator fan speed command data is now visible in simulation results.
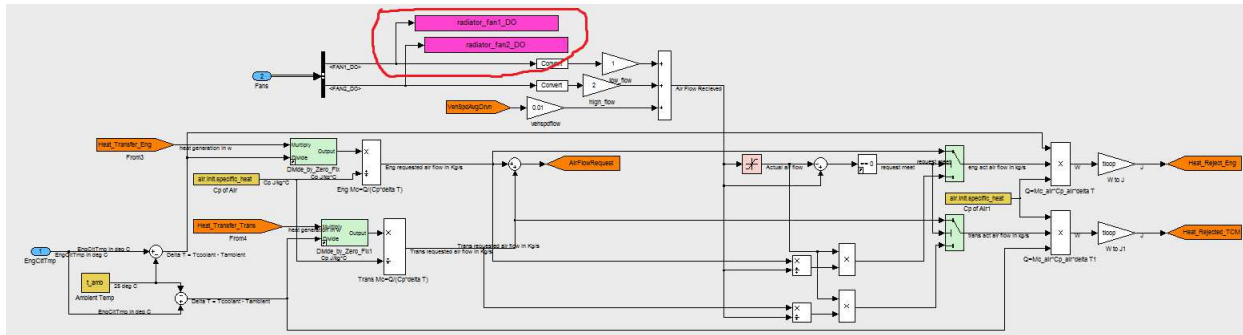
Figure 3-69. Motor thermal model advancement: radiator fan speed command data is now saved during simulation.

3.7.6. Gear Reducer

The motor gear reducer is a separate component than the rear differential, but it does not have its own plant model. The gear reducer is embedded within the rear differential plant model as one of two terms of the RFD.Ratio, shown in Figure 3-70.

Figure 3-70. Gear reducer embedded in the rear differential plant model.

The Rear Final Drive Ratio (RFD.Ratio) was updated from 7.12 to 6.853 by replacing the obsolete belt and pulley reducer ratio (2.57) with the new gear reducer ratio (2.474). The rear differential ratio of 2.77 remained unchanged. The RFD.Efficiency was missing the term for the reducer, it only had a term for the rear differential. A term was added to the RFD.Efficiency and a value of 0.97 (97% efficient) was assigned. The 97% is in line with typical efficiencies of a gear pair (95% - 97%), according to both Guzzella [21] and Ehsani [24]. The gear reducer prior to the addition of 97% efficiency was effectively at 100% efficiency in the simulation.

- **7.12** (2.77 x 2.57) → **6.853** (2.77 x 2.474) rear final drive ratio   (4% decrease)

- 100% → 97% gear reducer efficiency   (3% decrease)

3.7.7. Rear Differential

The rear differential efficiency was updated from 99% to 97% to bring it in line with typical efficiencies of a gear pair (95% - 97%), according to both Guzzella [21] and Ehsani [24]. Also, an error was discovered with the efficiency calculation for negative motor torque, the efficiency ended up being 103% instead of 97%. This error was fixed by inverting the 97% efficiency when the motor torque is negative, shown in Figure 3-71.

- 99% → 97% rear differential efficiency update   (2% decrease)

- 106% → 94% (rear differential + gear reducer) efficiency when torque is negative   (11% decrease)
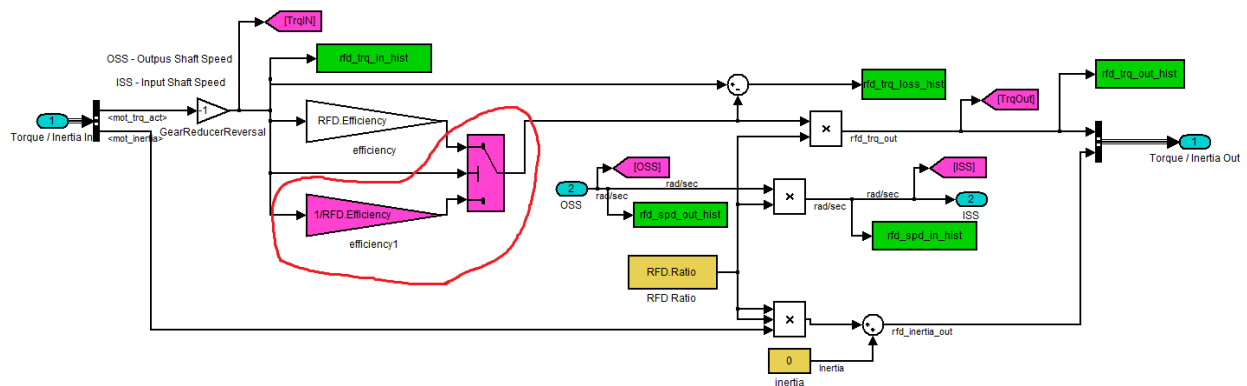
Figure 3-71. Plant model advancement: rear differential efficiency fixed for negative torque (regen).

3.8. Internal Combustion Engine Powertrain Plant Model Advancement

3.8.1. Engine Efficiency

The Internal Combustion Engine (ICE) efficiency error of negative efficiency during braking events previously identified in Figure 2-18, has been fixed. The fix was to limit bound efficiency between 0% and 100% and is shown in Figure 3-72.
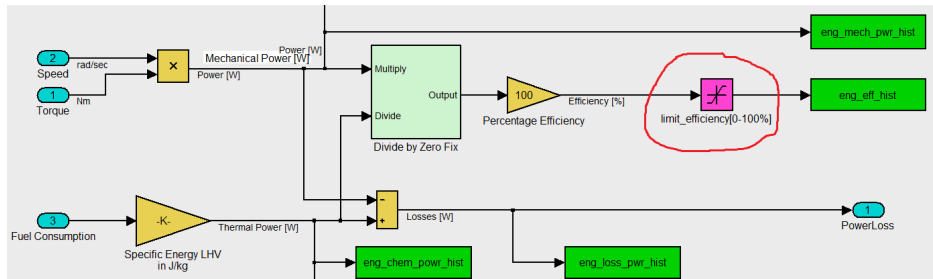
Figure 3-72. Plant model advancement: engine negative efficiency eliminated.

Engine efficiency never goes below zero anymore, shown in Figure 3-73, previously a problem during braking events.
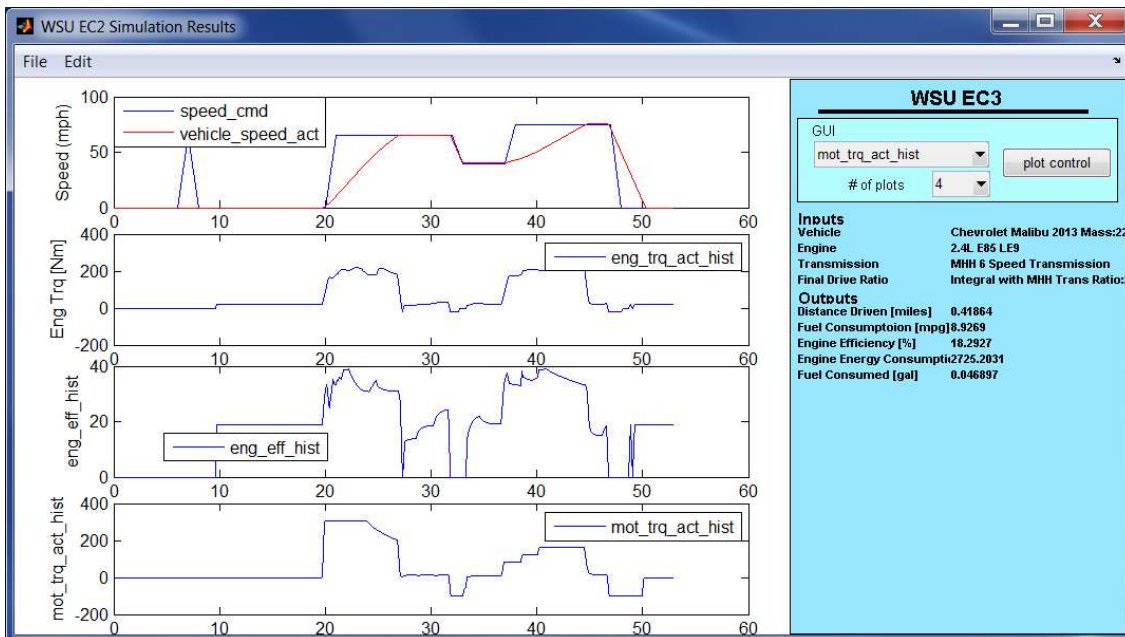
Figure 3-73. Thesis simulation results for acceleration (0-60, 50-70) and braking (60-0), shows ICE efficiency never going below zero.

3.8.2. Engine Rotational Inertia

The rotational inertial of the engine was increased from an initial assumption of 0.10 kg m^2 to a new assumption of 0.25 kg m^2. The new value was from another team's experimental data from performing engine coast downs (no fuel) with the engine decoupled from the transmission by disengaging the clutch while the vehicle was stationary in Park [34] and accounting for previously determined engine friction. Although the other team's value of 0.25 kg m^2 is for a different engine (the other team used a 1.8L four cylinder compared to WSU's 2.4L four cylinder engine), this update to inertia is directionally correct and brings the model closer to reality.

- 0.10 kg m^2 $\rightarrow$ 0.25 kg m^2 engine inertia   (150% increase)

3.8.3. Transmission

The transmission has the same type of error in efficiency as the rear differential for negative torque (engine braking) where the efficiency is greater than 100%. The same fix for the rear differential also applies here when torque goes negative: invert the efficiency for negative torque. The fix is shown in Figure 3-74.
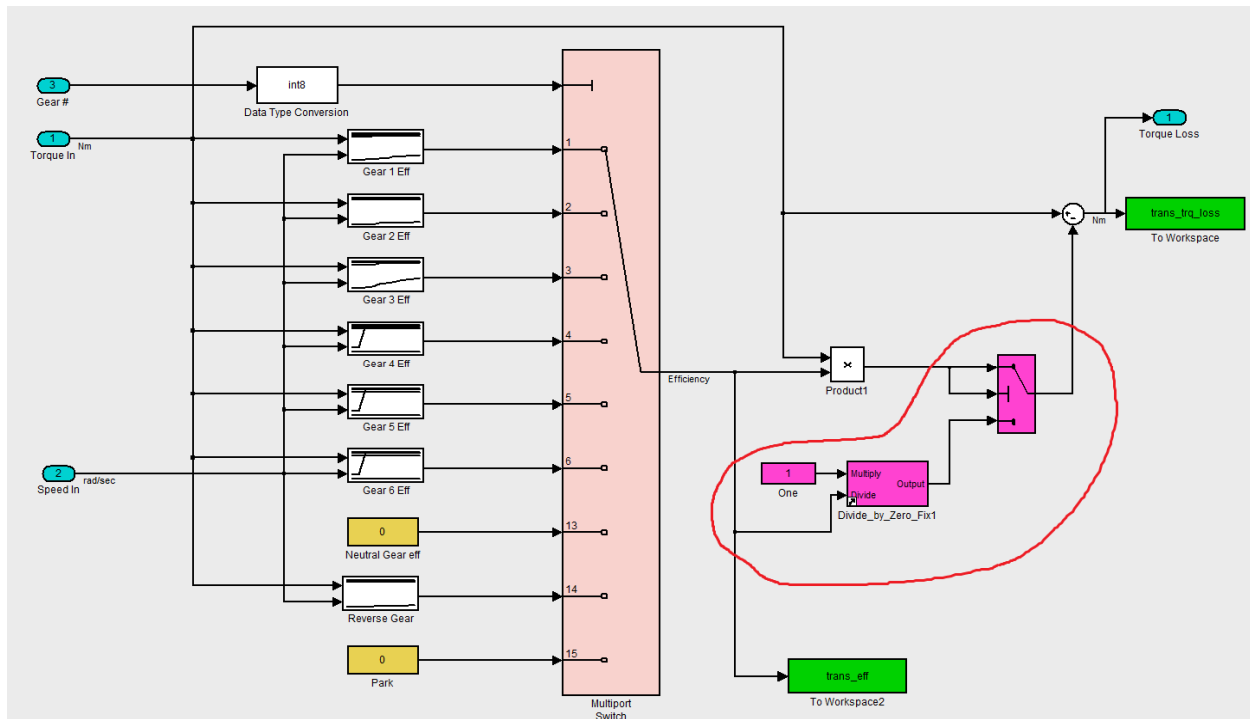
Figure 3-74. Plant model advancement: transmission efficiency fixed for negative torque (engine braking).

3.8.4. Front Differential

The front differential efficiency was updated from 99% to 97% to bring it in line with typical efficiencies of a gear pair (95% - 97%), according to both Guzzella [21] and Ehsani [24]. Also, an error was discovered with the efficiency calculation for negative engine torque (engine braking), the efficiency ended up being 103% instead of 97%. This error was fixed by inverting the 97% efficiency when the engine torque is negative, shown in Figure 3-75.

- 99% → 97% front differential efficiency update   (2% decrease)

- 103% → 97% front differential efficiency when engine torque is negative   (6% decrease)
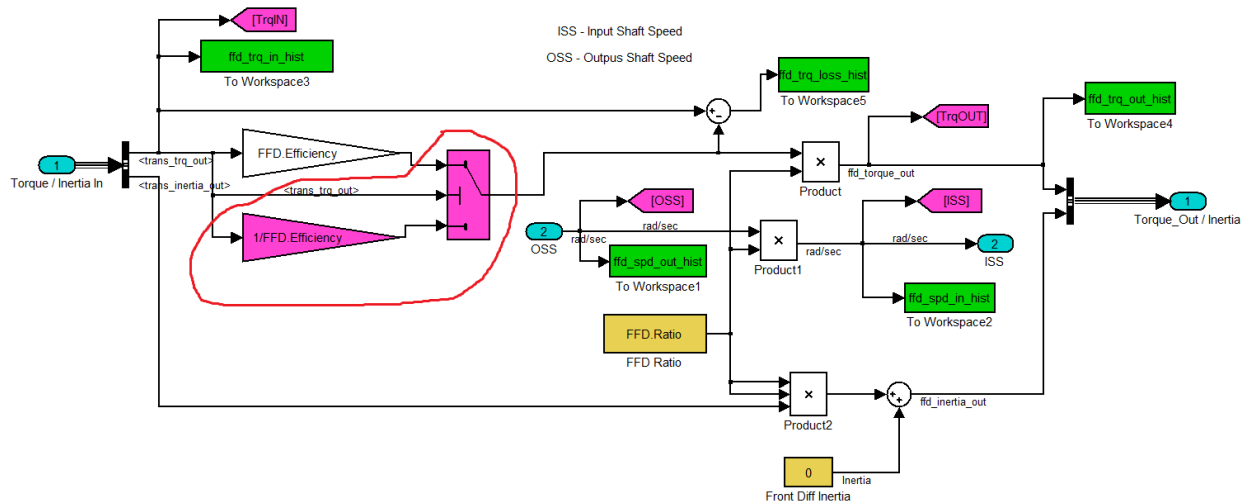
Figure 3-75. Plant model advancement: front differential efficiency fixed for negative torque (engine braking).

3.9. Total Effective Mass from including Rotational Inertias

All of the rotational inertia updates from the previous sections of Chapter 3 resulted in the rotational inertia effective mass increase becoming an average of 6.0%, up from 3.2%. This is directionally correct, as the original 3.2% effective mass increase from rotational inertia was unrealistically low. If the component inertias are unknown, then for a reasonable static, single value estimate of the overall rotational inertia effective mass, Larminie suggests using 5% [22] and Husain suggests a range of 8% -10% [20].

The thesis average of 6.0% rotational inertia effective mass increase comes from averaging the dynamic values for rotational inertia effective mass increase. One portion is with the electric motor's rotational inertia

connected through the gear reducer and then the rear differential to the rear wheels – this portion is the static portion and it increased from 2.4% to 3.6% by increasing the motor and both front & rear wheel rotational inertias described previously in section of Chapter 3 plant model advancements. The other portion is the dynamic portion which is the Internal Combustion Engine (ICE) effective rotational inertia due to the transmission gear selected (0 = neutral, 1st gear – 6th gear) through the front differential through the front wheels, shown in Figures 3-76 & 3-77.
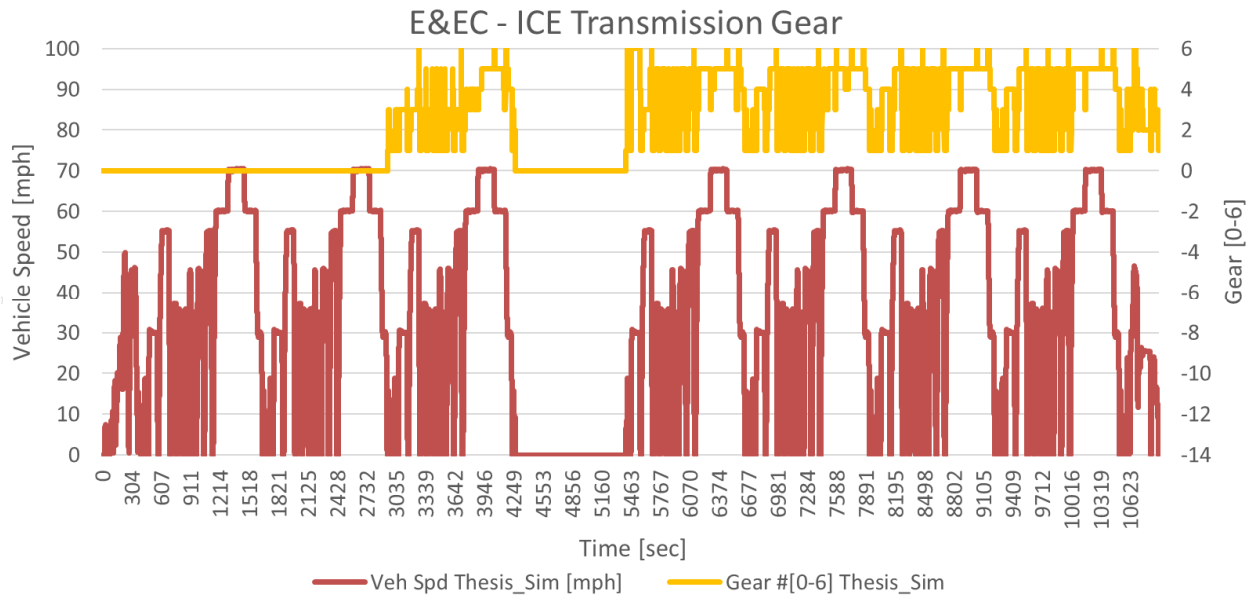
Figure 3-76. ICE transmission gear selection during E&EC drive cycle.

In Figure 3-76, the first portion of the E&EC drive cycle (1st & 2nd City Highways), the driving is electric only, so the engine is off and the transmission is in neutral gear. With the transmission in neutral gear, the engine is decoupled from the front wheels and does not contribute any rotational inertia, this is why the total effective mass is a constant value for this portion of the E&EC drive cycle.
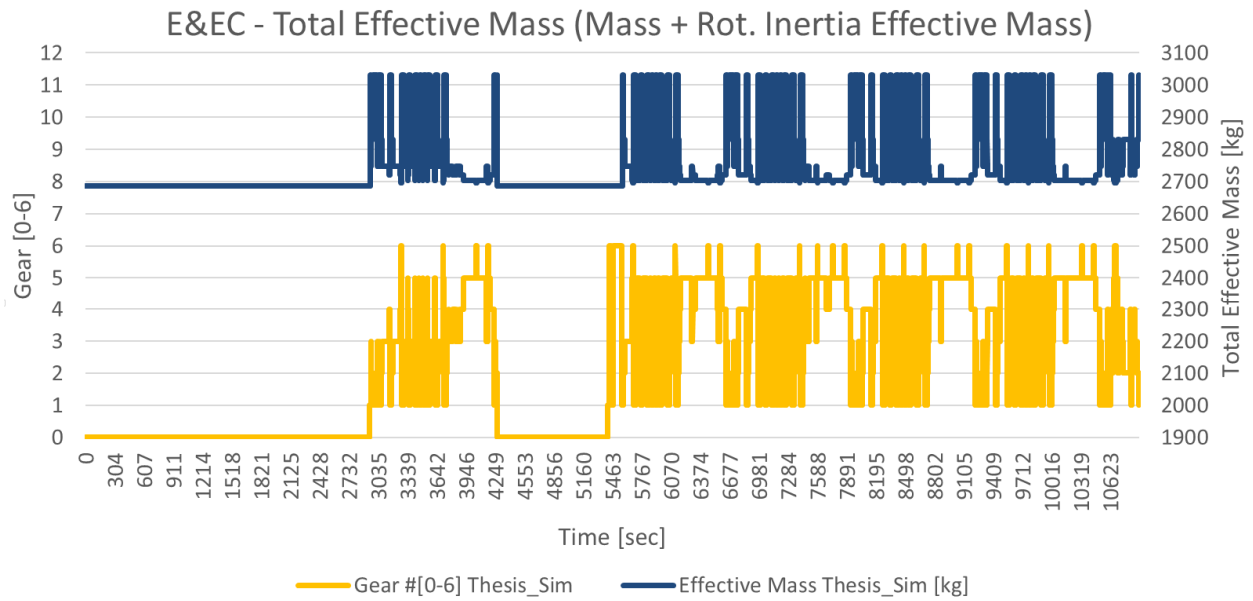
Figure 3-77. Total Effective Mass – Vehicle and Trailer Mass plus Rotational Inertia Effective Mass.

After the first 2 City Highways, the ESS is depleted and the engine turns on. When the engine is on, the 6 speed automatic transmission selects the appropriate gear to have engaged based on vehicle speed and driver demand (accelerator pedal position). The mass of the vehicle (2250 kg) and the emissions instrumented trailer (344 kg) is 2594 kg. When the transmission is in:

Neutral gear (decoupled), the engine inertia's effective mass at the wheels is zero, resulting in a 2687 kg effective vehicle mass, a 3.6% increase over just the mass total

1st gear (4.58:1 ratio), the engine inertia's effective mass at the wheels is the most, resulting in a 3031 kg effective vehicle mass, a 16.8% increase over just the mass total and 12.8% more than when in neutral

6th gear (0.75:1 ratio), the engine inertia's effective mass at the wheels is the least non-zero effective mass, resulting in a 2696 kg effective vehicle mass, a 3.9% increase over just the mass total and only 0.3% more than when in neutral

The variation of the total effective mass is quite large (12.8%, 3031 kg / 2687 kg) between engine on low speed driving (1st gear, 16.8%) and engine off (neutral gear, 3.6%), shown in Figure 3-78.
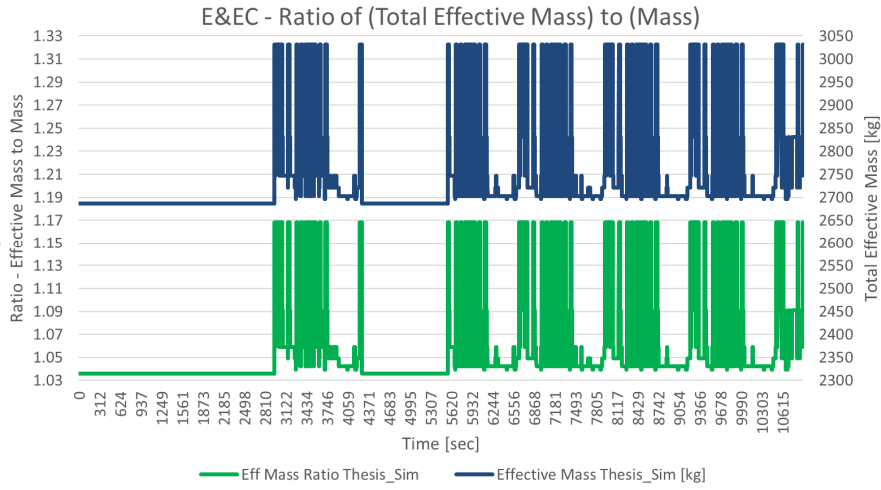
Figure 3-78. Ratio of (Total Effective Mass) to (Mass).

The thesis plant model advancement to the rotational inertias significantly shifted the effective total mass up, shown in Figure 3-79. The average of the thesis simulation effective mass is 6.0%, which is considerably more than the original WSU PTTR simulation effective mass average of 3.6%.

- 3.6% → 6.0% total average effective mass   (67% increase)
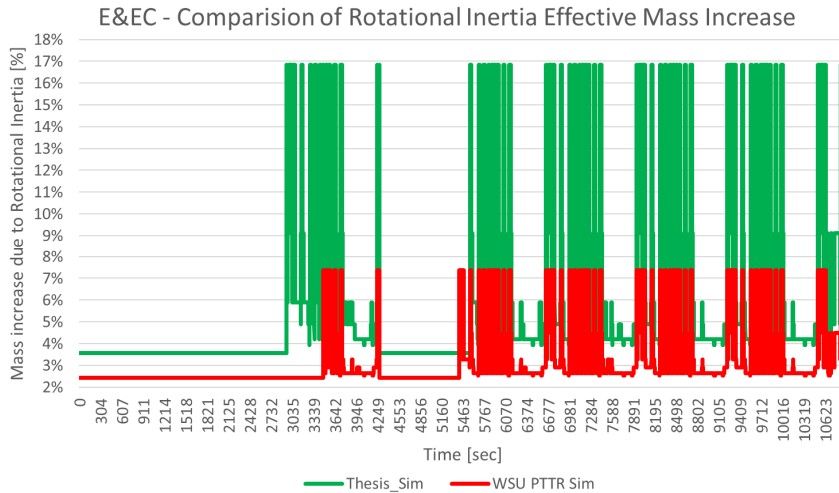
Figure 3-79. Plant model advancement – updated Effective Mass ratio from updated Rotational Inertias

3.10. Accessory Load Plant Model Advancement

3.10.1. Accessory Loads

Almost all of the accessory loads are electrical and therefore are easily quantifiable by the CAN message data from the APM input current or by the ESS discharge current when the APM is the only load on the high voltage bus. The engine's water pump and oil pump are the only mechanical accessory loads, but they are already accounted for in the engine's overall efficiency/fuel flow map.

The average accessory loads were increased from an initial assumption 900 W up to 1,150 W based on data from E&EC drive cycle. The E&EC drive cycle was run at night (headlights on, temperate ambient air temperature: 16.5°C/62°F).

- 900 W → 1,150 W accessory loads   (28% increase)

3.10.2. AC Plug-In Charging

Immediately after the E&EC drive cycle, the vehicle was plugged in and the ESS was charged back up to 100% SOC. The AC charging current and voltage was measured by the competition organizers and the results provided to the team: 73% charging efficiency. This compared poorly to the typical 87% charging efficiencies of teams from the previous EcoCAR competition. The On Board Charger (OBC) was a 3.3 kW Brusa unit, same as the previous EcoCAR competition, the difference was with the team's controls code keeping more items awake and running (pumps, controllers) during the charging event, decreasing the efficiency of charging. The charging efficiency has been updated from 87% to 73% and used in all the energy calculations for the E&EC results (see Table 2-2 from previous chapter and Table 4-2 in next chapter).

- 87% → 73% charging efficiency   (16% decrease)

CHAPTER 4. VEHICLE PLANT MODEL VALIDATION

4.1. Dynamic Performance Validation

After incorporating all of the plant model advancement changes into the thesis vehicle plant models, the dynamic performance of the WSU PTTR PHEV was re-run for:

1. 0-60 mph Acceleration

2. 50-70 mph Acceleration

3. Braking Distance, 60-0 mph deceleration

Table 4-1 shows the thesis simulation results for the dynamic performance compared to the stock vehicle, the competition targets, the actual experimental data, and the WSU PTTR simulation results.

- 0-60 Acceleration results no longer have any significant error

- 50-70 Acceleration results have increased error - mainly due to the large reduction adjustment of motor torque in the motor plant model at motor speeds above the motor's base speed to bring the motor plant model closer to experimental data (detailed in Section 3.7.2)

- Braking distance results have decreased error and is now acceptable

Table 4-1. Thesis simulation results for Dynamic Performance compared to experimental data.

EcoCAR 2 Vehicle Technical Specifications (VTS) - **Dynamic Performance**	Production 2013 Chevy Malibu (eAssist)	EcoCAR2 Competition Design Target	WSU PTTR Y3 E85 Experimental Data	THESIS E85 Simulation Prediction	WSU PTTR Y3 E85 Simulation Prediction
Acceleration 0-60 mph [0-96.6 kph]	8.2 sec	9.5 sec	6.4 sec	6.4 sec **(0% error)**	5.8 sec **(9% error)**
Accel. 50-70 mph [80.5-112.6 kph]	8.0 sec	8.0 sec	3.2 sec	3.8 sec **(19% error)**	3.7 sec **(15% error)**
Braking 60-0 mph	43.7 m [143.4 ft]	43.7 m [143.4 ft]	40.2 m [132 ft]	38.9 m [128 ft] **(3% error)**	25.3 m [82.9 ft] **(37% error)**

Figure 4-1 shows the thesis simulation results graphically plotted in the simulation tool GUI for the dynamic performance events of 0-60 accel, 50-70 accel, and 60-0 braking.
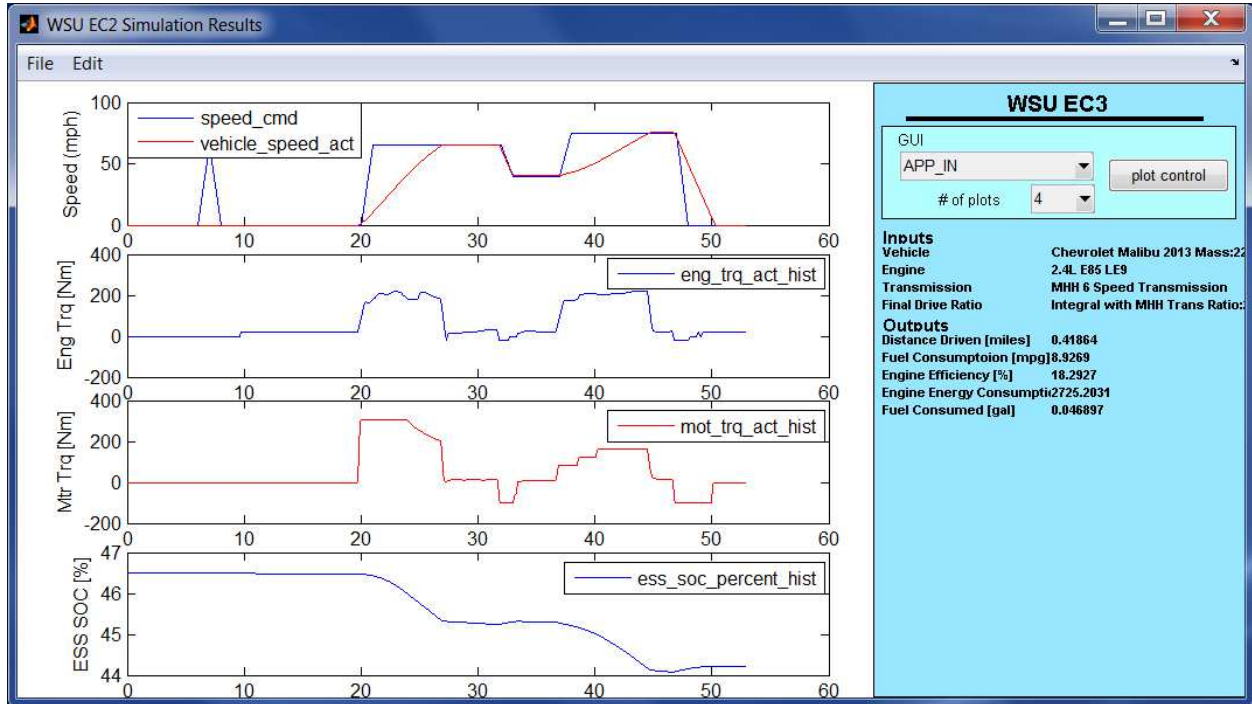
Figure 4-1. Thesis simulation results for acceleration (0-60, 50-70) and braking (60-0).

A before and after graphical comparison of the dynamic performance for the WSU PTTR simulation results

to the thesis simulation results is shown in Figure 4-2.
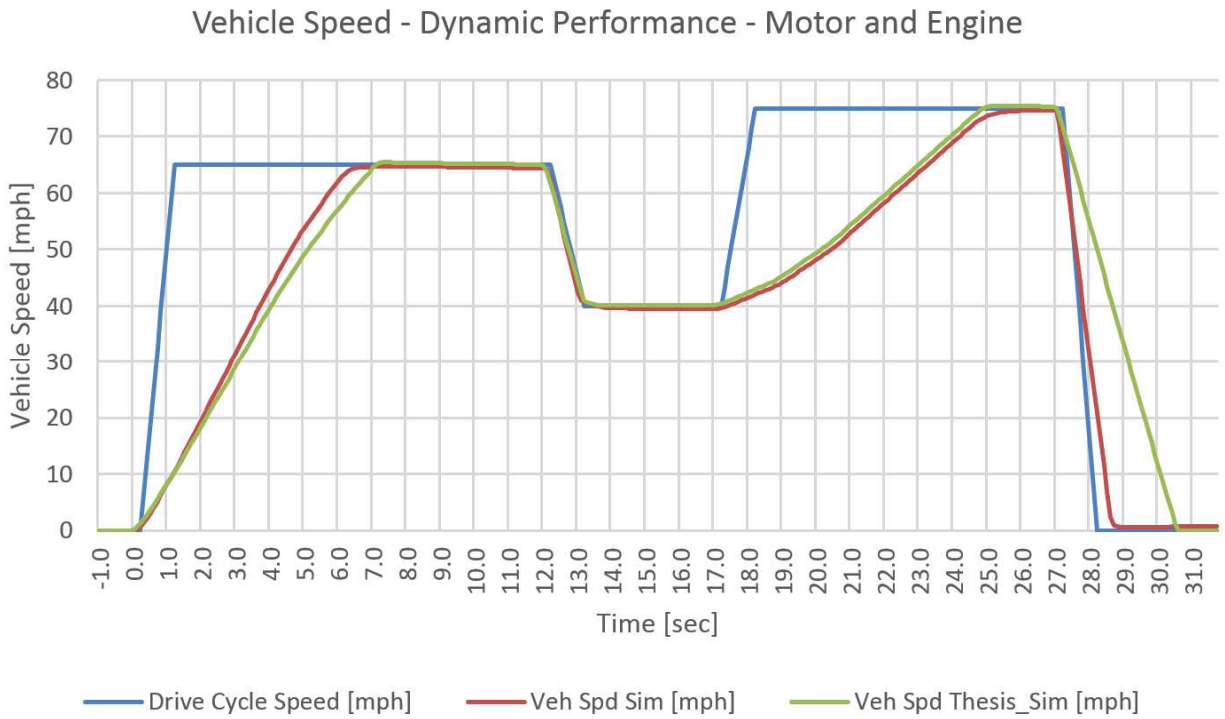
Figure 4-2. Thesis simulation results compared to WSU PTTR simulation results for acceleration (0-60, 50-70) and braking (60-0).

A before and after graphical comparison of the zoomed in view of the 0-60 accel for the WSU PTTR simulation results to the thesis simulation results with the experimental data is shown in Figure 4-3.
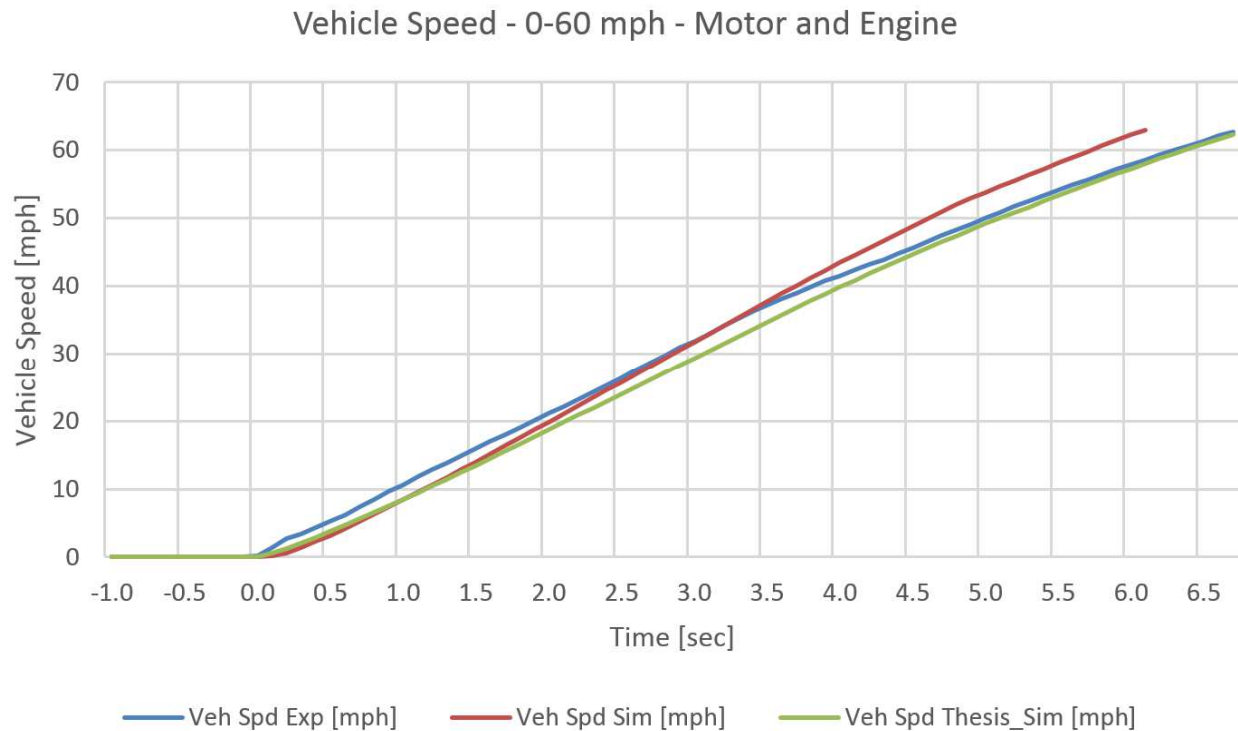
Figure 4-3. Thesis simulation results for acceleration 0-60 compared to experimental data and WSU PTTR simulation results.

Plant model advancement has completed an iteration loop of improvement on the electric motor powertrain and the vehicle chassis components, but has not been completed on the engine powertrain (skipped Engine, Transmission, and did not insert Torque Converter). Thesis comments on plant model advancement with respect to dynamic performance:

1. Electric motor performance in simulation is now acceptable – see motor only 0-60 accel back in Chapter 3.7.2.

2. E85 engine needs a Torque Converter plant model added to the vehicle model between the engine and the transmission. This is expected to be the largest factor in improvement to make dynamic performance behavior and results closer to experimental data.

2.1   The torque converter is in an unlocked state in 1st gear with 100% accel pedal - this provides a very significant torque multiplication on the engine's output torque, which would help shift the thesis simulation curve closer to the experimental data curve in Figure 4-3 for the duration of 1st gear (around the 4 seconds seen in Figure 4-3 where the experimental data curve leads the thesis simulation results curve).

2.2   After the approximately 4 seconds, in the experimental data, the transmission executes an upshift to 2nd gear and the torque converter is no longer unlocked. The upshift delay with the lack of an unlocked torque converter and the higher gear would reduce the lead of the curve, as seen in Figure 4-3.

3. Transmission gear shift execution time of ~0.5 sec could also be added along with the accompanying reduced engine output torque for the duration of each shift to make behavior and results closer to experimental data. This is expected to be a more significant factor for dynamic performance results than for energy consumption.

4.2.   Energy Consumption Validation

After incorporating all of the plant model advancement changes into the thesis vehicle plant models, the Emissions & Energy Consumption (E&EC) for the WSU PTTR PHEV was re-run for the following metrics:

1. Total Vehicle Range (ESS + Fuel Tank)

2. CD Range

3. CD Fuel Consumption

4. CS Fuel Consumption

5. UF-Weighted Fuel Energy Consumption

6. UF-Weighted AC Electric Energy consumption

7. UF-Weighted Total Energy Consumption

8. UF-Weighted WTW Petroleum Energy Use

9. UF-Weighted WTW GHG Emissions

Table 4-2 shows the Emissions & Energy Consumption (E&EC) comparison of the stock vehicle, the actual experimental data, the thesis simulation results, and the WSU PTTR simulation results. The AC charging efficiency

was updated from 87% (first EcoCAR competition population samples) to 73% for the WSU PTTR actual measured efficiency during competition.

Six of the eight metrics still have significant error. It is expected that this remaining error would significantly decrease if there was time to have the thesis scope cover adding in the missing torque converter plant model between the engine and transmission plant models, and also the validation & refinement of the engine & transmission plant models.

- Total vehicle range error reduced by more than half, but is still high at 16%

- Charge Depleting Range no longer has any significant error

- Charge Sustaining Fuel Consumption error reduced by half, but is still high at 24%

- UF-Weighted Fuel Energy Consumption error reduced by nearly half, but is still high at 27%

- UF-Weighted AC Electric Energy Consumption no longer has any significant error

- UF-Weighted Total Energy Consumption error reduced by nearly half, but is still high at 21%

- UF-Weighted WTW Petroleum Energy Use error reduced by nearly half, but is still high at 26%

- UF-Weighted WTW GHG Emissions error reduced by a quarter, but is still high at 31%

Table 4-2. Thesis simulation results for E&EC compared to experimental data.

EcoCAR 2 VTS - Emissions & Energy Consumption "On-Road Competition" Drive Cycle with SEMTECH instumentation trailer	Production 2013 Chevy Malibu (eAssist Hybrid) Experimental Data	WSU PTTR Y3 E85 Experimental Data	THESIS E85 Simulation Prediction	WSU PTTR Y3 E85 Simulation Prediction
Total Vehicle Range CD+CS (59.8 L [15.8 gal] stock tank, PTTR Y3 tank 34.2 L [9.04 gal])	606 km @ 59.8 L 383 km @ 37.9 L	243.3 km @ 34.2 L 151.2 mi @ 9.04 gal	281.2 km [174.8 mi] (16% error)	363.5 km [225.9 mi] (49% error)
Charge-Depleting (CD) Range	N/A	48.7 km [30.3 mi]	48.7 km [30.25 mi] (0.2% error)	54.1km [33.6 mi] (11% error)
Charge-Depleting (CD) Fuel Consumption	N/A	0	0	0
Charge-Sustaining (CS) Fuel Consumption	9.87 lge/100km	13.7 lge/100km	10.46 lge/100 km (24% error)	7.86 lge/100 km (43% error)
UF-Weighted Fuel Energy Consumption	9.87 lge/100km [842 Wh/km]	7.47lge/100km [665 Wh/km]	5.47 lge/100km [487 Wh/km] (27% error)	3.99 lge/100km [356 Wh/km] (47% error)
UF-Weighted AC Electric Energy Consumption	N/A	182 Wh/km	180 Wh/km*** (1% error)	166 Wh/km*** (9% error)
UF-Weighted Total Energy Consumption	842 Wh/km	848 Wh/km	666 Wh/km (21% error)	522 Wh/km (38% error)
UF-Weighted WTW Petroleum Energy (PE) Use	829 Wh PE/km	216 Wh PE/km	160 Wh PE/km (26% error)	118 Wh PE/km (45% error)
UF-Weighted WTW GHG Emissions	279 g GHG/km	351 g GHG/km	243 g GHG/km (31% error)	201 g GHG/km (43% error)

*** Includes 73% actual efficiency measured for WSU PTTR charging system and battery for grid AC electricity

Figure 4-4 shows the thesis simulation results graphically plotted in the simulation tool GUI for the E&EC drive cycle. The inverter fault was forced in the simulation at the same point as it actually occurred in the competition E&EC event.
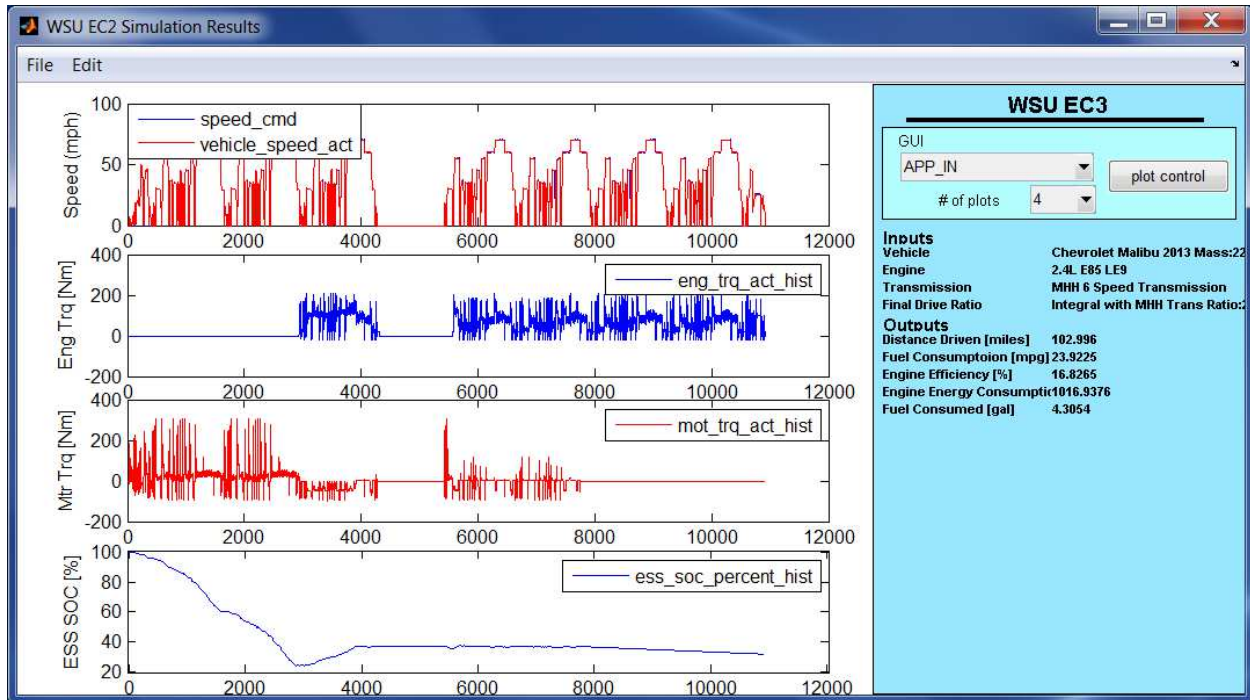
Figure 4-4. Thesis simulation results for E&EC drive cycle, including the inverter fault forced on.

The thesis simulation result for the speed trace of the E&EC is compared to the WSU PTTR simulation result in Figure 4-5.
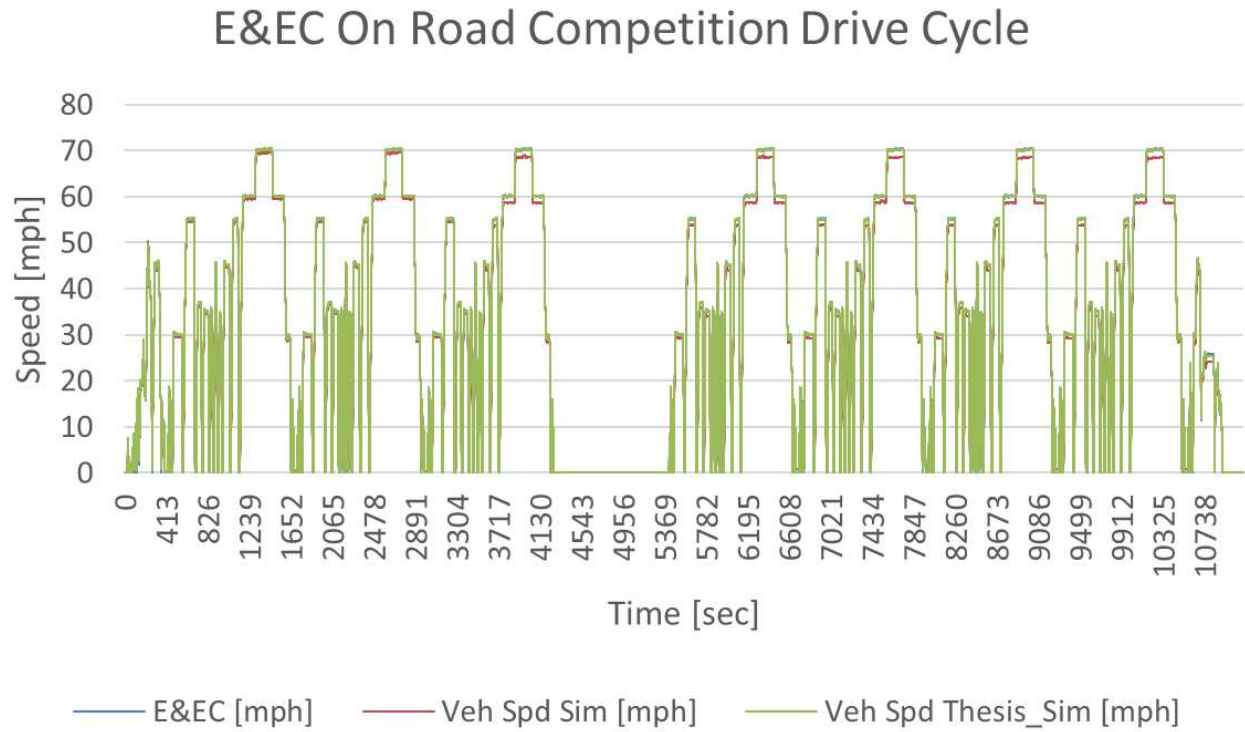
Figure 4-5. Thesis simulation results for E&EC drive cycle compared to the WSU PTTR simulation.

The 1st City Highway period is used to compare trace miss of the thesis simulation speed trace result to the WSU PTTR simulation speed trace result, shown in Figure 4-6.

- WSU PTTR Simulation Results: 7.6% trace missed by over 2 mph (99 out of 1299 seconds driving)

- Thesis Simulation Results: 0.0% trace missed by over 2 mph (0 out of 1299 seconds driving)
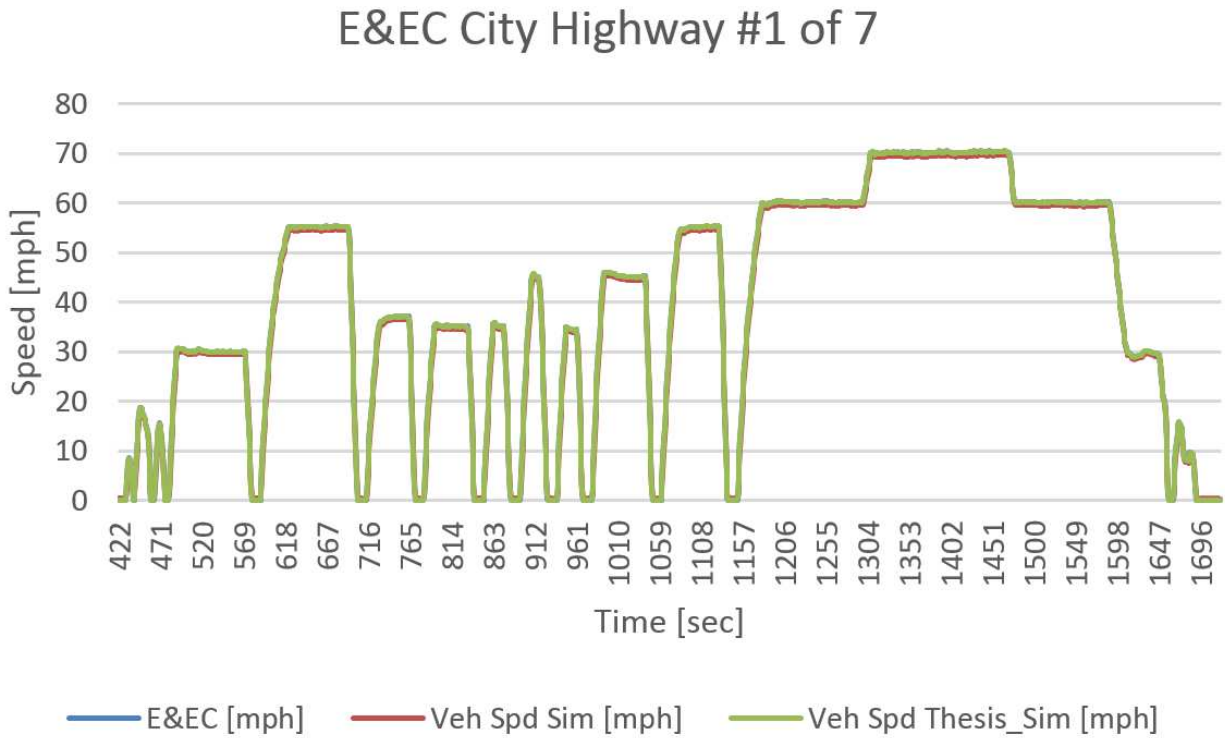
Figure 4-6. E&EC 1st City Highway comparison between thesis simulation and WSU PTTR simulation.

The 7th City Highway period is used to compare trace miss of the thesis simulation speed trace result to the WSU PTTR simulation speed trace result, shown in Figures 4-7, 4-8, and 4-9.

- WSU PTTR Simulation Results: 9.5% trace missed by over 2 mph (123 out of 1294 seconds driving)

- Thesis Simulation Results: 0.5% trace missed by over 2 mph (7 out of 1294 seconds driving)

- Thesis Driver PI controller model does much better at following the drive cycles than the original Driver PI controller model
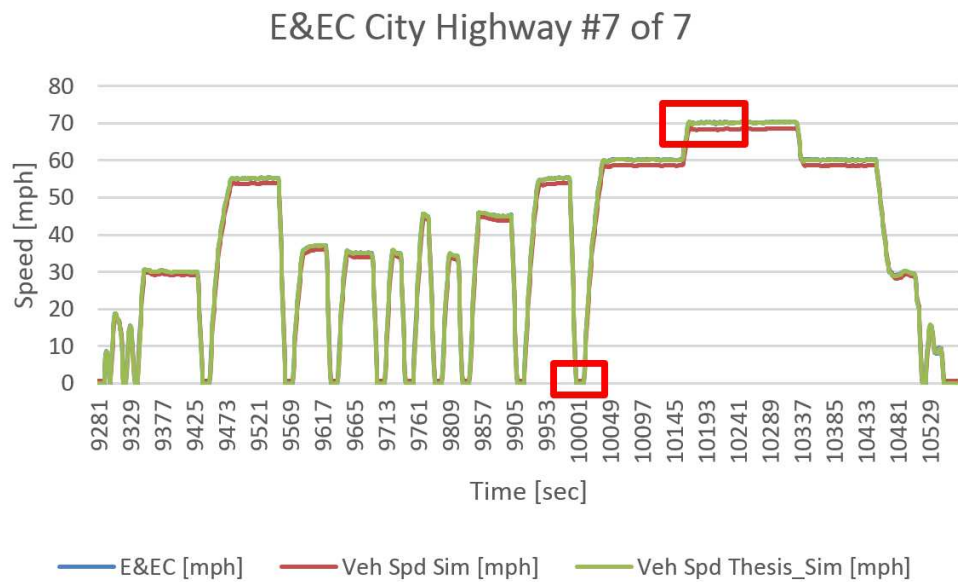
Figure 4-7. E&EC 7th City Highway comparison between thesis simulation and WSU PTTR simulation.
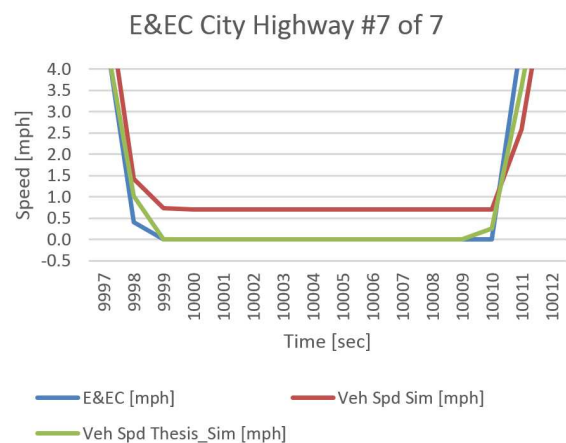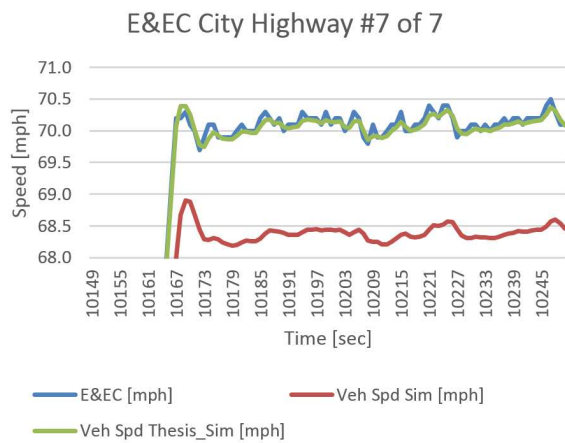
Figures 4-8 & 4-9. E&EC 7th City Highway comparison detail trace miss at 70 mph and 0 mph target speeds.

The Thesis simulation results for distance driven is closer to both (a) E&EC drive cycle distance and (b) experimental data distance, than the WSU PTTR simulation results.

- Distance driven for 103.7 mile E&EC drive cycle:

    o 103.0 miles driven in thesis simulation

        ▪ 0.7% error distance driven from E&EC

        ▪ 0.3% error distance driven from experimental data

    o 101.5 miles driven in WSU PTTR simulation

        ▪ 2.1% error distance driven from E&EC cycle

        ▪ 1.2% error distance driven from experimental data

    o 102.7 miles driven in experimental data

        ▪ 1.0% error distance driven from E&EC cycle

The thesis simulation result for the SOC trace of the E&EC is compared to the WSU PTTR simulation result and the experimental data in Figure 4-10.

- Thesis simulation result for SOC now follows the experimental data for SOC for charge depletion with acceptable error

- After transitioning to charge sustaining, the thesis result SOC climbs back up much faster from charging through the road while driving than the experimental data SOC

    o Potentially more work may be needed for charging mode in the motor (generator mode) and inverter

    o Engine and Torque Converter have not been covered by the thesis work, it is very probable that improvement to these would also affect the charging rate and SOC climbing rate
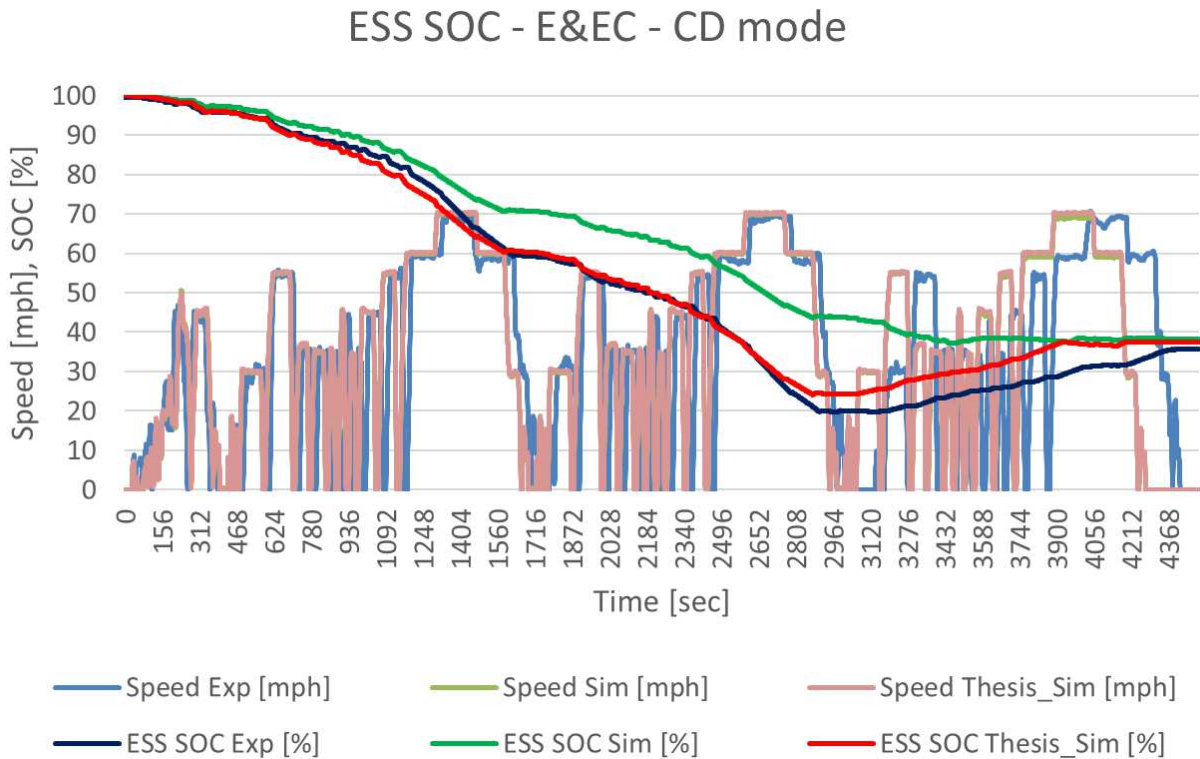
Figure 4-10. ESS SOC from E&EC - validation failure of simulation results to experimental data.

As previously discussed in Section 2.5 (see Figure 2-30), the driving on the oval test track for the experimental data did not strictly follow the timing of the E&EC drive cycle, as the experimental data is time shifted by various amounts throughout the entire 103.7 mile drive cycle. Because of the time shifting, direct comparison and validation is not possible on the E&EC cycle as a whole, so direct comparison was done on individual City Highway periods. The first two City Highway periods are compared individually after time shifting to speed align the data, shown in Figures 4-11 & 4-12.

- 3.4% error for thesis sim SOC used in 1st City Highway (was 28% error for WSU PTTR sim)

    o 35.7% SOC used in thesis simulation results (3.4% error)

    o 36.9% SOC used in experimental data

    o 26.6% SOC used in WSU PTTR simulation results (28% error)

- 7.7% error for thesis sim SOC used in 2nd City Highway (was 31% error for WSU PTTR sim)

    o 35.9% SOC used in thesis simulation results (7.7% error)

    o 38.9% SOC used in experimental data

    o 26.6% SOC used in WSU PTTR simulation results (31% error)
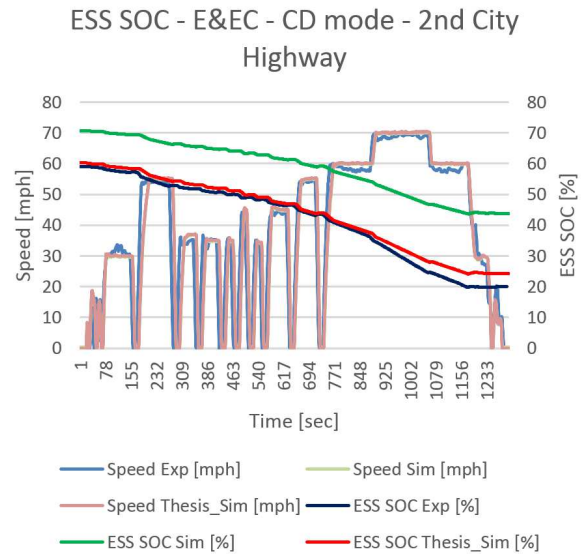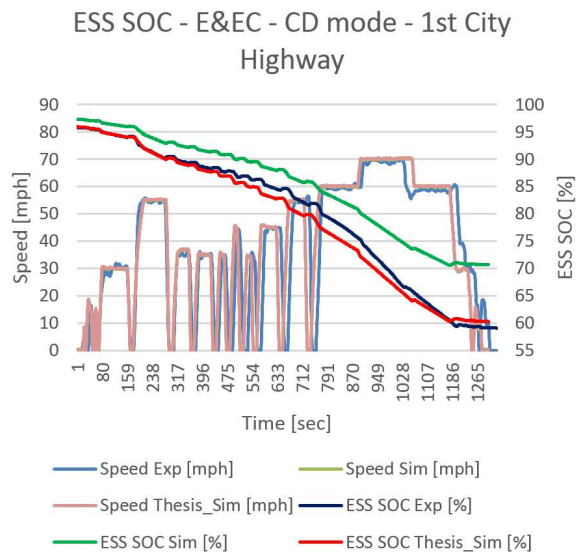
Figures 4-11 & 4-12. First two City Highway's speed aligned with ESS SOC compared by drive cycle trace.

Thesis comments on plant model advancement with respect to energy consumption after an iteration loop of improvement on the electric motor powertrain and the vehicle chassis components, but not on the engine powertrain (skipped analysis on Engine and Transmission, did not add a Torque Converter to the model):

1. ESS SOC simulation results are now much closer to actual experimental data with the advancements made in the plant models for this thesis.

2. E85 engine needs a Torque Converter plant model added to the vehicle model between the engine and the transmission. The high losses with a torque converter when it is not locked up are expected to be the largest factor in improvement to make energy consumption results closer to experimental data.

3. For energy drive cycles like the E&EC, transmission gear shift execution time of ~0.5 sec with the accompanying reduced engine output torque for the duration of each shift is expected to be less of a factor than for the dynamic performance type drive cycles.

4.3. Summary of Plant Model and Simulation Advancements

Advancements made for this thesis for error reduction to the original WSU PTTR plant model are summarized from the previous chapter into Table 4-3. Also, the E&EC drive cycle used for simulations was updated by adding an 18 minute soak (shift from Drive to Park, key off, soak 18 min, key accessory, key run, key crank, key run, shift from Park to Drive) between the 3rd City Highway and the 4th City Highway, to exactly match the actual soak period from the experimental data from competition. The original E&EC drive cycle used for simulations did not have any soak time, the addition of the soak time did not change the E&EC metrics results, but now the vehicle behavior in simulation better matches the experimental data.

Table 4-3. Thesis plant model advancements made to the original WSU PTTR simulation.

Plant Model Advancement - Summary of Chapters 3.6 - 3.10	Error Reduced?			
	0-60	50-70	Braking	E&EC
Driver PI Controller: Integral gain reset problem fixed by model code change.	na	na	**Yes**	**Yes**
Driver PI Controller: Brake pedal command not enough to hold vehicle at a stop, fixed by model code change.	na	na	**Yes**	**Yes**
Driver PI Controller: PI gain combination not large enough for vehicle speed to ever reach target speed, fixed by **130+% increase** in proportional	**Yes**	**Yes**	**Yes**	**Yes**

gains, **70% decrease** in of integral gain.				
Driver PI Controller: Accel & Brake Pedal rate of change updated, full travel occurs now occurs in 0.3 seconds, was 0.1 seconds (this was too fast, not matching reality), **200% increase**.	na	na	na	**Yes**
Driver PI Controller: Controller too reactive (lagging trace), not reading ahead in anticipation like real driver, added look ahead feature.	na	na	na	**Yes**
Driver PI Controller: Controller pedal command oscillation between Accel & Brake fixed when speed error is very small, fixed with +/-1% dead zone.	na	na	na	**Yes**
Driver PI Controller: Integral windup was too large, fixed with an additional speed based gain added in parallel to proportional and integral gain.	na	na	na	**Yes**
Wheel: Effective radius was too large, fixed by **4.3%/4.9% (Front/Rear) decrease** affecting component speeds and rotational inertia (shaft speeds and rotational inertia increased after fix).	**Yes**	**No**	**Yes**	**Yes**
Wheel: Wheel total rotational inertia low (rubber tire, alloy wheel, iron brake disc), fixed by **increasing 33%** to 1.60 kg m^2 (was 1.2 kg m^2).	**Yes**	**No**	**Yes**	**Yes**
Wheel: Wheel slip plant model now detecting wheel slip on front wheels after motor torque reductions, fixed temporarily with bypass around wheel slip model since experimental results did not indicate any wheel slip, this just allowed the altered thesis model to once again follow the drive cycle trace rather than getting stuck in a limp mode.	na	na	na	na
Braking force: Force was sent instead from driver PI controller to wheels instead of torque (this was a very significant error), wheel plant model expected torque as input, fixed by converting force to torque before sending to wheels (**67% decrease**).	na	na	**Yes**	**Yes**
Braking force: Total brake force changed from Y1 to Y2/Y3 due to change of mass at rear axle, resulting CG change, and resulting vehicle pitch change of rear lower than front, fixed by updating total braking force based off Y3 experimental braking distances (**increased force 29%**).	na	na	**Yes**	**Yes**
Braking force: Force split front/rear not used, all force went to front wheels, fixed by splitting total braking force between front & rear, assumed 60% of force to front (was 100% of force).	na	na	na	na

Emissions Instrumentation Trailer for E&EC: Trailer mass missing from inertial term of road load in chassis plant model (inertial term had only (1)vehicle mass and (2) rotational inertia equivalent mass are accounted for, was missing (3) trailer mass), fixed by changing model to include trailer mass (**15% increase**).	na	na	na	**Yes**
Emissions Instrumentation Trailer for E&EC: Trailer mass wrong by 10 kg too low, was 334 kg, fixed to 344 kg (**3% increase**).	na	na	na	**Yes**
ESS: ESS does not have coulombic losses, only has ohmic losses. Added an assumed 1% coulombic loss to both charge and discharge current (**1% decrease** in efficiency).	na	na	na	**Yes**
Motor: Adjusted peak and continuous torque curves down slightly and shifted base speed in model to match experimental data, resulting in very significant torque reduction at speeds above the newly fixed based speed.	**Yes**	**No**	na	**Yes**
Motor: Reduced entire motor efficiency table down by 8% (multiplied all values by 0.92), these adjustments were iterative based on repeated simulations of the E&EC drive cycle electric range to get a closer ESS % SOC match to the experimental data (**8% decrease**).	na	na	na	**Yes**
Motor: Reduced inverter initial assumed constant efficiency down from 97% to 92%, these adjustments were iterative based on repeated simulations of the E&EC drive cycle electric range to get a closer ESS % SOC match to the experimental data (**5% decrease**).	na	na	na	**Yes**
Motor: Increased motor rotational inertia based on finding manufacturer's specification actual value, initial assumption was too low, so after fixing, rotational inertia **increased 38%**.	**Yes**	**No**	**Yes**	**Yes**
Motor: Inverter: Error with inverter switching losses for regen reducing the losses for motoring. Fixed by adding absolute value to the inverter losses so they are always accumulating, never decreasing for regen.	na	na	na	**Yes**
Motor: Increased pump speeds due to trace miss of drive cycle from motor component high temperature fault as a result of the changes made to reduce motor and inverter efficiencies. No more over temp faults after adjustments.	na	na	na	na
Gear reducer: Gear reducer has no losses (can't be 100%), added efficiency of 97% (**3% decrease**).	**Yes**	**No**	na	**Yes**

Gear reducer: Gear reducer ratio is wrong (still using 2.57 belt reduction ratio instead of 2.474 gear reduction ratio), fixed by changing to 2.474 ratio (**4% decrease**).	**Yes**	**No**	na	**Yes**
Front & Rear differentials: Both differentials assumed to be 99% efficient, reduced to 97% efficiency (**2% decrease**).	**Yes**	**No**	na	**Yes**
Front differential: Efficiency wrong for negative torque (regen, engine braking), the efficiency is inverted for negative torque (i.e. what should be 97% efficiency wrongly becomes 103% efficiency for negative torque), fixed by model code change (**6% decrease**).	na	na	na	**Yes**
Rear differential & gear reducer: Efficiency wrong for negative torque (regen, engine braking), the efficiency is inverted for negative torque (i.e. what should be 94% efficiency wrongly becomes 106% efficiency for negative torque), fixed by model code change (**11% decrease**).	na	na	na	**Yes**
Engine: Engine efficiency in 0-60 & 50-70 goes negative during decel, can't have negative efficiency, fixed by model code change to limit efficiency to 0-100%.	na	na	na	na
Engine: Engine rotational inertia increased to 0.25 kg m^2 from initial assumption of 0.1 kg m^2, choose 0.25 based on a published paper from another team (**150% increase**).	**Yes**	**No**	**Yes**	**Yes**
Accessory loads: Increased average accessory loads to 1,150 W, up from 900 W (**28% increase**).	na	na	na	**Yes**
Plug-In AC Wall Charging: Reduced charging efficiency from assumed 87% to actual 73% (**16% decrease**).	na	na	na	**Yes**

na - not applicable

Finally, there are two major advancements that had no direct impact on the error reduction, but did have an indirect impact because of actions taken as a result of the output from these additions:

1. Added trace missed by 2 mph in simulation tool (missed time total & percent), helps one to understand how useful their results may be, also check to see for E&EC On-Road what % the simulation missed trace

2. Added Energy flow (in, out, %efficiency) for each component to debug and check for reasonableness. Also check total overall efficiency for each component and the interface from one component to its

adjoining neighbors, making sure energy isn't "lost/gained" where it shouldn't be. Adding energy helped find errors in the negative torque through the front & rear differentials

CHAPTER 5. DISCUSSION

Energy Flow: The addition of energy flow through each component was accomplished by adding code for each plant model, examples shown in Figures 5-1 & 5-2. Energy flow is a critical part of any simulation for fuel economy & energy consumption, this allows energy audit for reasonableness and errors. Other fuel economy modeling and simulation tools like Autonomie [23] and VTool [35] (another team's self-developed tool) track energy flow through each component. Several items for investigation in the model were discovered by adding energy flow to the WSU PTTR tool for this thesis:

1. Efficiency of negative (reverse) torque/energy for front & rear differentials was inverted 103% efficient for negative torque instead of using the same 97% efficient that the positive torque used, the efficiency inversion was fixed in the code so that positive and negative torque used the same efficiency (details in Chapters 3.7.7. Rear Differential Efficiency and 3.8.4. Front Differential Efficiency).

2. No engine braking during vehicle deceleration when in transmission is in drive, but no changes made, investigating the engine ended up falling outside of the scope of this thesis due to time constraints.

3. Efficiency of negative (reverse) torque/energy for transmission was also inverted (no actual effect due to lack of modeled engine braking during decel), fixed by inverting efficiency for negative torque, further investigation of the transmission ended up falling outside of the scope of this thesis due to time constraints.

4. Motor Inverter power losses were being underreported because the regen losses were being subtracted from the motoring losses, instead both losses needed to be added together (details in Chapter 3.7.4. Motor Inverter).

5. ESS efficiency seems marginally high, so it was adjusted down by 1% [28] (details in Chapter 3.7.1. Energy Storage System (ESS)).

6. Engine efficiency may be a little high, but no changes made, investigating the engine ended up falling outside of the scope of this thesis due to time constraints.
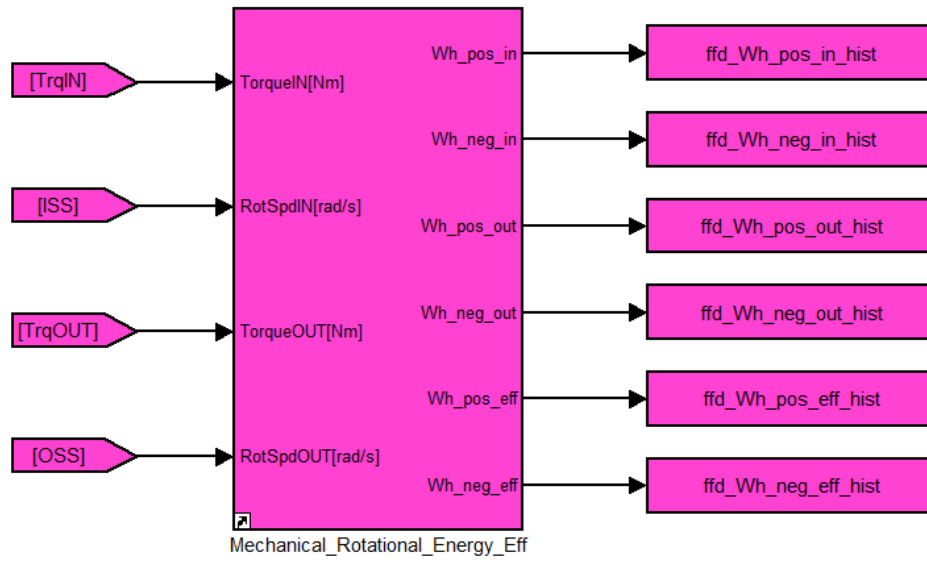
Figure 5-1. Example of mechanical energy flow input/output accounting added to differential plant model.
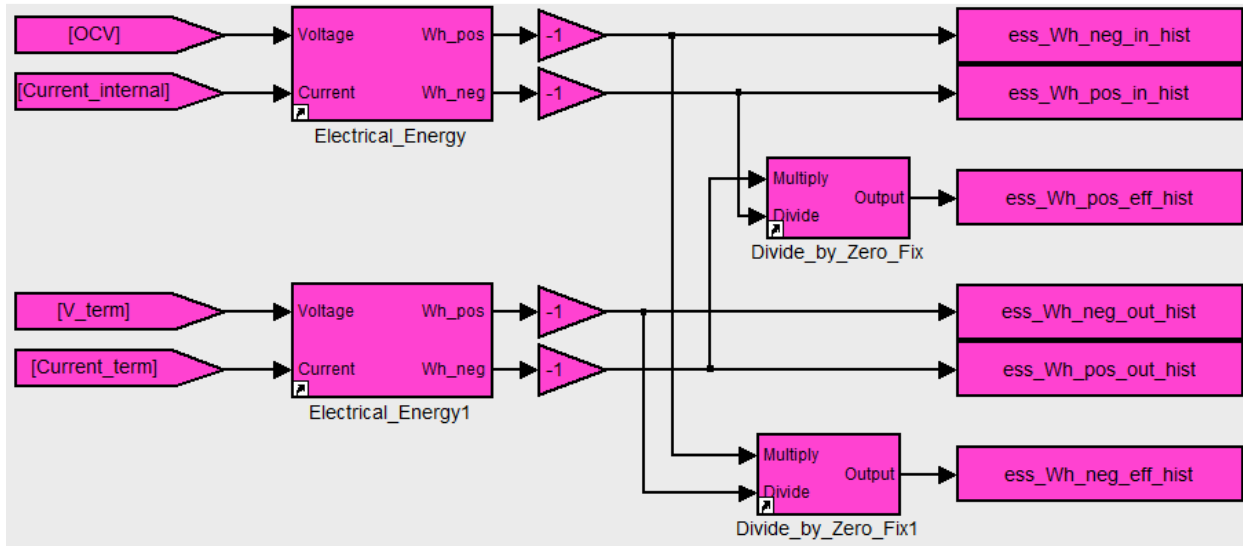
Figure 5-2. Example of electrical energy flow input/output accounting added to ESS plant model.

Vehicle road load was updated to separate the positive (tractive) load form the negative load (decel) and is shown in Figure 5-3. By having the energy separated by positive and negative, following all of the energy is possible from one component plant model to the next for all vehicle behavior. It is not possible to follow all of the energy if both the positive and negative energy are combined together.
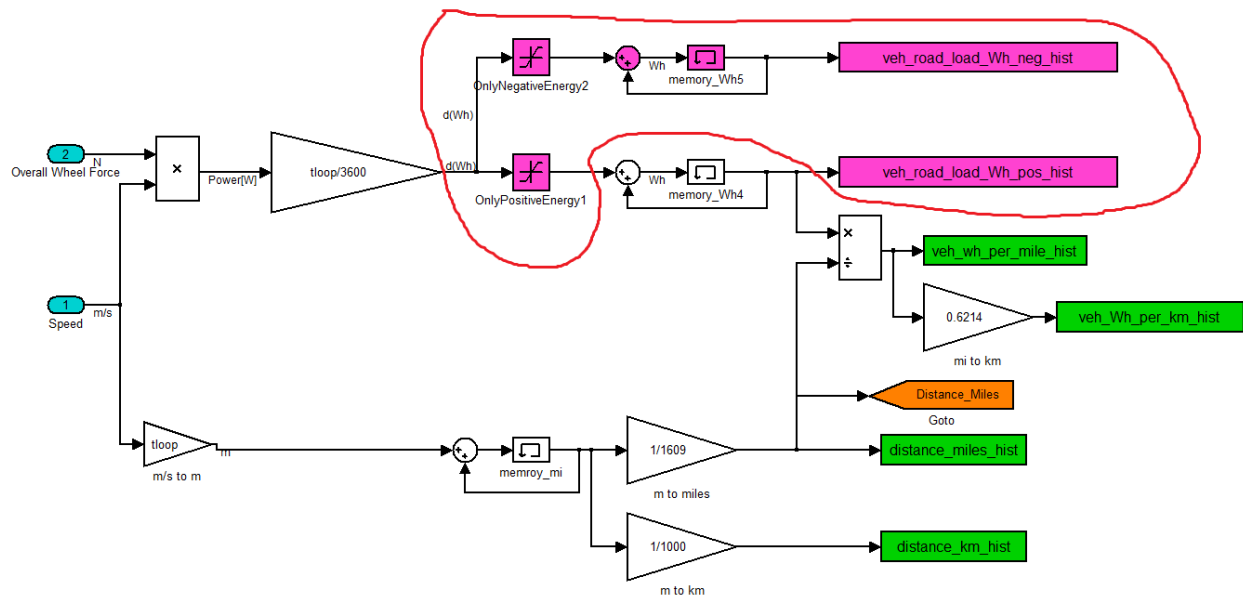
Figure 5-3. Road load separation of the positive and negative loads.

The newly added energy flow report from the thesis simulation for the E&EC competition drive cycle is shown in Table 5-1. The positive road load of 227.6 Wh/km was checked for reasonableness to a spreadsheet calculation result of 245.0 Wh/km, a 7.1% discrepancy. The spreadsheet calculation is inherently less accurate than desired, as it used the E&EC drive cycle at the original 1 Hz data rate while the simulations used interpolation to create a 100 Hz high resolution version of the E&EC drive cycle.

The spreadsheet calculation also used a constant 6.0% addition to the vehicle mass to simulate the addition of an average total rotational inertia to the effective mass while the simulation dynamically calculated the rotational inertias based on the current transmission gear. The average effective mass increase of the dynamically calculated rotational inertia was 6.0%, which was nearly double the original 3.6% rotational inertia effective mass from the WSU PTTR simulation model. The 6.0% was much more reasonable than 3.6%, as sampling of other publications shows Larminie suggests 5% [22] and Husain suggests 8%-10% [20].

Table 5-1. Energy flow through each powertrain component for E&EC on road competition drive cycle.

Trace missed by more than 2 mph	0.2	%
Distance Driven	103.0	mi
Distance Driven	165.7	km
Vehicle Chassis Energy positive	37,718.0	Wh
Vehicle Chassis Energy negative	-11,170.2	Wh
Accessory Losses	3,306.2	Wh
Accessory Losses	1.1	kW
Road Load (positive)	227.6	Wh/km
Front Wheel energy pos	31,456.4	Wh
Rear Wheel energy pos	11,461.8	Wh
Front Wheel energy neg	-4,592.9	Wh
Rear Wheel energy neg	-11,777.5	Wh
Rear Diff energy pos out	11,461.8	Wh
Rear Diff energy neg out	-8,668.8	Wh
Rear Diff energy pos in	12,181.8	Wh
Rear Diff energy neg in	-8,156.5	Wh
Rear Diff energy pos eff	94.1	%
Rear Diff energy neg eff	94.1	%
Front Diff energy pos out	31,526.4	Wh
Front Diff energy neg out	0.0	Wh
Front Diff energy pos in	32,501.5	Wh
Front Diff energy neg in	0.0	Wh
Front Diff energy pos eff	97.0	%
Front Diff energy neg eff	0.0	%
Trans energy pos out	32,501.5	Wh
Trans energy neg out	0.0	Wh
Trans energy pos in	34,409.5	Wh
Trans energy neg in	-174.0	Wh
Trans energy pos eff	94.5	%
Trans energy neg eff	0.0	%
Mot + MCU energy pos out	12,181.8	Wh
Mot + MCU energy neg out	-8,156.5	Wh
Mot + MCU energy pos in	16,024.7	Wh
Mot + MCU energy neg in	-6,482.9	Wh
Mot + MCU energy pos eff	76.0	%
Mot + MCU energy neg eff	79.5	%
Engine energy pos out	34,956.4	Wh
Engine energy pos in	104,740.5	Wh
Engine energy pos eff	33.4	%
Engine energy neg out	-174.0	Wh

DCDC energy pos out	2,975.6	Wh
DCDC energy pos in	3,306.2	Wh
DCDC energy pos eff	90.0	%
ESS energy pos out	18,833.0	Wh
ESS energy neg out	-5,985.0	Wh
ESS energy pos in	19,354.4	Wh
ESS energy neg in	-5,862.7	Wh
ESS energy pos eff	97.3	%
ESS energy neg eff	98.0	%

Trace missed by 2 mph: The addition of the percent trace missed by 2 mph allowed quantification of the how much excessive error there was in following the drive cycle. The larger the amount of trace miss, the less useful the simulation results become, and the less they approximate reality. Trace miss is an appropriate metric for fuel economy drive cycles, but not an appropriate metric for dynamic performance where the drive cycle is a series of step functions that always have excessive trace miss.

The added metric showed the improvement of the thesis simulation Driver PI controller model to the original WSU PTTR simulation Driver PI controller where trace missed by 2 mph was reduced by 95%:

7.6% → 0.0% on 1st City Highway

9.5% → 0.5% on 7th City Highway

Accessory Load: The 1,150 W average accessory load of the experimental data from the E&EC drive cycle is high partially due to the headlights & taillights being on because the drive was done during the night. The difference from the 900 W in the WSU PTTR simulation to the 1,150 W in experimental data is mainly attributed to the headlights & taillights that were not considered as it was expected that the E&EC driving be done during the day. It does not appear that the simulation was updated to include headlights & taillights after the team learned in Year 2 that the E&EC driving is done at night.

Wheel Effective Radius: An interesting future work item would be to increase rear tire pressure from 45 psi to 50 psi to see if the rear became even closer to the front for wheel effective radius. The additional 5 psi would reflect bringing the rear tires to the same ratio axle load to tire pressure as the front tires.

Electric Traction Motor: The motor efficiency map based on speed and torque used in the simulation does not handle zero motor speed and near zero motor speed very well. This is a high loss region of the motor operation and the efficiency map does not do the best job of delivering expected torque output and losses. For

example, at zero rpm speed and any torque, the efficiency is zero, yet the motor efficiency map needs to have a significant non-zero efficiency (say 40+%), otherwise excessive current beyond the ESS capability would be required to provide the torque necessary to get the motor spinning and produce initial vehicle movement. A future work improvement would be to replace the motor efficiency map with a motor power loss map based on speed and torque, which avoids the above mentioned compromised situation. Another team in EcoCAR competition ended up doing just this. In [6], Waldner describes the creation of such a map for their implementation.

Also, the simulation model only uses the peak motor torque curve and never de-rates to the continuous torque curve. This would normally be a problem in the simulation results, but the battery peak output de-rates down to the battery continuous output faster than the motor de-rates, so there isn't currently a problem with the simulation results. However, if the motor or battery are changed, there could easily be a problem with the simulation results in the future.

Driver PI controller plant model: With the evolution of the plant model increasing in features added to the control logic, there is probably the opportunity to remove some of the earlier changes like the integral summation gain reset as the integral windup gain limiter is now +/-15% instead of +/-100%. So revisiting the fixes to Problems 1 & 2 to see if the fixes can be deleted from the plant model for simplification (complexity reduction) reasons. Initially, no Driver PI controller plant model changes were expected, however upon the first close analysis of dynamic performance showed that many items were in need of fixing. Now drive cycles' intended road loads and distance traveled are achieved with the thesis Driver PI controller, so results are closer to experimental data. Driver PI controller is now probably "too good" in that it follows the drive cycle better than any human driver could, so some decreasing of the proportional gains and increasing lag (integral gain increase) are areas of further exploration. Experimental data from oval test track showed significant human driver error: difficulty for a test driver to drive a vehicle on a road while trying to follow the drive cycle speed trace on a driver's aid display (chassis dyno testing allows test driver to focus solely on following the drive cycle speed trace on a driver's aid display since they don't have the distraction of driving on a road).

Wheel slip plant model: The temporary fix of bypassing wheel slip is an opportunity for future work to get wheel slip model matching experimental data and not falsely preventing the following of a drive cycle trace. The wheel slip model should be altered such that it reduces torque enough to wheels that are slipping to stop the slip and still provide substantial torque to the wheels that were slipping. It should allow the vehicle to continue driving

without undue impairment or undue speed degradation, to resume following a drive cycle, as all of the EcoCAR drive cycles are on dry road surface conditions.

Braking force split between front and rear: The thesis updated assumption of 60% braking force always going to front wheels and the thesis manual calculation of total braking force from experimental data could be replaced with equations to dynamically calculate total braking force and front/rear spit based on mass, Center of Gravity (CG) height location & longitudinal location, and angle of the vehicle from horizontal (is the rear squatting lower than the front, level, or above the front). The actual changes to the team's vehicle added 478 kg (1053 lbs) mass to the rear of the vehicle, altering the CG locations and the rear of the vehicle became lower than the front (the team's rear heavy vehicle had more resistance to the typical tendency of a vehicle rear to lift and the front to nose dive under full braking). The assumption of 60% for the front brake force portion is reasonable based on an example from Husain (64% front) [20] because the team's vehicle had more rear weight bias, although the team's CG height was not known.

Unchanged Item(s) - Electrical conduction wiring losses (I^2R): No wiring electrical conductor I^2R losses were modeled as a part of electrical energy conduction from the cells within the ESS over to the motor. Although these are small losses, they might not be negligible during the high electrical energy period of CD mode when considering changes needed to close the gap between simulation results and experimental data for energy cycles like the E&EC.

- Electrical conductors within the ESS from cell to cell, module to module, from the ESS to the inverter, then from the inverter to the motor

- Especially the relatively higher resistances for very short distances at harness connections, bus bar joints, and wire splices

Unchanged Item(s) – Torque Converter: The vehicle has a torque converter between the engine and the transmission but the simulation vehicle plant model dos not. Adding a torque converter to the vehicle plant model is probably the single most significant change left to do that has not been done by the scope of the thesis work. Torque converters are typically the second highest loss component, right after the engine with the highest loss [36]. The only period when the torque converter is not the second largest component energy loss is when driving steady state at highway speeds where the torque converter is locked up (no slip) and therefore not producing any loss. Figure 5-4 shows powertrain component losses for a conventional mid-sized sedan for the EcoCAR "4-Cycle" drive cycle

using Autonomie modeling and simulation software [23] which shows the torque converter as the second largest component loss, right after the engine.

Conventional Powertrain Component Losses Ranked by Drive Cycle
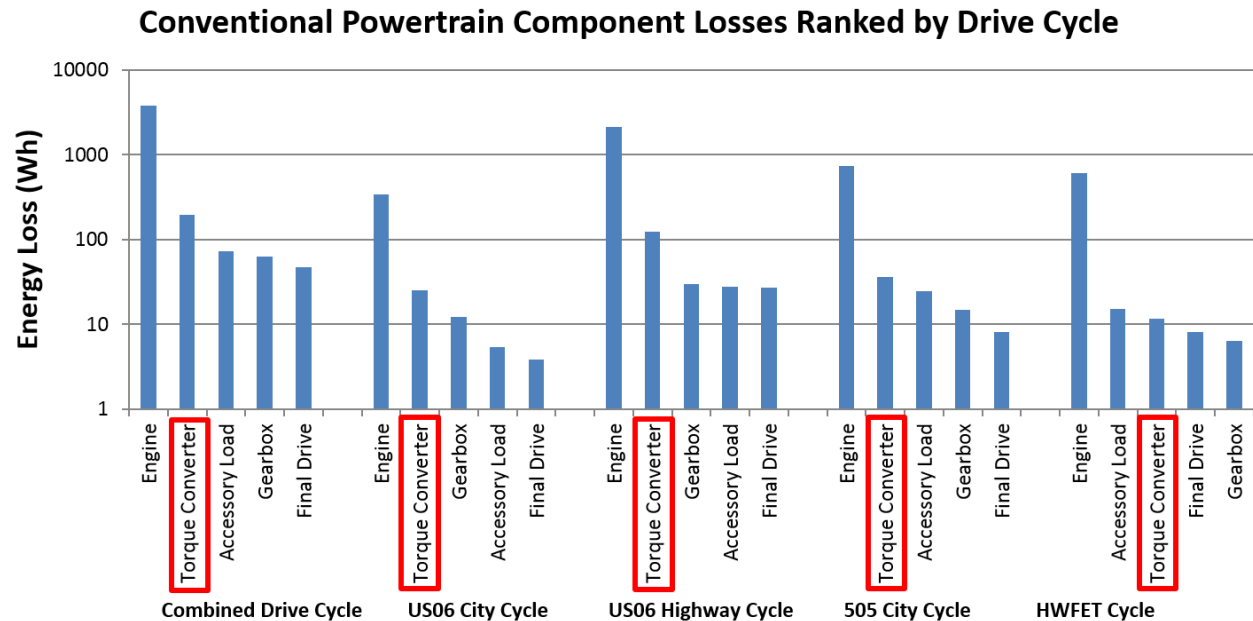
Figure 5-4. Powertrain component losses by drive cycle for a conventional mid-sized sedan [36].

Unchanged Item(s) - Transmission: Transmission items that were not changed at all in vehicle plant models for this thesis but are opportunities for future work:

1) Transmission gear shift execution in simulation does not reduce engine torque for duration of shift like the actual vehicle's experimental data. Shift duration is typically ~0.5 seconds and the engine torque reduction may range from 30% to 90% reduction depending on which gear is being shifted to and the current engine torque output. The lower the gear and more torque output, the larger the engine torque reduction. The first gear shift on a 0-60 accel is the shift from first gear to second and the torque reduction is at the large end of the range, up to a 90% reduction. This is a very significant factor in the 0-60 & 50-70 acceleration drive cycle where transient behavior is a substantial component affecting the metric, but low significance for the E&EC drive cycle.

2) The simulation has only one pair of transmission gear upshift and downshift maps (schedules) – the shift maps are based on accelerator pedal position and vehicle speed. With these two inputs an upshift

or downshift gear can be determined. The shift map pair the team received for the 6 speed transmission may be a generic map pair or may be only one of many shift map pairs that are programmed into the transmission. Multiple shift map pairs are programmed into automatic transmissions, with default map pairs used for optimal fuel economy (eco mode), but other map pairs would be for maximum acceleration performance (sport mode), for cold transmission temperature, for overly hot transmission temperature, for towing, etc. The simulation could be advanced by reviewing the experimental data and creating two pairs of shift maps, one for fuel economy and one for acceleration performance.

Unchanged Item(s) - Engine: Engine items that were not changed at all in vehicle plant models for this thesis but are opportunities for future work:

1) E85 engine overall average efficiency (33.4%, from Table 5-1) seems like it could be a little high as the team's hybrid controls code was underdeveloped and unlikely to achieve anywhere close to the engine efficiencies of commercially available hybrids. Expectations would be at either the high end of conventional vehicle engine efficiency or the low end of hybrid vehicle engine efficiency. Conventional vehicle engine efficiencies commonly range from 28% to 32%, depending on drive cycle [37] and hybrid vehicle engine efficiencies commonly range from 31% to 35%, depending on drive cycle [38]. Analysis and validation of engine data from Yuma E&EC (ICE only) and TRC Chassis Dyno (ICE only) would help to see if an adjustment to fuel rate table is needed and by how much, but only after the simulation vehicle plant model is updated by adding in a torque converter. The thesis simulation result was 4.31 gallons of E85 used during the E&EC drive cycle, compared to 5.95 gallons from experimental data (28% error). Adding a torque converter is expected to significantly reduce this error and some of the remaining error may be with the engine efficiency from the engine fuel map.

2) No engine "braking" modeled. During deceleration, the transmission typically stays in the highest gear possible and the engine fuel is cut to a low level to sustain combustion, with the force of the combustion is so low that it ends up being a negative output torque from the engine to the transmission, providing some mild engine "braking" (driveline drag) in actual production vehicles. Experimental data could be used to determine how much drag the engine produces for various speeds

and gears and update the vehicle plant models in the simulation. This would reduce the amount of regen available for recapture during CS mode when the engine is on.

3) Engine idle torque in simulation is different than experimental data in both 1st gear (Drive) and also in Park, results in different fuel consumption for idle, this is a small factor, but might not be insignificant for E&EC.

4) Validating E85 engine fuel mass flow with experimental data:

   a) Steady state stairs on chassis dyno to simulation results (engine only, no motor)

   b) E&EC from Year 2 at Yuma (engine only, no motor) to simulation results – the detailed logger data was not lost from the Year 2 Yuma E&EC drive cycle.

5) Validating E85 engine reported torque & speed. These have not been validated for the team's engine, but have to assume that GM has performed tuning and calibration to have low error for speed and low error for torque when using certified/quality E85 fuel. Could potentially validate peak torque curve during 0-60 and 50-70 accel with experimental data from Year 2 Yuma (engine only, no motor) and Year 3 Milford (engine only, no motor due to inverter fault).

Lessons Learned during EcoCAR competition: These are items included to document knowledge transfer to future WSU student teams, but are not directly related to this thesis topic of modeling and simulation validation and advancement.

- **Electric traction motor** – replace oil cooled motor to water cooled motor, as the increase in accessory loads (the 2 oil pumps add 50 W – 100W to the accessory loads), decrease the energy efficiency of the powertrain, and the gain from oil cooling in continuous torque and motor service life were not needed for competition purposes, but may be needed for a production intent design. The added complexity of the external oil thermal system, packaging, cost, more fluid leaks, etc., makes oil cooled an undesirable option. When the oil was around 75°F ambient temperature, the oil filter and especially the oil cooler were severe flow restriction points, easily visible by how much the blue tubing swelled up. When the oil was warmed up, the oil filter was more restrictive than the oil cooler. If the oil cooling is kept for future use, then would recommend having 2 oil filters in parallel and completely replacing the oil cooler heat exchanger with a large capacity unit of the counter flow layered plate construction style

that are dominate in automotive OEM use. Also recommend stainless steel braiding to go over the tubing to prevent swelling too much to the point of bursting.

- **Motor Thermal System** - WEG cooling flow for motor inverter and oil cooling – the motor inverter was the main restriction of the cooling loop and therefore limits how much the WEG coolant flows to cool the oil heat exchanger. Adding another WEG coolant pump is not desired, nor is trying to add a bypass loop around the motor inverter. The team ended up having swap a 100 W WEG coolant pump in for the 50 W WEG coolant pump to keep the motor from overheating, due to the high restriction of the motor inverter and the potentially undersized oil cooler heat exchanger. Switching from one 100 W WEG pump to two 50 W WEG pumps in parallel, one for the motor inverter and the other for the oil cooler heat exchanger, would be a better solution than the single 100 W pump. Ideally the inverter would not have such a restricted coolant path so a single 50 W WEG pump would then be enough for both motor and inverter.

- **CAN message data** – in post processing CAN data during analysis after drive cycles, it would have been helpful to have CAN data for the team's hybrid supervisory controller controlled outputs. The team could create a new CAN message on the team's High Voltage (HV) CAN bus that does not conflict with existing messages. The new message ideally could contain the commanded pump speeds (PWM duty cycle for each of 4 pumps), radiator fan control (2 digital outputs controlling 2 relays), the transmission IMS outputs, and the driver indicator light outputs (Ready, Charging, Ground Fault).

- **Project timing** – not having all hardware designed, specified, procured, and mounted on the vehicle in Year 2 of the competition as per EcoCAR 2 schedule, resulted in hardware (gear reducer, motor mount) still being worked on and not mounted until about a month before the Year 3 Final Competition – which left no meaningful time for debugging components (motor resolver faulting out inverter) and controls code. The hardware complexity must be managed to keep simple enough for the team to handle and the team must stay on track enough per the competition timeline to ensure all engineering disciplines get a chance to perform and contribute per the EcoCAR competition intent.

- **Plug-In Charging** – the low efficiency of 73% for AC charging of the ESS (87% expected) is due to having more modules awake than needed (motor inverter) and thermal system on (pumps running) when actually not needed. The motor inverter is only needed to be turned on to do a quick discharge

(active discharge) the high voltage bus after charging completes and ESS contactors are open. Very little heat is generated in the ESS during the 3.3 kW plug-in charging that there is no need for the thermal system to run, as no outside charging in hot desert daytime was done by any team.

- **Transmission Aux Pump** – the team used an electric auxiliary oil pump for the transmission to provide cooling and lubrication for the transmission components on the output side that rotated during the vehicle's electric only driving with the transmission in neutral. This was directionally correct for a production design, but for competition purposes, the transmission will survive long enough without the aux pump, just make sure at the end of every electric only driving, the engine is started and vehicle briefly driven with engine on to lubricate all transmission components. The omission of the aux pump has been proven by other teams to be successful in competition. A significant reduction of 100 W of accessory load could then be realized during CD mode.

- **Front & Rear Seats** – the team accidentally cut out too much of the left side rear seat sheet metal to provide clearance for the electric motor, thereby compromising the right side sheet metal for the structural integrity of the right side rear seat latch. This increased the rear seat penalty from 25 points for no left side rear seat to 50 points for no rear seats on both sides. Also, the replacement of the leather full power front seats with manually adjustable cloth seats for light weighting, added headache between the team and organizers questioning if air bag safety system would be intact with the seat swap (seats had side air bags), and kept the vehicle from being showcased to the media (leather downgraded to cloth) during the ride and drive at the end of the competition.

- **ESS Enclosure** – the team used steel for all of the ESS enclosure which added undesirable weight to the vehicle, causing the action to replace the front seats with lighter versions for light weighting. If the team had replaced the ESS sides and top with aluminum or composite, like other teams ESS enclosures, then less drastic light weighting actions would have been pursued and the nice original full power leather front seats could have been retained.

- **ESS Thermal System** – the team used a very nice chill plate and liquid cooling system that included a refrigerant to liquid heat exchanger (chiller) tied into the air conditioning compressor. This was directionally correct for a production design, but for competition purposes, the ESS could be air cooled by cabin air and then the hot air exhausted outside like some production HEV vehicles do. This saves

complexity and cost. For competition purposes, the ESS starts off fully charged in a climate controlled garage and the E&EC drive cycle is done during the night, so the ESS stressful charge depletion driving ends up being done under moderate ambient conditions, so liquid cooling and tying into air conditioning refrigerant is not needed for competition purposes. The omission of the liquid ESS cooling has been proven by other teams to be successful in competition.

CHAPTER 6. CONCLUSION

This thesis detailed plant model validations and advancements that brought the plant model directionally closer to the actual vehicle's experimental data and error was reduced for most metrics, but not all metrics. Most of the remaining error can be addressed by the future work suggested in Chapter 5, especially the addition of the torque converter to the vehicle plant model. Many of the advancements were to update overly optimistic initial component assumptions with more thoroughly researched values. As a last resort, iterative simulation trial and error was used where researched values could not be found. The advancement of the electric motor powertrain and the vehicle chassis portions of the vehicle plant model provided significant error reduction (at least a 10% reduction) in:

- 2 of 3 Dynamic Performance metrics, 8 of 8 Emissions & Energy Consumption (E&EC) metrics

    However, significant error (more than 10%) still exists and more work is needed in:

- 1 of 3 Dynamic Performance metrics, 6 of 8 Emissions & Energy Consumption (E&EC) metrics

Table 6-1 shows the thesis simulation results for the dynamic performance compared to the stock vehicle, the competition targets, the actual experimental data, and the WSU PTTR simulation results.

- 0-60 Acceleration results no longer have any significant error

- 50-70 Acceleration results have increased error - mainly due to the large reduction adjustment of motor torque in the motor plant model at motor speeds above the motor's base speed to bring the motor plant model closer to experimental data (detailed in Section 3.7.2)

- Braking distance results have decreased error and is now acceptable

Table 6-1. Thesis simulation results for Dynamic Performance compared to experimental data.

EcoCAR 2 Vehicle Technical Specifications (VTS) - **Dynamic Performance**	Production 2013 Chevy Malibu (eAssist)	EcoCAR2 Competition Design Target	WSU PTTR Y3 E85 Experimental Data	THESIS E85 Simulation Prediction	WSU PTTR Y3 E85 Simulation Prediction
Acceleration 0-60 mph [0-96.6 kph]	8.2 sec	9.5 sec	6.4 sec	6.4 sec **(0% error)**	5.8 sec **(9% error)**
Accel. 50-70 mph [80.5-112.6 kph]	8.0 sec	8.0 sec	3.2 sec	3.8 sec **(19% error)**	3.7 sec **(15% error)**
Braking 60-0 mph	43.7 m [143.4 ft]	43.7 m [143.4 ft]	40.2 m [132 ft]	38.9 m [128 ft] **(3% error)**	25.3 m [82.9 ft] **(37% error)**

Table 6-2 shows the Emissions & Energy Consumption (E&EC) comparison of the stock vehicle, the actual experimental data, the thesis simulation results, and the WSU PTTR simulation results. The AC charging efficiency was updated from 87% (first EcoCAR competition population samples) to 73% for the WSU PTTR actual measured efficiency during competition.

It is expected that this remaining error would significantly decrease if there was time to have the thesis scope cover adding in the missing torque converter plant model between the engine and transmission plant models, and also the validation & refinement of the engine & transmission plant models.

- Total vehicle range error reduced by more than half, but is still high at 16%

- Charge Depleting Range no longer has any significant error

- Charge Sustaining Fuel Consumption error reduced by half, but is still high at 24%

- UF-Weighted Fuel Energy Consumption error reduced by nearly half, but is still high at 27%

- UF-Weighted AC Electric Energy Consumption no longer has any significant error

- UF-Weighted Total Energy Consumption error reduced by nearly half, but is still high at 21%

- UF-Weighted WTW Petroleum Energy Use error reduced by nearly half, but is still high at 26%

- UF-Weighted WTW GHG Emissions error reduced by a quarter, but is still high at 31%

Table 6-2. Thesis simulation results for E&EC compared to experimental data.

EcoCAR 2 VTS - Emissions & Energy Consumption **"On-Road Competition"** Drive Cycle **with SEMTECH instumentation trailer**	Production 2013 Chevy Malibu (eAssist Hybrid) Experimental Data	WSU PTTR Y3 E85 Experimental Data	THESIS E85 Simulation Prediction	WSU PTTR Y3 E85 Simulation Prediction
Total Vehicle Range CD+CS (59.8 L [15.8 gal] stock tank, PTTR Y3 tank 34.2 L [9.04 gal])	606 km @ 59.8 L 383 km @ 37.9 L	243.3 km @ 34.2 L 151.2 mi @ 9.04 gal	281.2 km [174.8 mi] **(16% error)**	363.5 km [225.9 mi] **(49% error)**
Charge-Depleting (CD) Range	N/A	48.7 km [30.3 mi]	48.7 km [30.25 mi] **(0.2% error)**	54.1km [33.6 mi] **(11% error)**
Charge-Depleting (CD) Fuel Consumption	N/A	0	0	0
Charge-Sustaining (CS) Fuel Consumption	9.87 lge/100km	13.7 lge/100km	10.46 lge/100 km **(24% error)**	7.86 lge/100 km **(43% error)**
UF-Weighted Fuel Energy Consumption	9.87 lge/100km [842 Wh/km]	7.47lge/100km [665 Wh/km]	5.47 lge/100km **(27% [487 Wh/km] error)**	3.99 lge/100km **(47% [356 Wh/km] error)**
UF-Weighted AC Electric Energy Consumption	N/A	182 Wh/km	180 Wh/km*** **(1% error)**	166 Wh/km*** **(9% error)**
UF-Weighted Total Energy Consumption	842 Wh/km	848 Wh/km	666 Wh/km **(21% error)**	522 Wh/km **(38% error)**
UF-Weighted WTW Petroleum Energy (PE) Use	829 Wh PE/km	216 Wh PE/km	160 Wh PE/km **(26% error)**	118 Wh PE/km **(45% error)**
UF-Weighted WTW GHG Emissions	279 g GHG/km	351 g GHG/km	243 g GHG/km **(31% error)**	201 g GHG/km **(43% error)**

*** Includes 73% actual efficiency measured for WSU PTTR charging system and battery for grid AC electricity

The thesis validation and advancement work done now provides higher confidence and higher accuracy (in most cases) for the simulation results. This makes the vehicle plant model significantly more useful for evaluating fuel economy improvement results when testing the team's controls code changes for fuel economy optimization. This thesis also provides several lessons learned and future work for modeling and simulating vehicle Dynamic Performance and Emissions & Energy Consumption metrics.

Highlights of the team's performance in the EcoCAR 2 competition and resulting experimental data are:

- The WSU team succeeded in reengineering the donated Chevrolet Malibu into a functioning plug-in hybrid electric vehicle with a 49 km [30 mile] range when pulling the emissions trailer and a projected 58 km [36 mile] electric range without the trailer. During the competition, the vehicle was plugged in for charging the ESS up to 100% SOC, then driven in electric only CD mode until the ESS was depleted. Once the ESS was depleted, the vehicle drove in hybrid mode with the E85 fueled engine providing the propulsion energy.

- Fuel energy was reduced 21% primarily through displacement by grid AC electrical energy stored in the high voltage battery pack.

- Petroleum oil usage was reduced 74% primarily by using E85 instead of gasoline.

- The total energy consumption from driving was not significantly changed (0.7% increase) from stock even though the stock vehicle mass of 1640 kg [2616 lbs] was increased 26% by 432 kg [953 lbs] from the addition of the electric powertrain and high voltage battery to the rear of the vehicle.

- However, the Green House Gas emissions increased, mainly due to a CO tailpipe emission increase of 212% more than the stock vehicle, primarily from heavy engine loading right after switching into CS mode due to the engine providing propulsion for the vehicle and charging the ESS from 20% to 39% as the CS target SOC was 38-39%.

- Dynamic performance was improved over the stock vehicle in all areas: 0-60 & 50-70 acceleration (22% & 60% respectively), braking (8%), maximum lateral acceleration, and autocross.

- The team finished in 7th place out of the 15 university teams in Year 3 of the competition, improving up from 8th place in Year 2 and 12th place in Year 1.

REFERENCES

[1] SAE International Surface Vehicle Recommended Practice, 2010, SAE Standard J1711, "Measuring the Exhaust Emissions and Fuel Economy of Hybrid-Electric Vehicles, Including Plug-in Hybrid Vehicles."

[2] Argonne National Laboratories, 2014, "EcoCAR 2 Non-Year-Specific-Rules," Rev. N.

[3] Kahn Ribeiro, S., S. Kobayashi, M. Beuthe, J. Gasca, D. Greene, D. S. Lee, Y. Muromachi, P. J. Newton, S. Plotkin, D. Sperling, R. Wit, P. J. Zhou, 2007, "Transport and its infrastructure. In Climate Change 2007: Mitigation."

[4] U.S. Energy Information Administration, 2013, "Energy Explained: Nonrenewable Sources: Oil and Petroleum Products," http://www.eia.gov/energyexplained/index.cfm?page=oil_home#tab2, accessed December 2014.

[5] U.S. Environmental Protection Agency, 2012, "Sources of Greenhouse Gas Emissions," http://www.epa.gov/climatechange/ghgemissions/sources.html, accessed December 2014.

[6] Waldner, J., 2009, "Development of a 2-Mode AWD E-REV Powertrain and Real-Time Optimization-Based Control System," M.S. thesis, University of Victoria, Victoria, British Columbia, Canada.

[7] Crain, T., 2014, "Hybrid Vehicle Supervisory Controller Development Process to Minimize Emissions and Fuel Consumption in EcoCAR 2," M.S. thesis, University of Washington, Seattle, Washington, USA.

[8] Wilhelm, E., 2007, "Model-Based Validation of Fuel Cell Hybrid Vehicle Control Systems," M.S. thesis, University of Waterloo, Waterloo, Ontario, Canada.

[9] Syed, F., Kuang, M., Czubay, J., Ying, H., 2006, "Derivation and Experimental Validation of a Power-Split Hybrid Electric Vehicle Model," IEEE Transactions on Vehicular Technology, Vol. 55, No. 6, Nov. 2006.

[10] Browne, G., 2011, "A Driven Approach to Proper Vehicle Modeling and Model Validation," M.E. thesis, Memorial University of Newfoundland, St. John's, Newfoundland, Canada.

[11] Walsh, P., Alley, J., 2013, "Safety Tech Pre-Competition Inspections and Emissions Testing Event," Argonne National Laboratory.

[12] Argonne National Laboratory, 2014, EcoCAR 2 Event Operations Description, "Emissions and Energy Consumption."

[13] Argonne National Laboratory, 2014, EcoCAR 2 Event Operations Description, "Acceleration 0- 60 & 50-70 MPH and Braking Events."

[14] Argonne National Laboratory, 2014, EcoCAR 2 Event Operations Description, "Autocross Event."

[15] Argonne National Laboratory, 2014, EcoCAR 2 Event Operations Description, "Maximum Lateral (Max Lat) Acceleration."

[16] Argonne National Laboratory, 2014, EcoCAR 2 Event Operations Description, "Dynamic Consumer Acceptability (DCA)."

[17] Argonne National Laboratory, 2014, EcoCAR 2 Event Operations Description, "AVL Drive Quality."

[18] Argonne National Laboratory, 2014, EcoCAR 2 Event Operations Description, "Gradeability."

[19] Argonne National Laboratory, 2014, EcoCAR 2 Event Operations Description, "On Road Safety Evaluation (ORSE)."

[20] Husain, I., 2011, "Electric and Hybrid Vehicles – Design Fundamentals," second edition, CRC Press, Boca Raton, FL, United States, pp. 29-44, p. 422.

[21] Guzzella, L. and Sciarretta, A., 2007, "Vehicle Propulsion Systems – Introduction to Modeling and Optimization," second edition, Springer, Berlin, Germany, pp. 13-24, p. 51.

[22] Larminie, J. and Lowry, J., 2003, "Electric Vehicle Technology Explained," John Wiley & Sons Ltd., West Sussex, England, pp. 184-189.

[23] Autonomie is a powertrain and vehicle modeling and simulation tool for improving fuel economy, http://www.autonomie.net/, 2009, "Help Part 10 - Main Plant Models Description," Argonne National Laboratory, U.S. Department of Energy.

[24] Ehsani, M, Gao, Y., and Emadi, A., 2010, "Modern Electric, Hybrid Electric, and Fuel Cell Vehicles – Fundamentals, Theory, and Design," second edition, CRC Press, Boca Raton, FL, United States, pp. 19-65.

[25] GM Powertrain, "2012 Product Guide," 2012 – 2015 model years available as of March 2015 from http://www.gmpowertrain.com/VehicleEngines/Introduction.aspx.

[26] GM Powertrain, "2013 Product Guide," 2012 – 2015 model years available as of March 2015 from http://www.gmpowertrain.com/VehicleEngines/Introduction.aspx.

[27] GM differential ratios, http://www.Buick.com, accessed 2013.

[28] A123 Systems, 2011, "Battery Sub-System Design Specification Interface Control Document."

[29] A&D Technology, 2012, "WSU Traction Motor Test Stand."

[30] Rinehart Motion Systems, 2013, "RMS PM100 Software User Manual," rev. 2.7, http://rinehartmotion.com/support.html.

[31] Rinehart Motion Systems, 2013, "Setting up the PM Controller to run with Remy Motors," rev. 1.4.

[32] WSU Hybrid Warriors, 2014, "Year 3 Design Progress Report 3 for EcoCAR 2," rev. G.

[33] Mason, S., The Effects of Rotational Inertia on Automotive Acceleration,

http://stephenmason.com/cars/rotationalinertia.html, accessed 2014.

[34] Hyde, A., Midlam-Mohler, S., and Rizzoni, G., 2014, "Development of a Dynamic Driveline Model for a

Parallel-Series PHEV," SAE Int. J. Alt. Power. 3(2):2014, doi:10.4271/2014-01-1920.

[35] Alley, R., Nelson, D., White, E., and Manning, P., 2013, "VTool: A Method for Predicting and Understanding

the Energy Flow and Losses in Advanced Vehicle Powertrains," SAE Technical Paper 2013-01-0543,

doi:10.4271/2013-01-0543.

[36] WSU Hybrid Warriors, 2011, "Year 1 Design Progress Report 1 for EcoCAR 2," rev. C.

[37] U.S. Environmental Protection Agency, " Where the Energy Goes: Gasoline Vehicles,"

http://www.fueleconomy.gov/feg/atv.shtml, accessed March 2015.

[38] U.S. Environmental Protection Agency, " Where the Energy Goes: Hybrids,"

http://www.fueleconomy.gov/feg/atv-hev.shtml, accessed March 2015.

ABSTRACT

ADVANCEMENT AND VALIDATION OF A PLUG-IN HYBRID ELECTRIC VEHICLE MODEL UTILIZING EXPERIMENTAL DATA FROM VEHICLE TESTING

by

KEVIN SNYDER

May 2015

Advisor: Dr. Jerry Ku

Major: Electric-drive Vehicle Engineering

Degree: Master of Science

The objective of the research into modeling and simulation was to provide an iterative improvement to the Wayne State EcoCAR 2 team's math-based design tools for use in evaluating different outcomes based on hybrid powertrain architecture tweaks, controls code development and testing. This thesis includes the results of the team's work in the EcoCAR 2 competition for university student teams to create and test a plug-in hybrid electric vehicle for reducing petroleum oil consumption, pollutant emissions, and Green House Gas (GHG) emissions.

Plant model validations and advancements brought the vehicle plant model directionally closer to the actual vehicle's experimental data and achieved a significant error reduction in 10 of 11 metrics detailed in the research. The EcoCAR 2 competition events provided the opportunity for the team to get experimental data of the vehicle's behavior on the vehicle chassis dyno and the vehicle on road testing from General Motors proving ground test tracks. Experimental data was used from 5 sources to validate and advance the vehicle plant model:

1. Component Test Benches

2. HIL Test Bench

3. Component on Dynamometer (Dyno)

4. Vehicle on Chassis Dyno

5. Vehicle On Road

The advancement of the electric motor powertrain and the vehicle chassis portions of the vehicle plant model provided significant error reduction (at least a 10% reduction) in:

- Dynamic Performance metrics (2 of 3 had more than 10% error reduction):

- o 9% → 0%   0-60 mph Acceleration

- o 15% → 19%   50-70 mph Acceleration

- o 37% → 3%   Braking Distance, 60-0 mph deceleration

- Emissions & Energy Consumption metrics (8 of 8 had more than 10% error reduction):

  Utility Factor (UF) is from SAE J1711 standard for measuring the exhaust emissions and fuel economy of HEV's and PHEV's

  - o 49% → 16%   Total Vehicle Range (ESS + Fuel Tank)

  - o 11% → 0.2%   Charge Depletion Range

  - o 43% → 24%   Charge Sustaining Fuel Consumption

  - o 47% → 27%   UF-Weighted Fuel Energy Consumption

  - o 9% → 1%   UF-Weighted AC Electric Energy consumption

  - o 38% → 21%   UF-Weighted Total Energy Consumption

  - o 45% → 26%   UF-Weighted Well To Wheel Petroleum Energy Use

  - o 43% → 31%   UF-Weighted Well To Wheel GHG Emissions

However, significant error (more than 10%) still exists and more work is needed in:

- 1 of 3 Dynamic Performance metrics

- 6 of 8 Emissions & Energy Consumption metrics

Future work includes adding a torque converter plant model between the engine plant model and the transmission plant model on the front wheel drive powertrain, implementing identified advancements into the engine and transmission plant models, and additional analysis for validation of the engine and transmission plant models.

The vehicle plant model now provides higher confidence and higher accuracy (in most cases) for the simulation results, making the vehicle plant model significantly more useful for evaluating fuel economy, dynamic performance, and emissions improvement results when testing the team's controls code changes for optimization.

AUTOBIOGRAPHICAL STATEMENT

Kevin Snyder has a Bachelor of Science in Electrical Engineering from the University of Tennessee and is currently a graduate student at Wayne State University, pursuing a Master of Science in Electric-drive Vehicle Engineering.

Kevin also acted as the Chief Engineer on the Wayne State University student team competing in EcoCAR 2, the U.S. Department of Energy's current three year Advanced Vehicle Technical Competition.

Kevin has held various engineering positions at Detroit Diesel and Chrysler and is currently in the Electrified Powertrain hybrid vehicle department at Chrysler, now Fiat Chrysler Automobiles (FCA).